Title
Charging Infrastructure, Network and Urban Mobility

Author
Zeng, Teng

Publication Date
2022

Peer reviewed|Thesis/dissertation

Charging Infrastructure, Network and Urban Mobility

by

Teng Zeng

A dissertation submitted in partial satisfaction of the

requirements for the degree of

Doctor of Philosophy

in

Engineering - Civil and Environmental Engineering

in the

Graduate Division

of the

University of California, Berkeley

Committee in charge:

Associate Professor Scott J. Moura, Chair
Professor Alexandre M. Bayen
Associate Professor Duncan Callaway
Associate Professor Marta C. Gonzalez

Fall 2022

Charging Infrastructure, Network and Urban Mobility

Abstract

Charging Infrastructure, Network and Urban Mobility

by

Teng Zeng

Doctor of Philosophy in Engineering - Civil and Environmental Engineering

University of California, Berkeley

Associate Professor Scott J. Moura, Chair

This dissertation shares a unique perspective to plug-in electric vehicle (PEV) charging infrastructure planning and operations, in which various optimization, control, and data analytic techniques are explored. The critical infrastructure supports to the rapid growth of plug-in electric vehicle adoption is lagging. To efficiently and cost-effectively build and operate a network of charging infrastructure, understandings toward the characteristics both at a single station level as well as at the complex network level are crucial to a societal success. This dissertation shares perspectives and advances knowledge to fill this gap.

First we emphasize the poorly understood and often neglected issue, the *overstay* problem at a single charging station level. The overstay problem is described when a PEV continues to occupy a charger even after its charging session has been completed. It significantly hinders the utilization of the charging infrastructure, leading to wasteful resources, disappointing customer satisfaction, and discounted revenue return. This motivates a strategy for increasing utilization by interchanging fully charged PEVs with those waiting for service. An interchange mechanism is defined and the planning and operation models are developed to account for the phenomena. Numerical experiments are conducted to illustrate the performance and demonstrate decreased planned chargers yet increased economic benefits.

Secondly, we seek to further improve the charging station efficiency through optimal operation strategies. This work stands out from the others by acknowledging and incorporating human users decision process. Human factor is a crucial element in the decision loop and cannot be forced. We achieve the control strategies by nudging users' choices with time flexibility and monetary incentives. The formal process will be defined in the corresponding chapter. The overall control framework is evaluated with three metrics, (i) net profits, (ii) overstay duration, and (iii) number of sessions served. Furthermore, this work served as proof-of-concept and has enabled multiple real life hardware testbeds, including the parking lots on the UC Berkeley and UC San Diego campuses. Pricing experiments have been conducted and the data will be shared to advance community understanding of PEV drivers'

sensitivity to charging flexibility and prices.

Thirdly, the scope is enlarged to consider a network of charging infrastructure. The context is electric trucking logistics with cargo movement. We propose an innovative modeling perspective to consider the non-cooperative nature between charging service provider and the fleet operator(s). Often, it is assumed a powerful system planner can control and management all assets. We, on the contrary, highlight the necessity to consider different entities within the context of transportation electrification.

The final phase proposes a computationally efficient and scalable framework to size the ride hailing fleet, manage it at large-scale, design and match the charging infrastructure. Contrary to current market trends, the results of this work reveal that neither large-battery-size AEVs nor high-power charging infrastructure is necessary to achieve efficient service. This effectively alleviates financial and operational burdens on fleet operators and power systems. Furthermore, strategic fleet management results in low mileage, reducing emissions detrimental to human health. Finally, the reduced travel time and emissions resulting from efficient fleet management create an economic value that exceeds the total capital investment and operational costs of fleet services. The associative policy implications are also revealed in the chapter.

In summary, this dissertation shares the unique perspectives and tackles the often poorly understood problems from practice. The chapters are organized in sequence from planning phase to operation phase, and from single atomic scale to large network level. Yet, each chapter is self-contained. Hence, readers may jump to any chapter depending on their interests and needs.

This dissertation is dedicated to Mom and Dad,

蔡如 (Ru Cai) and 曾志群 (Zhiqun Zeng),

to families, friends and myself,

who's been away from home 10 years.

Acknowledgments

First and foremost, I would like to extend my most sincere gratitude to my research advisor Professor Scott Moura. Flash back to five years ago, Prof. Moura and I were visiting the Tsinghua-Berkeley Shenzhen Institute (TBSI) during the summer period. It was a noon time in a casual day, Prof. Moura and I finished lunch and was riding the elevator. We started to discuss about my future steps. I wanted to apply for graduate school but absolutely lacked the confidence to apply for the Ph.D. programs directly. If it weren't for his classic smile (if you know him you know) and deepest encouragement, I would not be here writing my Ph.D. dissertation. Moreover, I thank Prof. Moura for his acute perspective, supportive caring, and detailed-oriented work reviews. He has been not only an advisor, but also a life mentor, a big brother, an old friend to me. I have become more mature to conduct research, more effective in communication, more open-minded to ideas, and more responsible and caring for junior mentees.

I am grateful to my qualifying exam and dissertation committee members, Prof. Alexandre M. Bayen, Prof. Duncan Callaway, Prof. Marta C. Gonzalez. They asked challenging questions and provided critical feedbacks to my work. I am also very grateful to my preliminary exam committee members, Prof. Max Zuo-Jun Shen and Prof. Joan Walker, for shaping my early research path. Prof. Shen and I developed a research collaboration. His unique angle to tell the story and highlight the contributions has enlightened me.

Many colleagues deserve special recognition for their mentorship and friendship along my research career. I am indebted to Dr. Dai Wang and Dr. Hongcai Zhang. Dr. Wang not only opened my door to "research" but also connected me with industry opportunities. His relentless patience and kindness enable multiple possibilities in my career. Dr. Hongcai Zhang strengthened my research skills and sharpened the perspectives during my doctoral journey. I cannot express enough my admire toward his work ethics. I thank Dr. Saehong Park and Dr. Sangjae Bae for sharing the nights in 626 Davis Hall, for endless knowledge and support, for discussions about family and love relationships. I benefit tremendously from their perspectives to life and career. Their successes further motivate me. I thank Dr. Dante Recalde and Dr. Tobias Massier who hosted me as a research intern in Singapore. It was an unique opportunity for me to open my eyes and learn more about Singapore. I thank Dr. Dong Zhang, Dr. Chao Sun, Dr. Zhe Zhou, Dr. Yiqi Zhao, Dr. Zaid Allybokus, Dr. Anna Robert, Dr. Xiaosong Hu, Dr. Andrea Pozzi, Dr. Zhijia Huang, Dr. Tong Xu, Dr. Soomin Woo, Dr. Lirong Deng, Dr. Bertrand Travacca, Dr. Colin J.R. Sheppard, Dr. Timothy Lipman, Dr. Milad Memarzadeh, Dr. Hector Perez, Dr. Laurel Dunn for their constructive skepticism, insights, advice, and collaborations. Dr. Zhang was my roommate for two years and was generous to all my asks. Dr. Zhe Zhou shared the office with me back when I was still an undergraduate student. We studied the machine learning related methodologies and constructed the neural network from scratch. She has always believed in me and been active to all of my research discussions. Dr. Zaid Allybokus, Dr. Anna Robert and Dr. Yiqi Zhao shared the same project as well as the same catastrophic moments, COVID-19, with me. During the lockdown periods, I was home alone for three months. Delivering results

biweekly was the only mental support to keep me healthy. I am thankful to meet Dr. Zhijia Huang, Dr. Tong Xu, Dr. Lirong Deng from TBSI, who came to Berkeley to exchange and study. In fact, it's my fortune to take classes, discuss projects, and collect advice from them.

I humbly appreciate the peers I have met along this journey as well. I thank Dylan Kato who "coincidentally" finished his four-year undergraduate study at Berkeley, who "coincidentally" decided to stay in the same lab, who "coincidentally" became my roommate, who shared my joys and tears, who has been so kind, supportive and knowledgeable. I thank Patrick Keyantuo, Ruiting Wang, Dimitris Vlachogiannis, Ayşe Tuğba Öztürk, Hassan Obeid, and Yi Ju for the collaborations and rigorous intellectual contributions. I thank Josh Bass for well organizing all the lab logistics. This lab cannot run as smooth without Josh. I thank all the people I have met at the Energy, Control, and Application Lab (eCAL) for the joyful happy hours, unforgettable retreats, creative discussions.

Given my unique situation, where I completed my undergraduate and graduate schools both at the University of California, Berkeley, I also want to thank all the people I have met here since 2014. Starting August 2014, and with these amazing people from all over the world, I learned, absorbed, grew, and finally became the person I am today. I thank Dennis Yuxiao Shang, Leo Yueyang Li, Danial He for being my roommates for three years. We shared too many important life moments. I thank Justin Luke for being the best study buddy. We shared the same vision to transportation electrification and renewable energy. He's one of the most brilliant and hardworking students I have met. He is a role model and a very good friend to me. I thank Maple Lin for the memories in the first two years. I thank Edison Huang, Jack Kefan Xu, Neo Lu, Siyang Liu, Iris Chen, and Vania Fong for suffering the classes together. We have supported each other. I thank Victor Huang, Vanessa, Kelly Zhao who I met in Singapore. Their supports and long-term friendships have made me feel home. Victor always believes in me and always pays for food when we hang out. Vanessa was so patient and generous to even help with my graduation school applications. Kelly always proposes to meet and suggested the go-to options. I thank team members Robert Yu, Michael Yu, Yuting Wang, Fonda Xu and Emily Fan for winning the 10th (in a row) National Wushu Collegiate in 2017. We shared three nights of practice every week in the Spring semester and I am very honored that our efforts paid out.

I am extremely grateful to have met all these best and talented people from all over the world here at Berkeley. Finally, I would also thank my host parents from high school, John and NovaLee Knopp. They are families to me. They have always supported me from behind. NovaLee kept telling me to pack and drive up whenever I feel uncomfortable staying in California. These people shaped who I am. I could not have completed my doctoral studies without them.

Contents

List of Figures

List of Tables

Chapter 1

Introduction

1.1 Research Objectives

1.1.1 Background Context

I first came across the term "plug-in electric vehicles" (PEVs) during my first year of undergraduate study (2014) at UC Berkeley. I was debating if I wanted to stay at the Environment Science major or transfer to a relatively newer major, named Energy Engineering. In one occasion, I was introduced to the potential of PEVs, not only the already obvious environment benefits, but also a technology called "vehicle-to-grid" (V2G), which unlocks an entire space of opportunities. Like many other young enthusiasts, I was immediately sold to this incredible idea, thinking that green energy revolution awaits my contribution. I switched major and spent a year and a half at Dr. Samveg Saxena's Vehicle-to-Grid Simulator (V2G-Sim) project at Lawrence Berkeley National Lab. We incorporated a detailed EV battery pack thermal model and EV powertrain model to capture the time-varying battery temperature and working parameters including current, internal resistance and state-of-charge (SOC), while an EV is driving and offering various grid services. We compared different scenarios and found that the increased wear from V2G is inconsequential compared with naturally occurring battery wear (i.e. from driving and calendar ageing) when V2G services are offered only on days of the greatest grid need (20 days/year in our study) [157].

It was indeed quite an interesting work, and the published paper attracts some attentions over the years. However, what I realized then was the enormous gap between this V2G ideology and the actual implementation. In particular, the physical infrastructure feasibility and the economic viability concerned me. Nevertheless, this first experience enriched my understanding of plug-in electric vehicles and I was convinced that in order to accelerate the transition from conventional vehicles to PEVs, something else more important needs to be realized. Range anxiety was, and yet still is, a concerning problem that hinders PEV adoption. To enable worry-free travel and extend range of movement, convenient access to recharge is the key.

Despite the past heat in research studies and hypes in real world project developments,

charging station and infrastructure network design and operation still encounter significant hurdles. This phenomena often time is resulted from gaps between the academia and the industry. I set out my Ph.D. journey by first identifying a real world problem at charging station, the overstay issue (I will formally define in the next chapter). Later on, this becomes the tone of my research projects - we have a research direction, we identify what's missing from both academia and real world, and finally we conduct the research.

1.1.2 Motivation

The United States is the second leading emitter of greenhouse gases in the world, and as a signatory to the Paris Climate Agreement, it bears outsized responsibility for reducing its emissions [53]. Furthermore, the transportation sector has been the largest greenhouse gas emitting source. It accounts for nearly a third of the greenhouse gas emissions of the United States [140]. Recognizing the value of EVs for this issue, the Department of Transportation, Department of Energy, and the General Services Administration are all contributing to help the United States meet the goals of transportation electrification [60]. Despite these efforts, the United States lags severely in the deployment of electric vehicles, with less than 1% of road vehicles being electrified [139]. Similarly, the importance of optimization methods for handling the influx of people, cars, and trucks in the United States – as well as the concerns over fuel and energy use – has been reinforced by U.S. Department of Energy funding for optimization research and by the U.S. Department of Transportation's recent development of an optimization tool for freight and fuel transportation.

Electrifying transportation brings profound environmental impacts. Plug-in electric vehicles (PEVs) and charging infrastructure research has been a hot topic in the past 10-15 years. As the theme of carbon neutrality attracts more mainstream awareness, more and more countries roll out policies to phase out sales of internal combustion engine vehicles and policies to incentivize developments of plug-in electric vehicles. Being the critical infrastructure supports to enhance the range of mobility, developments of PEV charging stations soar along. China strategically positioned charging infrastructure as one of the eight "New Infrastructure Constructions" [161] in 2020; U.S. passed and enacted the infrastructure bill in November 2021, in which a total $7.5 billion is designated to build a national wide network of PEV chargers [119]; majority of the European countries promotes charging infrastructure developments with monetary incentives since 2019 [111].

Charging infrastructure is deeply coupled with mobility, including both the human mobility and the cargo mobility. These movements drive energy usages and hence impacts on different systems, such as the transportation system and the power system. As a result, when considering infrastructure design and operation, it's truly a complex decision. We need to be mindful that all the analysis are plausible within their given contexts. Considering different customer types, both private PEVs and commercial PEVs in this dissertation, I present a body of work that advances our intellectual understanding to the following questions:

- When facing private PEVs, incorporating individual human behaviors,

  - how to optimally design a charging station?
  - how to optimally operate a charging station?

- When facing fleets of commercial PEVs,
  - how to optimally design and operate the entire charging infrastructure network for fleets serving human and/or cargo mobility on-demand?

1.2 Novel Contributions

The overarching goal of this dissertation is to share one perspective of optimally planning and operating the plug-in electric vehicle (PEV) charging stations, in which the demand uncertainties, human behaviors, movements and systems are deeply coupled. This objective is achieved with four layers of contributions to knowledge on optimizations for energy infrastructure. These layers are detailed throughout this dissertation and are based primarily on a body of publications by the author and his colleagues ([J1,J2,J3,J6] listed in Section 1.3). The other related efforts are also listed but the author refer interested audience to those publications directly.

Single charging station: the overstay problem (Chapter 2)

1. We identify and address an important but misunderstood issue, the overstay problem, for PEV charging stations which neither the literature nor the field operations has addressed well.

2. We use power and energy boundaries to quantify PEVs overstay issue, with which together we propose an innovative aggregate model to describe the station demand profile. This aggregate model is governed by four pairs of the PEV aggregated demand boundaries.

3. Based on the developed methods, we apply measured data from the Cal Poly San Luis Obispo campus to test the model and compare our result with the station's actual configuration.

Single charging station: human driver decision factor (Chapter 3)

1. We propose an operation process at a PEV charging station with distinguished charging service options, which also allows PEV drivers to refuse a charging service. We incorporate Discrete Choice Modeling (DCM) to capture PEV drivers' decision making process;

2. We formally propose a station level optimization model that considers customer charging demands and station operating costs. The framework leverages DCMs to apprehend

a choice probability of charging service options, and incorporates the overstay factor, both of which are responsive to the pricing policy;

3. We allow the model to re-optimize the charge schedules of the existing sessions in response to the new arrivals. The PEV charging station will dynamically operate around the "sweet-spot";

4. We transform the resulted non-convex problem into a three-block multi-convex problem. We efficiently solve this problem with Block Coordinate Descent (BCD) algorithm which enables real-time implementation.

Network and mobility: the cargo movements with electric truck fleet (Chapter 4)

1. Instead of assuming the existence of a powerful single entity who owns both the fleet and the charging network, a two-party model with the charging service provider and fleet operator is adopted. They have their own objectives and their interactions are captured via a Stackelberg game, whose results are closely analyzed. This modeling perspective, to the authors' best knowledge, has never been studied for the vehicle/location routing problem before. The necessity of such modeling perspective is revealed.

2. We propose an innovative partial time expanded network (PTEN) model on top of the customer-node based network [58, 71, 72, 92, 93, 126–128, 166, 170]. This network only expands at candidate charging station nodes to capture both the time domain index and the charger index. This enables us to track the simultaneous charging activities of E-trucks at each location. Therefore, we may incorporate not only the charging station location but also the size decisions. Based on this, the upgrade cost of transformers is also incorporated in the CSP cost calculation, which is actually an important factor in real-world operation but has been neglected in past research. The PTEN also keeps the overall model in the domain of mixed integer linear program, which is more tractable than a mixed integer non-linear program.

3. In order to solve this complex problem, the framework is broken down to be solved in an iterative fashion. An outer loop adopts the idea from [174] to capture the dynamics of the Stackelberg game while ensuring convergence. Within each iteration, three subproblems are solved for CSP, FO, and a feasibility check accordingly. Each subproblem can be solved by either an off-the-shelf solver or any customized algorithm. The contributions are emphasized on the modeling perspective, rather than a particular solution algorithm.

Network and mobility: the human movements with autonomous electric ride-hailing fleet (Chapter 5)

- Strategic fleet management is crucial for operating urban mobility and can reduce fleet size by up to 40%. In our simulated experiments, the number of autonomous conventional vehicles reduced from 13,437 to 8,100 if proper vehicle dispatch and trip matching are conducted. Furthermore, the unnecessary vehicle mileage traveled (VMT) to scout for the next customers (referred to as the "deadheading" effect) decreased drastically.

  Notably, because ride-hailing/taxi fleets exhibit significant deadheading VMT, these vehicles provide a disproportionately large contribution to total vehicle VMT, relative to the proportion of ride-hailing vehicles on roads. The results of the study reveal that managed fleets alleviate traffic congestion and increase traffic speeds by 4%. This "secondary" effect enables further reduction of the fleet size and facilitates considerable economic benefits. The study reveals that more than $250 million of time cost can be saved annually because of reductions in traffic congestion.

- Unlike the current market trend of large-battery-size EVs, we do not advocate long-range and large power AEVs within the context of urban mobility systems. With ample charging infrastructure support, a fleet of 9517 cheap 50-kWh AEVs can be used to satisfy the same level of mobility demands as that of a fleet of 8753 expensive 175-kWh AEVs in the New York City region. Detailed economic analysis reflects that using a fleet of 50-kWh AEVs equipped with a network of 50-kW chargers is the socially optimal strategy.

- Both electrification and automation were realized to transform the ride-hailing service fleet. Fleet electrification alone can result in 84% removal of carbon emissions. When both features are considered, over 90% reduction may be achieved. Additionally, electrification and optimal management via automation can significantly reduce PM2.5 emissions, and the corresponding human health impacts. The economic effect from reduced PM2.5 emissions and reduced healthcare costs for the New York City population can be up to 250 million USD/year.

1.3 Involved Projects and Publication Records

Since the start of my Ph.D. journey, I have been very fortunate to be involved in multiple research projects in my lab. I want to highlight them as well as the associated publications here. I thanks these advisors, mentors, collaborators, and sponsors sincerely.

Lead/Co-Lead Researcher

1. **NSF STTR Phase I: Intelligent Planning and Control Software for EV Charging Infrastructure (2018-2019)**

[J1] **Zeng, Teng**, Hongcai Zhang, and Scott Moura. "Solving overstay and stochasticity in PEV charging station planning with real data." *IEEE Transactions on Industrial Informatics* 16.5 (2019): 3504-3514.

2. **TotalEnergies Sponsored Project: Smart Learning Pilot for Electric Vehicles (SlrpEV, 2019-current)**

   [J2] **Zeng, Teng***, Sangjae Bae*, Bertrand Travacca, and Scott Moura. "Inducing human behavior to maximize operation performance at PEV charging station." *IEEE Transactions on Smart Grid* 12, no. 4 (2021): 3353-3363. (*equal)

   [J3] Obeida, Hassan*, Ayse Tugba Ozturka*, **Teng Zeng***, Sangjae Bae, Wente Zeng, Scott J. Moura. "Electric Vehicle Drivers Charging Preferences with Price Variations at Workplace Charging Stations." *submitted to Nature Scientific Data*. (*equal)

   [J4] Ozturka, Ayse Tugba, Hassan Obeida, **Teng Zeng**, Wente Zeng, Scott J. Moura. "Joint Price and Power Optimization for Workplace Charging Stations." *submitted to IEEE Transactions on Smart Grid*.

   [C1] Bae, Sangjae, **Teng Zeng**, Bertrand Travacca, and Scott Moura. "Inducing human behavior to alleviate overstay at PEV charging station." In *2020 American Control Conference (ACC)*, pp. 2388-2394. IEEE, 2020.

   [U.S. Patent] Customer-centric method and system for pricing options and pricing/ charging co-optimization at multiple plug-in electric vehicle charging stations

   [U.S. Patent] Methods and systems for optimal pricing and charging control of a plug-in electric vehicle charging station

3. **TotalEnergies Sponsored Project: E-truck Fleet Design, Routing and Infrastructure Placement (2019-2021)**

   [J5] Zhao, Yiqi*, **Teng Zeng***, Zaid Allybokus, Ye Guo, and Scott Moura. "Joint Design for Electric Fleet Operator an Charging Service Provider: Understanding the Non-Cooperative Nature." Early access on *IEEE Transactions on Intelligent Transportation Systems*. (*equal)

4. **Other side projects**

   [J6] **Zeng, Teng***, Hongcai Zhang*, Max Z.J. Shen, and Scott J. Moura. "Enhancing the Environmental and Economic Benefits of Automated Electric Vehicle Ride-Hailing Fleets in New York City." *completed 1st round revision at Nature Communications*. (*equal)

   [C2] **Zeng, Teng**, Scott Moura, Xue Li, Zhe Zhou. "Distributed Fleet Management for Shared Electric Vehicles in Coupled Power and Transportation Networks." *submitted to IFAC World Congress 2023*.

Contributing/Advisory Researcher

5. **DOE SMART Mobility Consortium: Advanced Fueling Infrastructure (2019)**

   [J7] Zhang, Hongcai, Colin JR Sheppard, Timothy E. Lipman, **Teng Zeng**, and Scott J. Moura. "Charging infrastructure demands of shared-use autonomous electric vehicles in urban areas." Transportation Research Part D: Transport and Environment 78 (2020): 102210.

   [Report] Smart, John, Bi, Zicheng, Birky, Alicia, Borlaug, Brennan, Burrell, Erin, Koutou, Eleftheria, Lee, Dong-Yeon, Lipman, Timothy, Meintz, Andrew, Miller, Eric, Mohamed, Ahmed, Moniot, Matthew, Moore, Amy, Motoaki, Yutaka, Needell, Zachary, Onar, Omer, Rames, Clement, Reincke, Nicholas, Roni, Mohammad, Salisbury, Shawn, Sheppard, Colin, Toba, Danho Ange Lionel, Walker, Victor, Weigl, Dustin, Wood, Eric, Xie, Fei, Yi, Yonggen, **Zeng, Teng**, Zhang, Hongcai, Zhou, Yan, and Zhou, Zhi. 2020. "SMART Mobility. Advanced Fueling Infrastructure Capstone Report". United States. https://doi.org/10.2172/1656701. https://www.osti.gov/servlets/purl/1656701.

6. **DOE VTO project: Connected and Learning Based Optimal Freight Management for Efficiency (2021-current)**

   [C3] Wang, Ruiting, **Teng Zeng**, Patrick Keyantuo, Jairo Sandoval, Aashrith Vishwanath, Hoseinali Borhan, and Scott Moura. "Optimal Dispatch & Routing of Heavy-Duty Electric Trucks - A Sensitivity Analysis with Fleet Data." *submitted to 2023 American Control Conference (ACC) invited session.*

   [C4] Keyantuo, Patrick, Ruiting Wang, **Teng Zeng**, and Scott Moura. "Distributionally Robust and Data-Driven Solutions to Commercial Vehicle Routing Problems." *submitted to IFAC World Congress 2023.*

7. **TotalEnergies Sponsored Project: Design, feasibility and techno-economic studies of Robo-Chargers (2022-current)**

   [J8] Ju, Yi, **Teng Zeng**, Zaid Allybokus, and Scott Moura "Robo-Chargers: Optimal Operation and Planning of a Robotic Charging System to Alleviate Overstay." *submitted to IEEE Transactions on Smart Grid.*

   [C5] Ju, Yi, **Teng Zeng**, Zaid Allybokus, and Scott Moura "Optimal Operation with Robo-chargers in Plug-in Electric Vehicle Charging Stations." *submitted to 2023 American Control Conference (ACC) invited session.*

1.4 Dissertation Outline

This dissertation is essentially a compilation of several publications, centered around PEV charging infrastructure and mobility, from the microscopic (single station) to the macroscopic level (infrastructure network and mobility). It is organized as follows. Chapter 2 advocates to

incorporate the *overstay* issue for public and workplace charging station planing. It proposes a data-driven robust planning model for one station. Subsequently, Chapter 3 proposes a human centric operation model for a single PEV charging station. The problem scale elevates to the network macroscopic level since Chapter 4, where a joint decision framework to design charging infrastructure network, electric truck fleet, and vehicle routes is proposed. In Chapter 5, societal impacts of charging infrastructure and fleet design for human mobility on-demand are discussed. Finally, the conclusion and the potential future research directions are summarized in Chapter 6.

Chapter 2

Single PEV Charging Station Planning: the Infamous "Overstay" Issue

2.1 Overview

This chapter studies optimal plug-in electric vehicle (PEV) charging station planning, with consideration for the "overstay" problem. Today, public PEV charging station utilization is typically around 15%. When un-utilized, the chargers are either idle or occupied by a fully charged PEV that has not departed. We call this "overstay". This motivates a strategy for increasing utilization by interchanging fully charged PEVs with those waiting for service - an issue which is not well-addressed in the existing literature. Thus, this chapter studies the PEV charging station planning problem taking strategic interchange into account. To our best understanding, this has not been studied in the literature. With interchange, the objective is to enhance charger utilization rate, and thus reduce the number of chargers. This potentially reduces capital investment and operational cost. A novel power/energy aggregation model is proposed, and a chance-constrained stochastic programming planning model with interchange is developed for a public charging station to incorporate customer demand uncertainties. Numerical experiments are conducted to illustrate the performance of the proposed method. Simulation results show that incorporating strategic interchange operation can significantly decrease the number of chargers, enhance utilization and economic efficiency.

This work originally appeared in the following publication:

Zeng, Teng, Hongcai Zhang, and Scott Moura. "Solving overstay and stochasticity in PEV charging station planning with real data." *IEEE Transactions on Industrial Informatics* 16.5 (2019): 3504-3514.

2.2 Introduction

This chapter addresses a single plug-in electric vehicle (PEV) charging station planning problem, with demand uncertainty and "overstay." PEVs are more energy efficient than conventional internal combustion engine vehicles [70] [118], and emit less greenhouse gases and noise emissions [147]. A recent study based on public charging station data forecasts that the anticipated number of PEVs will reach 1 million in the U.S market by 2020, and more than 50% of new cars sold globally will be electrified by 2040 [35]. However, the continuing growth of PEVs might be impeded by limited driving range and lack of public charging infrastructure. Although governments and private parties have put forth great efforts to deploy public charging systems, there remains a large gap between the current service capability and the expected PEV deployment. That is, PEV penetration has out-paced charging station deployment [88][11]. Furthermore, due to improper planning of station sizes and sites, the charging facilities experience significantly imbalanced utilization rates. In urban areas, especially central business districts, the competition for charging resources is intense. After a charger is plugged in, it can be occupied (even if the PEV is not charging) until the driver returns (from work, shopping, dining, etc.). We refer to this behavior as "overstay". Today, "overstay" can consume a charger for 6-8 hours in a typical day. In a recent study conducted in China, where the world's largest PEV charging station network is developed, 85% of the time these stations are idle [171]. The limited number of available chargers may result in unacceptable queuing and inconvenience that can significantly degrade the quality of service (QoS) [82, 171] . Therefore, properly planning and dealing with over-staying PEVs becomes an important yet still poorly understood issue.

2.3 Real Life Data Motivation

In this section, we briefly examine EV charge demand profiles from real data. The station is located in San Luis Obispo, California and is equipped with 12 level-2 (240V, 30A) chargers. It is heavily utilized with on average 703 charging sessions and 80 unique user identities per month. As shown in Fig. 2.1a, over 90% of the sessions occur within 4 hours and the average plug-in duration is around 3.5 hours.[1] Note in Fig.2.1b that the average charging duration is only around 2 hours. Over 90% of the PEVs tend to overstay and occupy the chargers for an extra 75% of the charging time. Furthermore, the longer the PEVs are plugged-in, the more severe the over-staying effects were [2]. Tesla has encountered this problem in late 2016. They introduced an idle fee at Superchargers to encourage owners to move when charging is over. Lately, Tesla has again adjusted the fee to discourage the

[1]There is a notable decrease after 4 hours of duration in Fig. 2.1a. This could be explained by the facility's pricing policy: free parking for the first 4 hours.

[2]In this region the overstay is a very important problem. However, it varies region by region. Ultimately, the key take away is the planning process instead of the absolute results from this analysis.

practice even more [84]. The overstay problem is thus a universal problem that many station operators have to overcome.

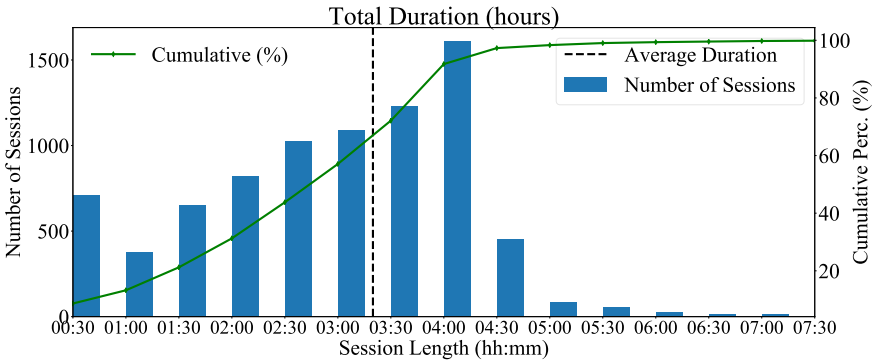

(a) Total Parking Duration

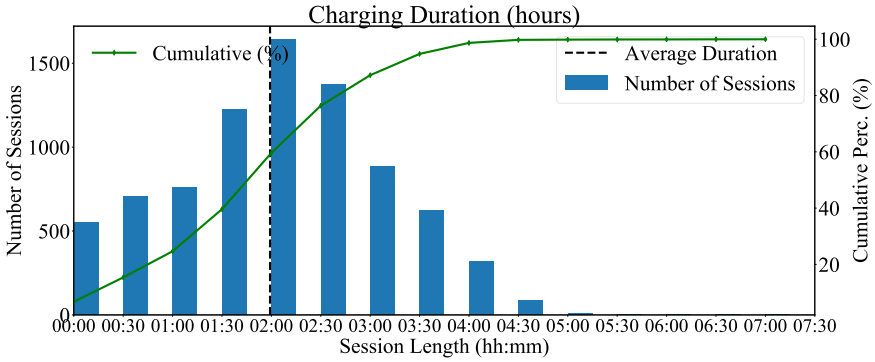

(b) Charging Duration

We discretized the day into 15-minute intervals. The aggregate power boundaries are shown in Fig. 2.2a and the PEVs' cumulative energy consumption at the station is shown in Fig. 2.2b. Since a year of demand profiles are plotted in the same figures, it is very messy and hard to read. The quantile curves thus visually provide readers a sense of the variance among the charging demands across the year. The aggregate methods are described in Sections 2.6 and 2.9. They are essentially the Minkowski Sum of the individual demands. Note that since there are always some overnight charging PEVs, the timelines on the plots are over 24 hours. As reflected from the two plots, the demand variance is non-trivial, with energy ranging from 20 kWh up to 700 kWh. Therefore, the rest of the chapter will address the following question: how to design a charging station that robustly provides high quality of service under uncertain demand while minimizing costs?

2.4 Relevant Literature

Low utilization has been partially addressed in the literature. Reference [86] identifies that fully recharged PEVs continuing to physically occupy the charging spaces creates a

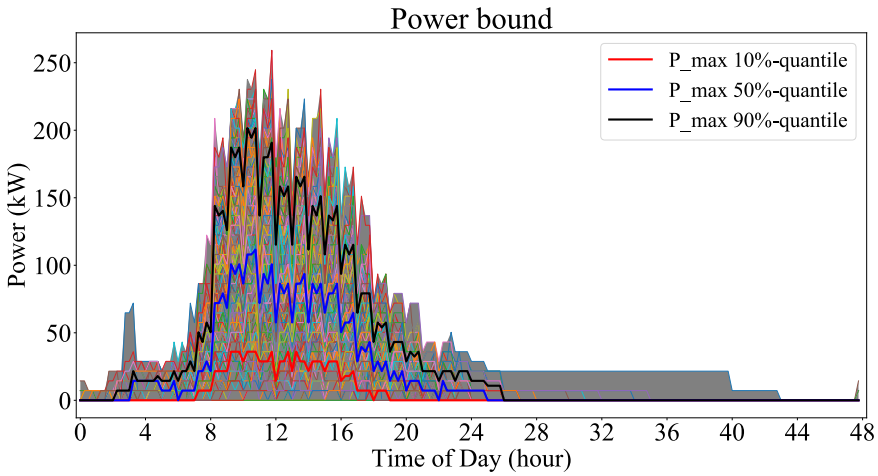

(a) Power boundaries (kW) of a day

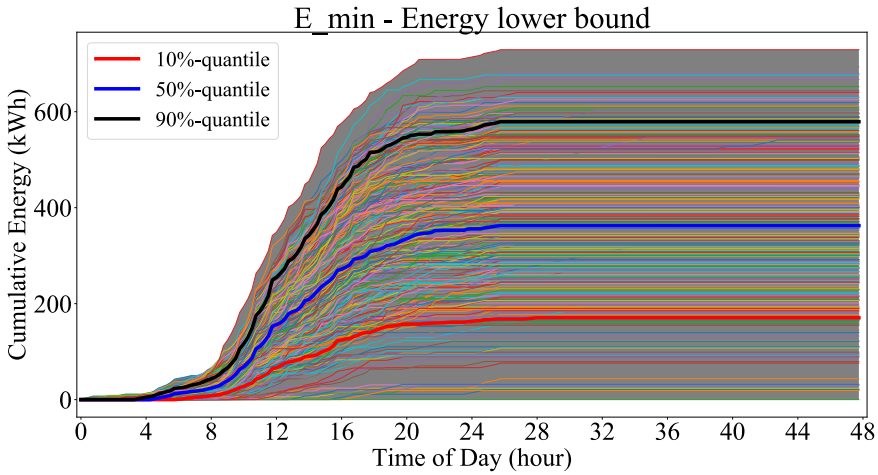

(b) Required energy (kWh) of a day

service bottleneck. To deal with this issue, reference [24] introduced a penalty function during operation. The penalty is activated once the actual charging session is finished, but the PEV is still occupying the charger. The trade off between the penalty price and the user acceptance probability is examined. Tesla has implemented a similar approach to address this exact issue. They impose an "idle fee," which is a penalty cost they apply to users, in USD/minute, when the PEV is fully charged [84]. Reference [164] proposed a sequential strategy for charging station planning considering charging demand growth, which avoids investment redundancy during early stages and enhances utilization rate.

On the other hand, most of the charging station planning literature focuses on the network-scale interaction, quantitatively measured through economic utilities (maximizing profits/social welfare). The focus is typically mitigating traffic congestion in a transportation system, or shaving the peak load in the distribution power system. For example, in [158], a multi-objective PEV charging station planning model considering traffic constraints was

proposed. Reference [168] studied coordinated planning of the integrated power distribution network and PEV charging systems; [61] oriented toward minimizing power losses and voltage deviation for the distribution system operator. Further, [159, 160] studied the planning problem with a transportation-electric coupled network. In [176], a planning framework for various types of charging facilities in an urban area was developed. The aforementioned literature focuses on the network level, and does not adequately address uncertainty at a single station level, particularly regarding utilization rate. Some publications focus on single stations and utilization rate. For example, [178] proposed the idea of single pole multiple cables. This allows multiple PEVs to simultaneously connect to one charging circuit, but only one PEV is charged at a time. Once the PEV is fully charged, the power output is switched to another PEV and thus increases the chargers utilization rate. A further extension to the method was proposed in [37], where a multiple-charger multiple-port charging system is proposed. However, the limitation of [37, 178] is that there does not exist proactive action to switch a charger to a waiting PEV. Therefore, the potential number of PEVs receiving charging services is still significantly limited by the number of charger cables at a station. To the authors' best knowledge, literature has not yet properly addressed the overstay issue at station planning stage. Moreover, due to the lack of real world data, charging demands (including the above literature) were mainly estimated according to either a hypothetical probability distribution (e.g. Poisson for arrival and Bernoulli for decision process [186]), agent-based simulations [36], or travel surveys. Therefore, the effectiveness of the planning method remains disconnected with real-world operation.

To address low utilization, it is critical to consider the problem from the planning stage. The benefits include less chargers with higher utilization rates, which leads to lower capital investment from chargers, transformer upgrades, and space. In this chapter we study PEV charging station planning, taking overstay and an interchange mechanism into account. The interchange concept is precisely defined in Section 2.5. We incorporate interchange along with PEV charging demand into the planning model. Results show that strategic interchange can significantly enhance station utilization rate. Since we take the perspective of the charging station owner and operator seeking to provide charging services, the planning objective is to minimize both investment and operational costs.

2.5 PEV Interchange Mechanism

To address the overstay problem, we formally define the interchange mechanism for station planning.

Definition 2.5.1 (*Interchange*)**.** One interchange (ITC) event occurs when a charger that has been occupied by PEV A is switched (either automatically by machine or manually by human) to another waiting PEV B, before PEV A's departure time. Mathematically, when $t_B^{\text{c.start}} < t_A^{\text{d}}$ holds, one interchange event occurs.

A schematic diagram of two PEVs A and B sharing one charger is shown in Fig. 2.3. Without proper management, PEV A occupies the charger after it is fully charged at $t_A^{\text{c.end}}$ and until PEV A departs at t_A^{d}. As a result, when PEV B arrives at t_B^{a}, it must wait until the charger is released. Note that the charger is blocked from providing charging service between $t_A^{\text{c.end}}$ and t_A^{d}. At a destination charging station, such as a workplace, the queued PEV may wait several hours. As a result, the infrastructure planner needs to deploy two chargers to satisfy the ongoing demands. However, if PEV B could be *interchanged* at $t_A^{\text{c.end}}$, such that there is no or little idle time, then utilization rate and quality of service increases and we can avoid investing in additional chargers. The interchange mechanism can be performed through several ways, including human actuated (e.g. a parking valet or end user) or machinery actuated (e.g. a specialized robot designed for such tasks). As a result, although interchange enables less capital investment, the mechanism inevitably accrues cost depending on the method. Our planning model optimally balances this trade off, which is illustrated in the case study and sensitivity analysis section.

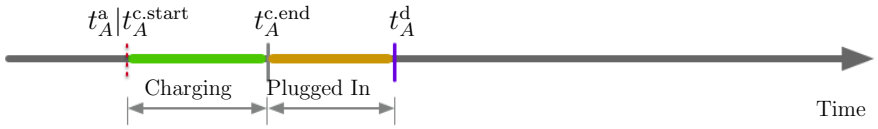

(a) Charging process of PEV A

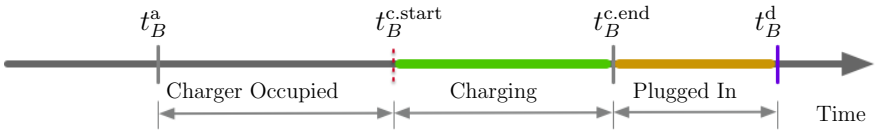

(b) Charging process of PEV B

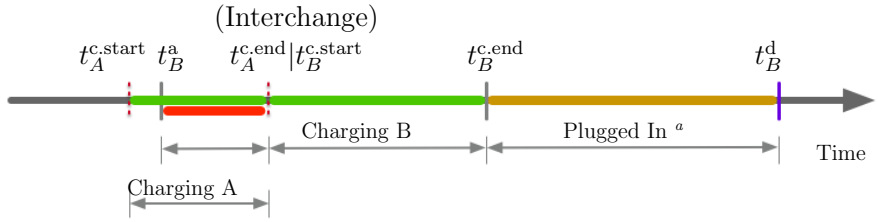

(c) Interchange process of the charger

[a] if there's a third PEV C coming in, the charger can again be unplugged from B and moved to C at $t_B^{\text{c.end}}$.

Figure 2.3: A schematic diagram of two PEVs sharing one charger through interchange.

2.6 PEV Aggregate Model

This section introduces an aggregate model to describe the macro-scaled power and energy demands with interchange at a charging station. We adopt and extend the aggregate formulations from [177], whose accuracy and efficient computational features are discussed within.

2.6.1 Aggregate Model for PEV Actual Demand

First, we define the Minkowski Sum, which will be instrumental in the aggregate model.

Definition 2.6.1 (*Minkowski Sum*)**.** Given two sets, $A, B \in \mathbb{R}^d$, their *Minkowski Sum*, $A \oplus B$, is their element-wise sum, namely the set $A \oplus B = \{a + b \mid \forall\ a \in A,\ b \in B\}$.

Reference [177] viewed all the PEVs requiring charging services during the same time interval as a fleet of vehicles. It proposed a method to aggregate the fleet's actual power and energy demand needs. Given the fleet of PEVs $\mathcal{N}$ parking at the same time interval t and each individual PEV's power boundaries $\{p_{i,t} \in [p^-_{i,t}, p^+_{i,t}],\ \forall i \in \mathcal{N}\}$, the Minkowski Sum of these sets results in (2.1):

$$P_t \in [p^-_{1,t}, p^+_{1,t}] \oplus \cdots \oplus [p^-_{i,t}, p^+_{i,t}] \oplus \cdots \oplus [p^-_{N,t}, p^+_{N,t}],\ \forall t \in T \tag{2.1}$$

in which, P_t denotes the PEV fleet's actual power demand. Since (2.1) is a summation of parallel line segments, the result is a lengthened line segment. Then the two endpoints of the resulting segment are denoted by p^-_t, p^+_t respectively.

Likewise, the corresponding Minkowski Sum of all the individual energy boundaries yields the aggregate energy lower and upper bounds, e^-_t and e^+_t.

$$\begin{aligned}\sum_{\tau=t_0}^{t} P_\tau \eta \Delta t \in &\left[\sum_{\tau=t_0}^{t} p^-_{1,\tau}\eta\Delta t, \sum_{\tau=t_0}^{t} p^+_{1,\tau}\eta\Delta t\right] \oplus \dots \\ &\cdots \oplus \left[\sum_{\tau=t_0}^{t} p^-_{N,\tau}\eta\Delta t, \sum_{\tau=t_0}^{t} p^+_{N,\tau}\eta\Delta t\right],\ \forall t \in T\end{aligned} \tag{2.2}$$

To simplify notations, (2.1) and (2.2) are equivalent to:

$$p^-_t \le P_t \le p^+_t,\quad \forall t, \tag{2.3}$$

$$e^-_t \le \sum_{\tau=t_0}^{t} P_\tau \eta \Delta t \le e^+_t,\quad \forall t. \tag{2.4}$$

Essentially, the above captures two extreme cases when a charging station is trying to provide the needed services. The extremes can be interpreted as "delay" charging and "immediate" charging. The "delay" charging seeks to satisfy the minimum needed demands

as delayed as possible and the "immediate" charging provides charging services as soon as the charger is connected until the PEV's battery is fully charged. Thus, the set $\{p_t^{+/-}, e_t^{+/-}\}$ becomes the PEV fleet's actual demand boundaries that the charging station needs to satisfy. For details, please refer to reference [177].

2.6.2 Aggregate Model for PEV Plug-in Demand

As motivated in Section 2.3, PEVs tend to overstay at the facility after charging, and the charger is blocked from providing service. To consider the blocked chargers that prevent service, we conceptualize a hypothetical consumption that PEVs extract from the charging station, which includes physical energy delivered and blocked energy. The station configuration thus should not be determined by the PEVs' physical electricity consumption (actual demands, Section 2.6.1); rather, it should be governed by the combined actual and hypothetical demands, plug-in power/energy, which we define and quantify next:

Definition 2.6.2 (*plug-in power*)**.** A PEV's *plug-in power* is the rated charging power of the plugged-in charger. It is the power that the PEV occupies but not necessarily consumes. Mathematically:

$$p_{i,t}^{\mathrm{p}} = \begin{cases} p_i^{\mathrm{rated}}, & \text{if PEV } i \text{ is plugged into a charger,} \\ 0, & \text{otherwise.} \end{cases} \tag{2.5}$$

Definition 2.6.3 (*plug-in energy*)**.** A PEV's *plug-in energy* is the combined actual and hypothetical energy consumed throughout the PEV's entire plug-in duration. Hypothetical energy quantifies the overstaying issue in terms of energy. Mathematically:

$$e_i^{\mathrm{p}} = p_i^{\mathrm{rated}} \eta \left(t_i^{\mathrm{unplug}} - t_i^{\mathrm{plug}} \right) = e_i^{\mathrm{need}} + e_i^{\mathrm{hypothetical}}, \tag{2.6}$$

where $t_i^{\mathrm{plug}} \leq t_i^{\mathrm{unplug}} \leq t_i^{\mathrm{d}}$.[3]

Both the plug-in power and energy are combined to form a PEV's plug-in demand. Note that the plug-in power and energy upper-bound PEV i's actual consumed power $p_{i,t}$ and energy $e_{i,t}$, respectively. Mathematically: $p_{i,t} \leq p_{i,t}^{\mathrm{p}}$ and $e_i \leq e_i^{\mathrm{p}}$, where $e_i = \sum_{\tau=t_0}^{t} p_{i,\tau} \eta \Delta t$.

A graphical illustration is featured in Fig. 2.4, where one PEV driver arrives to acquire charging service (15kWh in total), but overstays. The yellow portion indicates how much of the charging resource the overstaying problem has wasted.

Remark 1: The longer the PEV overstays, the more hypothetical energy the PEV consumes since $e_i^{\mathrm{hypothetical}} = e_i^{\mathrm{p}} - e_i^{\mathrm{need}}$. Thus, an interchange mechanism is crucial to help alleviate the wasted charging resource by advancing the unplug time. The hypothetical energy demand is also referred to as the *interchange energy demand*.

[3]For planning purposes, we assume that when the PEV arrives, it immediately plugs in to the charger to acquire service, i.e. $t_i^{\mathrm{plug}} = t_i^{\mathrm{a}}$ for planning modeling. Additionally, $t_i^{\mathrm{unplug}} = t_i^{d}$ as the PEV i user unplugs the charger upon departure.

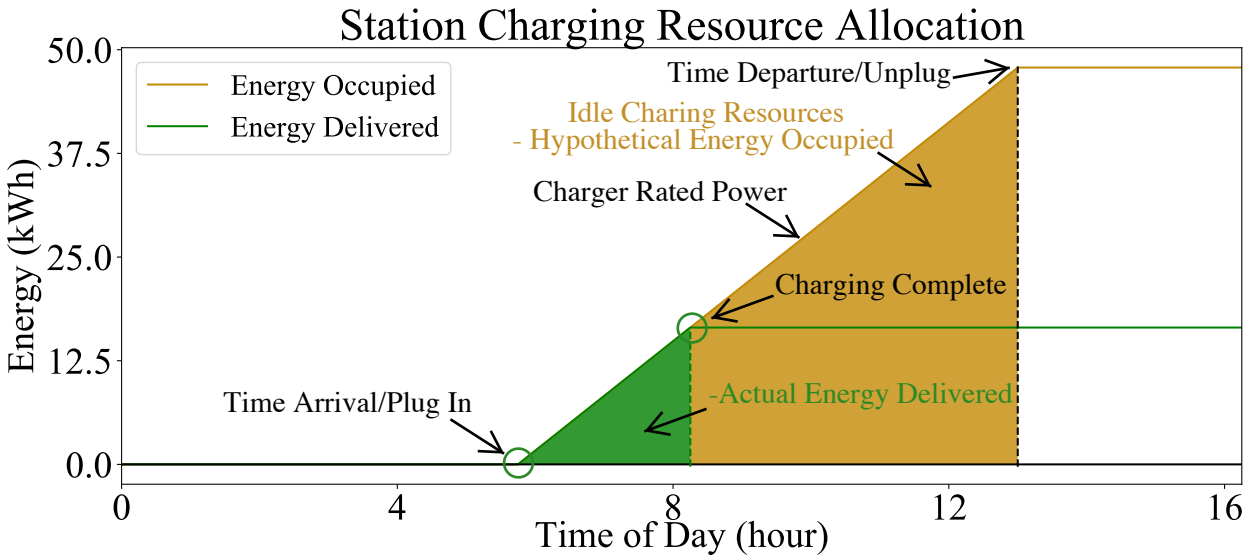

Figure 2.4: Plug-in Energy Illustration

In the following subsections, we propose an aggregate plug-in demand model for a PEV fleet with interchange.

Individual Plug-in Demand Model

Once a PEV i is fully charged, it may take up to Δt_i^{itc} time to interchange its charger to another PEV that has been actively waiting in the queue. Then, the PEV's minimum (required) plug-in energy need is:

$$e_i^{\text{pneed}} = e_i^{\text{need}} + p^{\text{rated}} \eta \Delta t_i^{\text{itc}}, \tag{2.7}$$

where the first term on the right hand side of (2.7) is the actual energy the PEV acquired upon its departure time. The second term is the additional plug-in energy resulting from the interchange time delay, immediately after PEV i is fully charged. Parameter Δt_i^{itc} can be estimated from historical interchange data.[4]

The plug-in energy upper bound of PEV i is determined by its expected plug-in duration, which we model as the parking duration, and can be calculated as:

$$e_i^{\text{pmax}} = p^{\text{rated}} \eta \left(t_i^{\text{d}} - t_i^{\text{a}} \right). \tag{2.8}$$

[4]In scenarios where interchange is performed by automatic machinery, the interchange delay could be approximated as fast as zero. In scenarios where human interactions are involved, the interchange delay could be several minutes to several hours.

The individual plug-in power and energy boundaries are thus:

$$p_{i,\tau}^{p+} = \begin{cases} p^{\text{rated}}, & t_i^{\text{a}} < \tau \leq t_i^{\text{d}}, \\ 0, & \tau > t_i^{\text{d}} \text{ or } \tau \leq t_i^{\text{a}}, \end{cases} \tag{2.9}$$

$$p_{i,\tau}^{p-} = 0, \quad \forall \tau, \tag{2.10}$$

$$e_{i,\tau}^{p+} = \begin{cases} e_i^{\text{pmax}}, & \tau > t_i^{\text{d}}, \\ \min\left(e_{i,\tau-1}^{p+} + p^{\text{rated}}\eta\Delta t, e_i^{\text{pmax}}\right), & t_i^{\text{a}} < \tau \leq t_i^{\text{d}} \\ 0, & \tau \leq t_i^{\text{a}}, \end{cases} \tag{2.11}$$

$$e_{i,\tau}^{p-} = \begin{cases} e_i^{\text{pneed}}, & \tau > t_i^{\text{d}}, \\ \max\left(0, e_i^{\text{pneed}} - p^{\text{rated}}\eta(t_i^{\text{d}} - \tau)\right), & t_i^{\text{a}} < \tau \leq t_i^{\text{d}}, \\ 0, & \tau \leq t_i^{\text{a}}, \end{cases} \tag{2.12}$$

Aggregate Plug-in Demand Model

For the aggregate plug-in model, we again utilize the summation of plug-in power and energy boundaries of all individual PEVs to represent the PEV fleet's plug-in demand boundaries.

$$e_\tau^{p+/-} = \sum_i e_{i,\tau}^{p+/-}, \forall \tau, \tag{2.13}$$

$$p_\tau^{p+/-} = \sum_i p_{i,\tau}^{p+/-}, \forall \tau. \tag{2.14}$$

This model describes the feasible set of all possible aggregate PEV plug-in power and energy consumption trajectories.

2.7 Planning Model

In this section, we propose a PEV charging station planning model considering the equivalent annual capital investment as well as the expected annual operational costs. Specifically, we examine the balance between installing more chargers at the investment stage and adopting more interchange operations at the operation stage. The planning model aims to minimize the total economic costs of the charging station, which includes the initial capital cost for the chargers, and the operation costs for electricity, interchange, and load shedding (due to limited electricity supply capacity).

Since human behavior is uncertain, parameters p_t^+, p_t^-, e_t^+, e_t^+, $p_t^{\text{p}+}$, $p_t^{\text{p}-}$, $e_t^{\text{p}+}$, $e_t^{\text{p}-}$ and p_t^{base} are random variables, colored in red for reading convenience. We consider variance among different individuals, and thus variance exists in the aggregate demand modeling. We propose a two-stage stochastic programming (SP) model with interchange, along with a set of finite representative scenarios Ω to capture the uncertainties. Further, we propose to

incorporate a chance constraint in the SP formulation. Reasons are addressed in subsection 2.7.2.

2.7.1 Two-stage Stochastic Programming Model for Planning

The problem is formulated as a two-stage stochastic program, where the optimization variables are colored blue for reading convenience:

$$f = \min_{X} \left\{ \underbrace{C^I(X)}_{\text{stage one}} + \underbrace{\mathbb{E}_p[Q(X,\omega)]}_{\text{stage two}} \right\} \tag{2.15a}$$

$$\approx \min_{X} \left\{ C^I(X) + \sum_{\omega\in\Omega} (\pi_\omega \cdot Q(X,\omega)) \right\} \tag{2.15b}$$

where:

$$C^I(X) = \frac{r(1+r)^N}{(1+r)^N - 1}(c^{\text{ch}} \cdot X) \tag{2.15c}$$

$$\begin{aligned} Q(X,\omega) = \min_{y} \Bigg\{ & 12c^{\text{ed}} \cdot P^{\text{grid}}_{\text{max},\omega} + 365 \sum_{t} (c^{\text{e}}_t \cdot P_{t,\omega} \\ & + c^{\text{loss}} \cdot P^{\text{loss}}_{t,\omega} + c^{\text{itc}}_{\text{plan}} \cdot P^{\text{pitc}}_{t,\omega}) \Delta t \Bigg\} \end{aligned} \tag{2.15d}$$

subject to $(\forall t, \forall \omega)$:

$$p^-_{t,\omega} \le P_{t,\omega} + P^{\text{loss}}_{t,\omega} \le p^+_{t,\omega}, \tag{2.15e}$$

$$e^-_{t,\omega} \le \sum_{\tau=t_0}^{t} \left(P_{\tau,\omega} + P^{\text{loss}}_{\tau,\omega} \right) \eta \Delta t \le e^+_{t,\omega}, \tag{2.15f}$$

$$0 \le P^{\text{pitc}}_{t,\omega} \le p^{\text{p+}}_{t,\omega}, \tag{2.15g}$$

$$P^{\text{p}}_{t,\omega} = p^{\text{p+}}_{t,\omega} - P^{\text{pitc}}_{t,\omega}, \tag{2.15h}$$

$$e^{\text{p}-}_{t,\omega} \le \sum_{\tau=t_0}^{t} P^{\text{p}}_{t,\omega} \eta \Delta t \le e^{\text{p+}}_{t,\omega}, \tag{2.15i}$$

$$P_{t,\omega} \le P^{\text{p}}_{t,\omega} \le p^{\text{rated}} X, \tag{2.15j}$$

$$P^{\text{grid}}_{t,\omega} = P_{t,\omega} + p^{\text{base}}_{t,\omega}, \tag{2.15k}$$

$$p^{\text{tran}}_{\text{min}} \le P^{\text{grid}}_{t,\omega} \le p^{\text{tran}}_{\text{max}}, \tag{2.15l}$$

$$P^{\text{grid}}_{t,\omega} \le P^{\text{grid}}_{\text{max},\omega}, \tag{2.15m}$$

$$\begin{aligned} & 0 \le X, \quad 0 \le P_{t,\omega}, \quad 0 \le P^{\text{loss}}_{t,\omega}, \\ & 0 \le P^{\text{p}}_{t,\omega}, \quad 0 \le P^{\text{pitc}}_{t,\omega} \end{aligned} \tag{2.15n}$$

Stage One

Stage one is planning, with decision variable X. The objective (2.15b) is to obtain optimal X to minimize the equivalent capital investment of a charging station. The first term in (2.15b) is calculated in (2.15c), in which, r is the discount rate and N is the service life of a charger. Therefore, $\frac{r(1+r)^N}{(1+r)^N-1}$ is the capital recovery factor, which converts the total investment cost into a stream of equivalent annual payments over the life cycle N years. Symbol c^{ch} is the total cost (USD) of a charger installation, including hardware and material costs, electrician labor costs, etc. [2]. The second term in (2.15b) is the expected annual operational costs, in which π_ω is the occurrence probability of scenario ω.

Stage Two

Stage two minimizes the monetary costs incurred during the operation stage. The decision variables include the demand charge, $P^{\text{grid}}_{\text{max},\omega}$, the charging power at each time interval t, $P_{t,\omega}$, unsatisfied (i.e. shed) power demand $P^{\text{loss}}_{t,\omega}$, and the (hypothetical) power demand shed due to the interchange mechanism, $P^{\text{pitc}}_{t,\omega}$. Therefore, $y = \{P^{\text{grid}}_{\text{max},\omega}, P_{t,\omega}, P^{\text{loss}}_{t,\omega}, P^{\text{pitc}}_{t,\omega}\}$. The first term in (2.15d) is the annual demand charge over 12 months and c^{ed} is the demand charge price. The second term is the annual electricity purchased, in which c^{e}_t is the corresponding electricity tariff, in USD/kWh. The third term is a measure of quality of service, where we penalize any unsatisfied energy demand. Parameter c^{loss} is the corresponding per-unit penalty cost, in USD/kWh. The last term is the cost of hypothetical energy shed due to interchange. Here we are experiencing a cost trade off between the installed number of chargers, the unsatisfied demand, and shed hypothetical demand. On one hand, since we want to minimize the number of chargers so that capital cost is lowered, charging demand conflicts among the PEV fleet may arise, which can lead to unsatisfied demand. This issue could be partially or even completely resolved through the interchange mechanism by actively unplugging the fully charged (or satisfied) PEVs. However, we need to take the cost of interchange into account ($P^{\text{pitc}}_{t,\omega}$), since it is an additional service the station is providing. On the other hand, it is wasteful to install any unnecessary chargers as overstaying PEVs continue occupying the chargers. This impacts the chargers' utilization rate. Therefore, the model seeks to optimally balance the number of chargers and the amount of interchange service the station provides.

Constraints

The optimization variables are colored blue to enhance clarity and expose structure. Note that the physical meaning of decision variables, $P^{\text{p}}_{t,\omega}$, $P^{\text{grid}}_{t,\omega}$ in stage 2, are the plug-in power demand and the grid net load respectively. They are defined in constraints (2.15h) and (2.15k) and by substitution, we could eliminate the equality constraints to reduce the problem dimensionality. Constraints (2.15e) and (2.15f) define the power and energy boundaries for the aggregate PEV charging profile, whereas constraints (2.15g) and (2.15i) define

the plug-in power and energy boundaries in association with interchange. Constraint (2.15j) determines the number of PEV chargers needed to satisfy the peak aggregate plug-in power demand; meanwhile it also ensures that the PEVs are only charged during their plug-in period. Constraint (2.15l) lower and upper bounds the total power demand from this charging station by the local transformer's capacity. Constraint (2.15m) determines the amount of demand charge and the last constraint defines the feasible domain sets of the variables.

2.7.2 Chance-constrained optimization

The quality of the stochastic programming results are directly affected by the number of representative scenarios. Namely, the law of large numbers says that as the number of scenarios goes to infinity, the sample average in (2.15b) will converge to the expected value. However, as the number of scenarios increases, the computational complexity can become intractable. In this paper, we combine chance-constrained programming and stochastic programming to effectively balance optimality and computational efficiency.

Any linear inequality constraint in (2.15e)–(2.15n) with a random variable can be formulated as follows:

$$b \leq \mathbf{a}^\intercal \mathbf{x}, \tag{2.16}$$

$$1 - \epsilon \leq \mathbf{Pr}(b \leq \mathbf{a}^\intercal \mathbf{x}), \tag{2.17}$$

in which, symbol b is the random variable, $\mathbf{x}$ is the decision variable, and $\epsilon \in [0, 1]$ is the reliability threshold. Solution robustness increases as $\epsilon \to 0$. Since the random variable separates from the decision variable, we can reformulate the problem into its deterministic counterpart given the cumulative distribution function (CDF) of the random variable b. [5] A basic approach to this individual chance constraint is to use quantiles as follows:

$$\mathrm{F}_b{}^{-1}(1 - \epsilon) \leq \mathbf{a}^\intercal \mathbf{x}, \tag{2.18}$$

where $\mathrm{F}_b{}^{-1}$ is the inverse CDF of b and $\mathrm{F}_b{}^{-1}(1 - \epsilon)$ represents the $(1 - \epsilon)$ quantile quantity of b, which is deterministic.

Simply turning all the constraints associated with random variables to chance constraints will significantly restrict the feasible domain of the problem and sometimes the restriction is so severe that the feasible domain is empty, i.e. no solution exists. As a result, uncertainty is accounted for in two ways, chance constraint and scenarios. For the scenario-independent decision variable, number of chargers X, we used chance constraints (2.15j). Note that this constraint is only lower bounded by one random variable $p^{p+}_{t,\omega}$, where the CDF can be modeled from measured charging station demand data. This chance constraint is reformulated into its deterministic counterpart following the procedure described above. For the remaining variables, we use a set of finite scenarios to capture the variety in charging demands.

The CDF of p^{p+} for different hours are shown in Fig.2.5. Each curve corresponds to a typical hour of the day. Throughout the day, higher power demands usually happen around

[5] The CDF can be modeled through empirical data.

10am-2pm; toward the night, the power demands decrease drastically, which correspond well with the school hours.

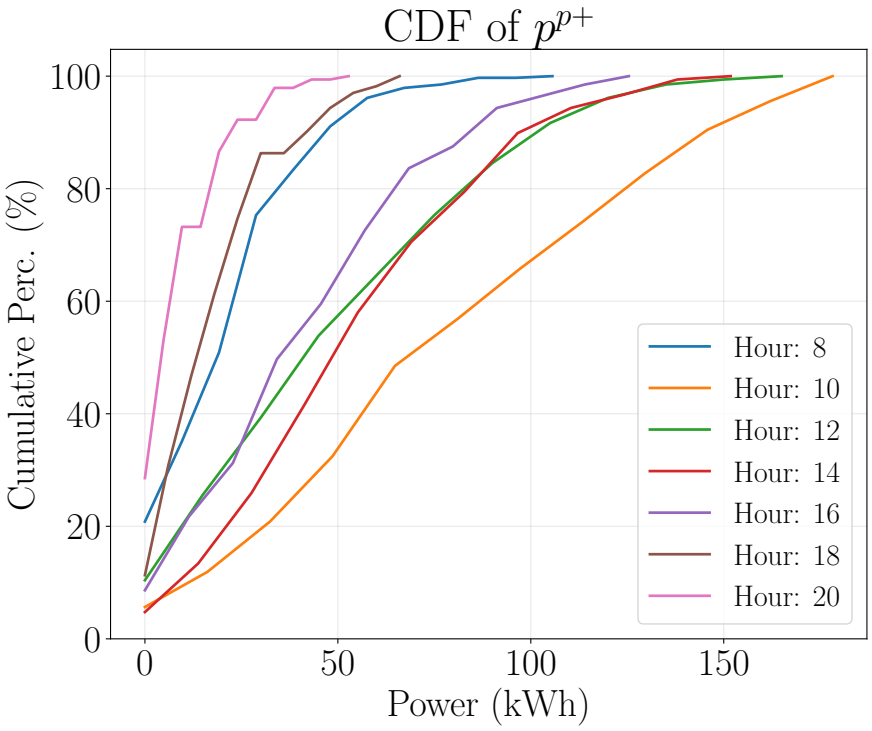

Figure 2.5: Cumulative Distributions of Power Upper Bound of Hour {8,10,12,14,16,18,20}.

2.8 Operation Model

Simulation to validate the performance of the planning results is included in Appendix B.3. This simulation is conducted at the real time operation level. We propose a rolling horizon based model [178, 189] with interchange mechanism. We choose to validate the setting from Case 4 (c^{ch} =\$4000, $c^{\text{itc}}_{\text{plan}}$ =\$0.003/kWh), which stresses the planning with minimum number of chargers. It will effectively push for more interchanges.

2.9 Numerical Studies

2.9.1 Parameter Settings and Case Overview

Data recorded at California Polytechnic State University, San Luis Obispo, California is used to verify the effectiveness of the proposed planning method. The time series data dates back to 2015 and we choose three complete calendar years 2016-2018 for this case study.

Regarding a small charging station, optimization is trivial and less useful. Therefore, we superimpose three years of data on one year, creating a "super" station with potentially on the order of 36 charging spots. We consider such a station large enough where optimal planning provides value. According to reference [2], we assume that one charger costs 4000 USD, including hardware material, installation, human labor, etc. We consider a charger lifetime of 15 years and discounted rate (refer to Eqn. 2.15c) of 6% [131]. The installed level-2 chargers are with $p^{\text{rated}} = 7.2$kw and $p^{\text{effi}} = 92\%$ [163]. Pacific Gas & Electric A-10, Medium General Time-of-Use Service is adopted as the time-of-use electricity plan.

Five cases are set up and compared with the real life scenario. Case 0 is the regular charging station planning where the overstaying issue and interchange mechanism are not considered. This is considered as the current practice. Case 1 and 4 capture scenarios at two ends. Case 1 ($c^{\text{itc}}_{\text{plan}} = \$0.3$/kWh [6]) represents one end, where the interchange mechanism cost mimic current practices in [84]; Case 4 ($c^{\text{itc}}_{\text{plan}} = \$0.003$/kWh [7]) represents the other end - a more futurist scenario, where interchange is performed a very low cost by, for example, a robot. The cost calculations are explained in detail in Appendices B.1 and B.2 respectively. Cases 2 and 3 are with interchange costs ($c^{\text{itc}}_{\text{plan}}$ =\$0.1/kWh and $c^{\text{itc}}_{\text{plan}}$ =\$0.05/kWh), which fall between Cases 1 and 4. The chance constraint captures the quantile of the extreme values, with $\epsilon = 0.5$ the median performance for the station. Then $\epsilon = 0$ designs the charging station with extreme robustness, even when encountering the day with the highest demand. We set $\epsilon = 0.1$ for better than median performance meanwhile avoiding overly conservative results. A sensitivity analysis in Section 2.9.2 examines different values of ϵ. Since the effective impact of the interchange mechanism is being examined, we specifically compare the capital investment cost (CAPEX) plus the interchange operational cost and unsatisfied demand costs (OPEX) across different cases. In Table 2.1, we calculate the portion of cost over the total investment process (CAPEX + OPEX, as illustrated above). The percentage values are included in the "$(\cdot)$" next to the numeric costs. Note, we have also specified the cost due to unsatisfied demands (penalty). The last column, "Cost Reduction", compares the cost savings among different cases relative to Case 0.

The number of chargers in Case 0, 36, aligns with the superimposed data. Trade-offs between installing more chargers to accommodate the demands or performing more interchange operation is also reflected in the table. As the interchange price decreases from Case 1 to 3, the portion of interchange operation costs increases. Meanwhile, the number of needed chargers and the corresponding investment cost decreases. This result clearly illustrates that the interchange mechanism is indeed useful for charging station planning. The mechanism effectively increases the chargers utilization rate, thus leading to less chargers. Comparing with the current practice (Case 0), the number of chargers decreases by a half, and the cost savings range from 20% to 50%. For Case 4, the number of chargers is equal to Case 3, reflecting that 18 chargers are the minimum number to ensure demand satisfaction - rather than sacrificing quality of service to lessen overall cost. Thus, further decreasing interchange

[6] See Appendix B.1

[7] See Appendix B.2

Table 2.1: Planning with Interchange Cost Saving Summary

Scenarios	Interchange Operation Cost [8]	Capital Investment Cost	Penalty (Unsatisfied Demand)	Chargers	Cost Reduction
Case 0	\$0 (0%)	\$14826.63 (100.0%)	0.0	36	0%
Case 1	\$745.14 (6.3%)	\$11119.98 (93.7%)	0.0	27	19.9%
Case 2	\$1504.06 (14.2%)	\$9060.72 (85.8%)	0.0	22	28.7%
Case 3	\$1882.30 (20.2%)	\$7413.32 (79.8%)	0.0	18	37.3%
Case 4	\$112.94 (1.5%)	\$7413.32 (98.5%)	0.0	18	49.2%

price only decreases the portion of the cost (20.2% to 1.5%).

2.9.2 Sensitivity Analysis

Sensitivity analysis among various interchange prices, charger prices and their influence on the cost is shown in Fig. 2.6. General trends are straightforward from the figure. When fixing one dimension, such as interchange price or charger price, and decrease the other, the total investment cost decreases. However, the trade-offs effect is also reflected from these two variables. For example, in cases (4000 USD/charger, 0.003 USD/kWh) and (3000 USD/charger, 0.44 USD/kWh), the total investment costs are \$7413.32 and \$8648.87. Decreased charger price with increased interchange cost could actually result in more investment for planning. Therefore, for the station operators, it is very important then to consider if installing more chargers (charger price is cheap) vs. providing better interchange service (interchange cost is cheap) to account for overstay PEVs. When the per unit interchange price is expensive (0.3-0.4 USD/kWh), but charger per unit price is cheap (500-1000 USD), then it is economical for the station operators to simply install enough chargers disregarding the interchange artifact. The same conclusion could also be drawn from Fig. 2.7. With some interchange, the total cost reduction of case (500 USD/charger, 0.44 USD/kWh) remains 13.9%. All of the other cases reach over 16.6% cost reduction. Cases without interchange mechanism are set as the comparison group. On the other hand, when the interchange per unit price decreases from 0.4 USD/kWh to 0.003 USD/kWh, increasing the charger per unit price from 500 to 4000 USD) will simply induce more interchange events and less chargers are installed. As shown in Fig. 2.7, the cost reduction increases from 14% up to 50%.

We choose to fix charger price at 4000 USD and vary the reliability factor ϵ and the interchange per-unit price to analyze the influence of robustness on overall capital investment. Fig. 2.8 shows the cost changes (%) across various ϵ and interchange price. Median value performance, $\epsilon = 0.5$ is chosen to be the base cases. The results show that chance constraint reliability factor ϵ also plays a significant role in overall cost performance. From the most conservative scenario to the median performance scenario, 14% of cost could be avoided. However, that may also lead to higher probability of charging congestion and lower quality of service. Thus, station operators should balance robust quality of service and capital investment cost when planning a charging station.

[8] *(·) indicates the portion of the cost over the total investment process (CAPEX + OPEX).*

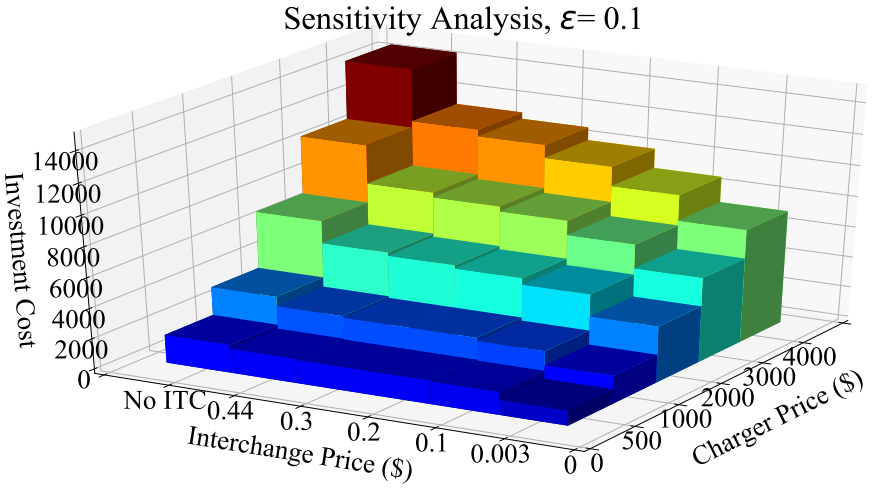

Figure 2.6: Sensitivity Analysis: ITC, Charger, Cost

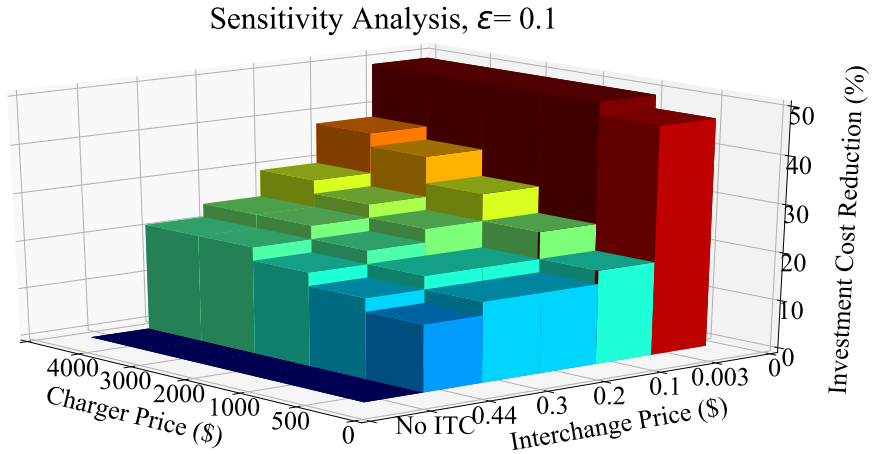

Figure 2.7: Sensitivity Analysis: ITC, Charger, Cost Reduction

2.10 Summary

In this chapter, we first identified the overstaying issue which severely harms charging station utilization in today's practice. We formally defined a mechanism to address the issue. Then we discussed a novel demand aggregate method to account for the overstaying problem and correspondingly proposed a planning model to increase charger utilization rate. Real data from Cal Poly San Luis Obispo campus has been applied to examine the model performance. The cost trade-off of various factors, i.e., interchange costs, charger costs, and reliability factor, have been examined. Planning results reflect that the interchange mechanism significantly reduces the needed number of chargers by having fully charged PEVs

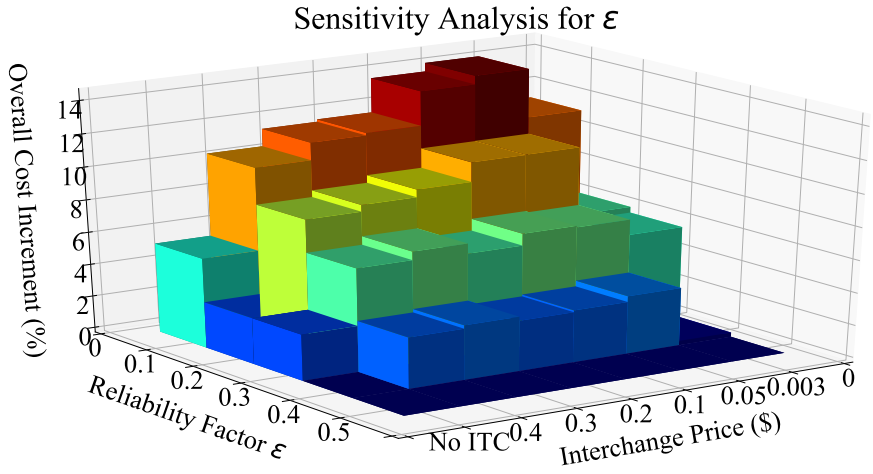

Figure 2.8: Sensitivity Analysis: ϵ, ITC, Cost Reduction

unplug to ensure charger availability. The capital investment costs are reduced accordingly. These findings provide an important perspective for reducing charging station operating costs, quality of service, and overall investments.

Chapter 3

Single PEV Charging Station Operation: User Choice Modeling and Differentiated Pricing

3.1 Overview

Plug-in electric vehicle (PEV) charging station service capability is physically limited by the charger availability and local transformer capacity. However, the station operation performance has become an increasingly important factor for enhancing charging service accessibility. In this work, we propose an innovative station-level optimization framework to operate charging station with optimal pricing policy and charge scheduling. This model incorporates human behaviors to explicitly and effectively capture drivers' charging decision process. We propose a menu of price-differentiated charging services, which differ in both the per-unit prices and the energy delivery schedule. Involving human in the loop, the operation model also exploits the capability to alleviate the *overstay* issue that occurs when a PEV's charging session has completed. We then propose a muli-block convex transformation methodology to reformulate the resulted non-convex problem via Fenchel-Young Inequality; the Block Coordinate Descent algorithm is applied to solve the overall problem and the efficiency enables real-time implementation. As a result, our simulation demonstrates that the proposed control polices can realize benefits in three aspects: (i) net profits gains, (ii) overstay reduction, and (iii) quality-of-service increase.

This work originally appeared in the following publication:

Zeng, Teng, Sangjae Bae, Bertrand Travacca, and Scott Moura. "Inducing human behavior to maximize operation performance at PEV charging station." *IEEE Transactions on Smart Grid* 12, no. 4 (2021): 3353-3363.

3.2 Relevant Literature

First, we provide a broad overview of PEV charging station operation. Then we examine literature on the overstay problem and human behavior, which are relevant to this manuscript's contributions.

Research on the operation of PEV charging stations can be generally organized into at least three different categories based on the system boundaries under consideration. Namely, from a broad to narrow perspective, these three categories involve (i) network level interactions with other systems, (ii) single station interactions with renewable energies, and (iii) single station operations without interacting with any outside resources. In category (i), the two interacting systems are the power system and transportation system. Charging stations serve as an intermediary agent that couple the transportation and electric grid networks and enable aggregated PEVs to participate in ancillary service markets [91, 157, 182, 188]. There are also extensive studies on the joint operation of coupled transportation-power networks [97, 184], whose objective is to simultaneously reduce congestion in both networks. For (ii), the operation problem typically involves power management of PEV charging, solar photovoltaic generation [165], and/or storage systems to enhance performance [32, 91]. In category (iii), the methodologies focus solely on single station operation: charging management, customer satisfaction, quality of service, etc. However, this body of literature rarely considers customer decision making. The operator-customer interaction is distinguished at levels of proactive vs. reactive. In reactive setting, the station operator manages charging with user experience taken into account, like [39]. In reference [39], charging costs and a so-called "user convenience factor" are simultaneously considered. The underlying assumption is that users would like their PEVs to complete charging as soon as possible. While this joint optimization model does enhance operation performance in minimizing users' wait times, it fails to optimally manage demand charge and acknowledge the overstay phenomenon. The overstay problem is further exacerbated as the station operator aims to complete charging as soon as possible. In the proactive setting, the station operator interacts with PEV drivers to influence charging decisions. Approaches include adding admission control upon drivers' arrival [153], introducing differentiated services and designing optimal pricing schemes [102], and this present work. The authors in [102] aim to design a menu of differentiated service options with service qualities tailored to customers. In their work, the authors propose optimal pricing and routing schemes with the focus of price-incentivizing PEV drivers to charge at designated sites to maximize social welfare. On the other hand, detailed charging operation is missing from this model and the overstay issue has been ignored. Another noteworthy difference is that in [102] the social operator tries to nudge potential customers to different stations, whereas our work incentivizes customers to different charging mode options at the station (to be defined concretely in Section 3.3.2). As a result, this present work aims to close the research gap in operating single charging stations by proactively interacting with customers.

Furthermore, overstay reduces station utilization and can lead to imbalanced charging demands across metropolitan areas throughout a day. Surprisingly, very few publications

have focused on this issue, in spite of the real world significance. The authors' previous study [175] introduces the idea of "interchange" operation which proactively unplugs fully charged PEVs. The study proposes a new station planning model as well as evaluates the financial burdens both to the station operator and the users. The other operation approach, which considers the overstay, is to explicitly apply an overstay penalty upon the complete of a charging session. The authors in [24] investigates the acceptance probability of such penalty, which is helpful in guiding the appropriate price settings. In 2018, a similar approach was adopted by Tesla Inc. to address this exact issue. They impose an "idle fee," which essentially is a penalty to users whose fully charged PEVs still remain connected [84]. However, the effectiveness of this penalty approach has not been studied and understood. On the other hand, in a philosophically similar line of work, the authors in [25] introduces the "deadline differentiated pricing" scheme to manage those deferrable loads. To this end, the customers are incentivized with a lower electricity price to defer their latest departure times, providing the station operator more charge schedule flexibility. However, this incentive system naturally increases the overstay, since the users are encouraged to occupy chargers longer. In this work, we address the overstay problem without a prior assumption such that deferring departure results in lower customer cost.

It is important to also recognize the "human-in-the-loop" dynamics that occur between the charging service provider and the customers (PEV drivers). When facing the need to charge, the customers must consider a parking spot availability, charger speed, prices for electricity and parking, overstay penalty, etc. The customers then decide whether to receive the charging service, and if so which service (if provided options). If the customers' decision making process is understood at the individual level, the station operators may strategically target charging prices to maximize profits as well as enhance overall station throughput. Human inputs can be significant, and there exists attempts to incorporate them into system operations, especially in the domain of Cyber-Physical & Human Systems (CPHS). In [14, 116], human inputs are modeled as system disturbances; in [106], humans are modeled as compliant agents; and in our previous work, humans are the system actuators [16, 17]. In [16], human behaviors are modeled from a new angle in the control system. The humans are regarded as amenable via designed incentives. We coin such systems as the "human actuated systems". We will adopt the same settings to incentivize customers to desired options.

3.3 Problem Overview and Behavioral Modeling

The motivating example from real world can again be referred to Chapter 2.3.

3.3.1 Definition and Evaluation of Overstay

Definition 3.3.1. *Overstay: The overstay duration is defined as the time duration after a PEV is fully charged but continues to occupy a charger* [175].

In this work, we propose to penalize the overstaying PEVs; however, the it is evaluated differently in the two charging options, i.e., *charging*-**FLEX** or *charging*-**ASAP** (to be defined in the next section). Upon arrival, the customer would first submit the needed energy and desired staying duration to the system. If *charging*-**ASAP** is chosen by the customer, the PEV would be penalized for overstay immediately after it is fully charged; on the other hand, if *charging*-**FLEX** is chosen as the service, then the penalty would not be applied until the stated parking duration. From the perspective of a charging service provider, it is beneficial to encourage the long-staying customers to accept the flexible charging option, since it draws economic benefits by strategically scheduling charging and avoiding heavy demand charges.

3.3.2 PEV Charging Station Operation

In this new PEV charging station framework, users are presented with three options upon requesting charging services. In this section we detail how each charging service is modeled. With following input information from user i: planned departure time, T_i, and desired energy requirement, $\mathrm{E}_i^{\mathrm{req}}$, station operator presents a pricing menu computed from the pricing policy controller (Fig. 3.1):

- *charging*-**FLEX**: z_i^{flex} and y_i^{flex}.
- *charging*-**ASAP**: z_i^{asap} and y_i^{asap}.
- ***leave***: $z_i^{\mathrm{leave}}(=0)$ and $y_i^{\mathrm{leave}}(=0)$.

We will formally introduce these three options, by describing the energy level evolution of the PEV with respect to each option.

charging-FLEX

In this service, user grants flexibility to the station operation, who may then control both charge schedule and rate. The station operator will ensure the needed energy delivered upon user's stated departure time (3.3). The PEV energy level constraints are defined as

$$e_{i,\tau_0} = 0, \tag{3.1}$$
$$e_{i,t+1} = e_{i,t} + \Delta t \cdot \eta \cdot p_{i,t} \quad \forall\, i \in \mathcal{A}_{\mathrm{flex}}, \tag{3.2}$$
$$\mathrm{E}_i^{\mathrm{req}} \leq e_{i,\mathrm{T}_i}, \tag{3.3}$$
$$0 \leq p_{i,t} \leq \mathrm{p}^{\max}. \tag{3.4}$$

charging-ASAP

In this service, no time flexibility is permitted. Thus, uncoordinated charging is performed by the station operator. The charging power is set to max throughout (3.6), until

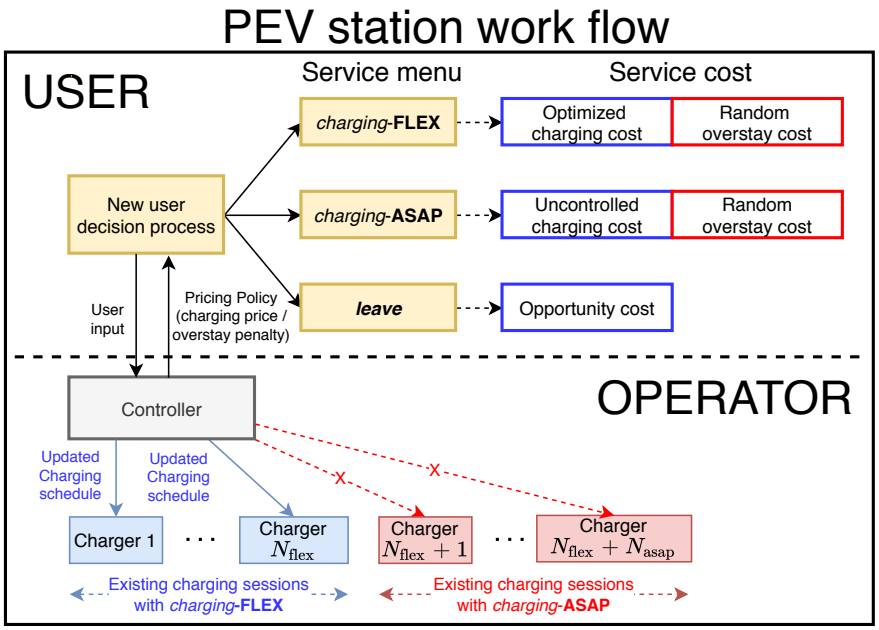

Figure 3.1: PEV charging station work-flow: how the station operator proactively interacts with the new users. The station-level controller not only proposes customized service tariffs, but also actively takes advantage of flexibility to adjust charge schedules of the existing *charging*-**FLEX** PEVs. The beauty of the proposed mechanism. An example of a station temporal status with respect to power, profit, cumulative services, etc., is presented in Fig.3.2.

the vehicle is unplugged or its battery is full (here we assume customers stay until their desired energy level is reached and the demand does not exceed the PEV battery capacity, i.e. $\mathrm{E}_j^{\mathrm{req}} \leq \mathrm{E}_j^{\mathrm{batt}}$). The constraints read

$$e_{j,t+1} = e_{j,t} + \Delta t \cdot \eta \cdot p_{j,t} \quad \forall\, j \in \mathcal{A}_{\mathrm{asap}}, \tag{3.5}$$

$$p_{j,t} = \mathrm{p}^{\max}, \quad \text{for } t = 0, 1, \cdots, \mathrm{T}_j \tag{3.6}$$

$$\mathrm{T}_j = \frac{\mathrm{E}_j^{\mathrm{req}}}{\Delta t \cdot \eta \cdot \mathrm{p}^{\max}}. \tag{3.7}$$

leave

User does not accept either proposed price set; thus leaves without charging. No state changes. However, the station operator is subject to service opportunity cost by losing one customer.

3.3.3 Discrete Choice Model (DCM) for Behavioral Modeling

From a system operator's point of view, each service alternative is associated with a specific operation cost (blue and red boxes in Fig. 3.1 next to the service menu). The effectiveness of capturing users' decision process dictates the service pricing policy. To quantitatively evaluate these behaviors, we adopt DCM model specifications in the preliminary version of this work [18]. In the model specifications, a charging price and overstay penalty are set as our control variables that adjust choice probabilities.

DCM is one of successful modeling techniques for analyzing human behaviors when their choice alternatives are limited to a discrete space. A representative model is "mulitinomial logit model" [96] which assumes each choice alternative is independent and choice probabilities follow a sigmoid function. We exploit this multinomial logit model in this study.

In DCM, the preference on each choice alternative is quantified by a utility function, and an alternative is chosen when its utility is higher than that of others. Formally, for the k-th alternative, $k \in \{1, 2, \cdots, K\}$, the utility function is

$$U_k \doteq \beta_k^\top z_k + \gamma_k^\top w_k + \beta_{0k} + \epsilon_k, \tag{3.8}$$

where z is the set of "incentive controls", w is the set of exogenous variables, β_k and γ_k are weights for the controllable inputs and uncontrollable inputs, respectively, β_{0k} is named the "alternative specific constant", and a latent variable ϵ_k accounts for any unspecified errors. In our context, the service prices and the overstay penalty are the "incentive controls"; time-of-the-day, parking duration, battery capacity, initial SOC, and needed energy are the exogenous variables. Interested readers can refer to [16] for details on human actuated system modeling.

The probability of alternative j chosen is captured with the multi-nomial logit model

$$\Pr\left(\text{alternative } j \text{ is chosen}\right) = \frac{e^{V_j}}{\sum_{n=1}^{M} e^{V_n}}, \tag{3.9}$$

where $V_j \doteq \beta_j^\top z_j + \gamma_j^\top w_j + \beta_{0j}$. Note that this model is non-convex in z and we will demonstrate how to address this particular issue in later sections.

Assumptions

[A1] All users follow the same behavioral model. They follow the same process in Fig. 3.1 when deciding on service options. This can be easily relaxed, by clustering users into archetypes, and then assuming each user falls within an archetype.

[A2] Three alternatives are probabilistically independent, a fundamental assumption of multinomial logit model.

[A3] At a time, each user chooses at least and at most one alternative among the three.

[A4] Each user is rational and selfish to maximize its individual utilities.

[**A5**] DCM parameters are deterministic, i.e., the system operator has collected sufficient observations on users' decisions to identify an accurate DCM.

[**A6**] Users' demographic information is unknown, i.e., only measurable data is utilized as attributes in the DCM.

Model Specifications for Charging Options

We collect Survey Preference (SP) data through 50 interviewees with the designed survey. The questions range from charging choices at specific scenario settings to user specific social-economic attributes. To highlight, they include initial energy level, energy need, staying duration, price, attitude toward sustainable energy, income, age, education level, etc. We then estimate the parameters with maximum likelihood estimation and the related tool, *pylogit* [30]. We also calculate the respective "p-values" for reference of statistical importance. As a result, *charging price* is identified as the statistically important incentive control input, and *initial energy level, energy need* as the statistically significant exogenous variables. This multinomial logit model is adopted to model drivers' decision process when designing the pricing scheme for the station operator. Note that this model specification relies heavily on the collected sample set. Relative to starting without any prior knowledge, this represents a reasonable starting point. In practice, as the station operator collects more user decision data, the model parameters may evolve and be updated.

3.4 PEV Charging Station Optimization Formulation

This section examines the mathematical foundations for the controller that finds optimal pricing and charging policies. Upon an arrival of a new user at the charging station, the controller finds new policies on real-time basis. We will start by describing overstay modeling.

3.4.1 Overstay modeling

"Overstay" is the amount of time the PEV blocks the charger after their charging session is complete. It's the period when a charging resource is wasted. We assume Poisson Distribution and model the overstay duration as random T^{overstay}. It is inversely dependent on the overstay price y. Consider a conditional probability model for overstay duration

$$\Pr\left(T^{\text{overstay}} = t \mid y\right). \tag{3.10}$$

Intuitively, as price y increases then the conditional probability distribution will shift toward shorter overstay duration. Then the expected revenue from overstay is

$$\Lambda(y) = y \cdot \mathbb{E}\left[T^{\text{overstay}} \mid y\right], \tag{3.11}$$

which has units of [USD].

3.4.2 Demand charge modeling

Demand charge is modeled by tracking the maximum total power consumption seen up to the current time. We use τ_0 to denote beginning of the control horizon ($\tau = \tau_0, \cdots, \mathrm{T_{end}}$), which is the current time index. This can be tracked with the following dynamics

$$G_\tau = \sum_{i \in \mathcal{A}_{\text{flex}}} p_{i,\tau} + \sum_{j \in \mathcal{A}_{\text{asap}}} \mathrm{p}^{\max}, \tag{3.12}$$

$$G_\tau \leq G_{\max}, \tag{3.13}$$

$$D_{\tau_0} = D_t, \tag{3.14}$$

$$D_{\tau+1} = \max\{G_\tau, D_\tau\}, \tag{3.15}$$

$$\mathrm{T_{end}} = \max\{\mathrm{T}_i \mid i \in \mathcal{A}_{\text{flex}} \cup \mathcal{A}_{\text{asap}}\}. \tag{3.16}$$

Eqn.(3.12) is the total station charging load including both services, *charging*-**FLEX** and *charging*-**ASAP**; Eqn.(3.13) limits the maximum power delivery of all time; Eqn.(3.14) records the previous peak power to initialize current control horizon; Eqn.(3.15) describes the peak power update dynamics and Eqn.(3.16) specifies the current control horizon length. Hence, we utilize this convex formulation to keep track of the peak power and later add to the station operation costs, in Eqn.(3.27) and Eqn.(3.32).

3.4.3 Optimization problem formulation

The overall objective of the station controller is to minimize the expected total cost (i.e. operational costs minus gross revenue), with quality of service (QoS) taken into account. The QoS is later evaluated through the number of fulfilled service as well as the overstay duration. The objective function reads

$$\min_{z,y,p} \quad \mathbb{E}\left[f(z, y, p, m)\right] \tag{3.17}$$

$$= \Pr\left(m = \text{flex}\right) f^{\text{flex}}(z^{\text{flex}}, y^{\text{flex}}, p^{\text{flex}}) \tag{3.18}$$

$$+ \Pr\left(m = \text{asap}\right) f^{\text{asap}}(z^{\text{asap}}, y^{\text{asap}}, p^{\text{asap}}) \tag{3.19}$$

$$+ \Pr\left(m = \text{leave}\right) f^{\text{leave}} \tag{3.20}$$

which is the weighted sum of revenue, over the control horizon, for each service option that the incoming vehicle might select. The weights, $\Pr(\cdot)$, are the probability of the user's selection. In addition, we must consider constraints for each service option

$$\text{subject to:} \quad \text{(constraints for Case 1: Flex, (3.1)-(3.4))}, \tag{3.21}$$

$$\text{(constraints for Case 2: ASAP, (3.5)-(3.7))}, \tag{3.22}$$

$$\text{(constraints for demand charge: (3.12)-(3.16))}. \tag{3.23}$$

Note that this optimization runs each time a new vehicle arrives and requests service. It's important to point out that the station optimization problem considers the new as well as the existing customers altogether. For existing *charging*-**FLEX** customers, the charging profiles will be re-evaluated to adapt to the new information and the changed environment. This will be jointly considered in Eqn.(3.18)-(3.20) when proposing price menu to the new customer. On the other hand, we do not make changes to the in-progress *charging*-**ASAP** customers.

Objective functions (3.18)-(3.20) will be expanded in the following sub-sections. Within a control horizon, we will use τ to index the rolling time step and keep t as the global time index.

Case 1: charging-FLEX

Provided with the two necessary information from the new user n, $\mathrm{E}_n^{\mathrm{req}}$ and T_n, we will consider the charging profile along with the existing customers

$$
\begin{aligned}
& f^{\mathrm{flex}}(z^{\mathrm{flex}}, y^{\mathrm{flex}}, p^{\mathrm{flex}}) \\
& = \sum_{\tau=t}^{T_n-1} (c_\tau - z_n^{\mathrm{flex}}) \cdot p_{n,\tau}^{\mathrm{flex}} \cdot \Delta t - \Lambda(y_n^{\mathrm{flex}}) && (3.24) \\
& + \sum_{i \in \mathcal{A}_{\mathrm{flex}}} \left[\sum_{\tau=t}^{\mathrm{T}_i-1} (c_\tau - \zeta_i) \cdot p_{i,\tau}^{\mathrm{flex}} \cdot \Delta t - \Lambda(\xi_i) \right] && (3.25) \\
& + \sum_{j \in \mathcal{A}_{\mathrm{asap}}} \left[\sum_{\tau=t}^{\hat{\mathrm{T}}_j-1} (c_\tau - \zeta_j) \cdot \mathrm{p}^{\max} \cdot \Delta t - \Lambda(\xi_j) \right] && (3.26) \\
& + c_D \cdot \left[D_{\mathrm{T}_{\mathrm{end}}^{\mathrm{flex}}} - D_{\tau_0} \right] && (3.27)
\end{aligned}
$$

subject to:

$$
\begin{aligned}
& \text{Energy constraints: } (3.1)-(3.4), (3.5)-(3.7), \\
& \text{Demand charge constraints: } (3.12)-(3.16), && (3.28)
\end{aligned}
$$

where $\hat{\mathrm{T}}_j = \frac{\mathrm{E}_j^{\mathrm{req}} - e_{j,t}}{\Delta t \cdot \eta \cdot \mathrm{p}^{\max}}$, is the updated departure time index from the remained needed energy of user j. In this choice, Eqn.(3.24) finds the optimal pricing and charging scheduling policy with given time-of-user electricity cost, c_τ. Eqn.(3.25) re-optimizes the charging profile for the in-progress *charging*-**FLEX** PEVs, with their already-determined prices. All of the PEVs with choice *charging*-**FLEX** are subject to the choice-specific constraints (3.1) - (3.4). However, we are restrained from optimizing for those in-progress *charging*-**ASAP** PEVs, which are thus modelled as uncontrollable loads with charging rate $\mathrm{p}^{\max}$, Eqn.(3.26). They are subject to constraints (3.5)-(3.7). The prices for all in-progress PEVs are locked down and fixed through their charging session.

Case 2: charging-ASAP

Provided the needed energy $\mathrm{E}_n^{\mathrm{req}}$ from the new user n, the controller then directly calculates the terminal charge time $\mathrm{T}_n^{\mathrm{asap}}$. If the user chooses this service option, their planned departure time will be enforced, i.e. $T_n = \mathrm{T}_n^{\mathrm{asap}}$. Then the revenue over the control horizon is

$$
\begin{aligned}
& f^{\mathrm{asap}}(z^{\mathrm{asap}}, y^{\mathrm{asap}}, p^{\mathrm{asap}}) \\
&= \sum_{\tau=t}^{\mathrm{T}_n^{\mathrm{asap}}-1} (c_\tau - z_n^{\mathrm{asap}}) \cdot \mathrm{p}^{\max} \cdot \Delta t - \Lambda(y_n^{\mathrm{asap}}) && (3.29) \\
&+ \sum_{i \in \mathcal{A}_{\mathrm{flex}}} \left[\sum_{\tau=t}^{\mathrm{T}_i-1} (c_\tau - \zeta_i) \cdot p_{i,\tau}^{\mathrm{asap}} \cdot \Delta t - \Lambda(\xi_i) \right] && (3.30) \\
&+ \sum_{j \in \mathcal{A}_{\mathrm{asap}}} \left[\sum_{\tau=t}^{\hat{\mathrm{T}}_j-1} (c_\tau - \zeta_j) \cdot \mathrm{p}^{\max} \cdot \Delta t - \Lambda(\xi_j) \right] && (3.31) \\
&+ c_D \cdot \left[D_{\mathrm{T}_{\mathrm{end}}^{\mathrm{asap}}} - D_{\tau_0} \right] && (3.32)
\end{aligned}
$$

subject to:

$$
\begin{aligned}
&\text{Energy constraints: } (3.1)-(3.4), (3.5)-(3.7), \\
&\text{Demand charge constraints: } (3.12)-(3.16). && (3.33)
\end{aligned}
$$

In this choice, Eqn.(3.29) aims to determine an optimal electricity price and overstay penalty for the new user. Since in the choice *charging*-**ASAP**, PEVs are delivered with full power at all time, the station operator does not optimize the charging profile in Eqn.(3.29). Hence, together with the existing *charging*-**ASAP** PEVs, their choice-specific energy constraints are all subject to (3.5)-(3.7). Similar to the other charging option, station operator is still able to re-optimize the charging scheduling profiles for the existing *charging*-**FLEX** PEVs to ease out the overall station-wide loads.

leave

We quantify the opportunity losses due to a leaving customer who chooses not to charge at the station. The reasons include but not are limited to unsatisfying charging prices, high penalty of overstay, etc. We leverage this option with the associated cost mainly to prevent generating unreasonable prices that drive away the customers. To keep the formulation of the entire objective function multi-block convex, this opportunity cost is computed as follow

$$
f^{\mathrm{leave}} = \sum_{\tau=t}^{T_n^{\mathrm{asap}}-1} (c_k - 0) \cdot \mathrm{p}^{\max} \cdot \Delta t. \tag{3.34}
$$

From the station operator perspective, this is essentially the cost of uncontrolled charging [1].

3.5 Reformulation into Multi-convex Problem

It is important to point out that the original form of the problem cannot be solved efficiently with standard off-the-shelf solvers. This is due to the highly non-linear and non-convex structure of the model structure (Eqn.(3.17)). We propose a transformation methodology to yield a three-block multi-convex structure. The resulted reformulation is then solved efficiently via Block Coordinate Descent (BCD). This reformulation process and proof are detailed in the Appendix C.1.

3.6 Numerical Studies

3.6.1 Scenario overview

Input Data Overview

For a case study, we consider a real-world dataset from the PEV charging station at the Cal Poly San Luis Obispo campus in California. The data represents a charging demand (a total of 201 charging events) over a week from Jan. 16th to 23rd, 2019. In the dataset, the parking duration is 3.25 hours on average, while the charging duration is 2 hours on average. That is, 38% of the parking duration is the overstay.

Time-of-Use Price

We adopt the Pacific Gas & Electric A-10 Medium General Time-of-Use service [123] for the price.

Parameter Settings for a Charging Station

The parameter settings of a charging station are as follows: a number of charging poles (8 [EA]), maximum charging power at each pole (7.2 [kW]), and operation hours (from 7 am to 10 pm).

The general behavior tendencies reflected from the DCM model include (i) the higher the per-unit electricity prices imposed to customers, the more likely they tend not to charge but leave; (ii) the more energy the customers need, the more likely they tend to charge (iii) the longer the customers tend to stay, the more likely they tend to charge and they tend to choose *charging*-**ASAP** by default to maximize their own convenience.

[1] Note that, it's not the focus of this paper how to capture the opportunity cost due to loss of customers. The purpose here is trying to properly capture as many customers as possible and thus to maximize station operator's profits.

3.6.2 Results and Discussion

For one day operation, a set of charging events (a total of 50) is sampled from an empirical distribution of charging events generated from the dataset. With the perceived utility, which depends on the charging prices and the overstay penalty, a user makes a decision to whether charge or leave, and which service if to charge. Both the charging price and overstay penalty are optimally determined online by the pricing controller. We first present an overview of the results in Fig. 3.2, which demonstrates a temporal profile for one episode of the charging station's power profile, net profit, overall occupancy, accumulated overstay duration, and the number of PEVs served. Note that the values of net profit, overstay duration and number of service are all accumulated over time. Subsequently, we will break down details including the real-time variations of the optimal prices (Fig. 3.3) and the resulting variations of the user decision process (Fig. 3.4). To concretely quantify the performance of the station controller, we considered three metrics: (i) overstay duration, (ii) total net profit, and (iii) quality-of-service, measured by the number of PEVs served (Fig. 3.6). We have also observed the effectiveness of peak power management at the station level in Fig. 3.7. Lastly, a sensitivity analysis is conducted on how station size impacts the total profit and the QoS (Fig.3.8).

Figure 3.3 illustrates the trajectories of charging prices and overstay penalty based upon TOU price. Note the optimizer heavily discounts *charging*-**FLEX** relative to *charging*-**ASAP** when customers stay through the peak hours (12:00-17:00), when the TOU price is high. For example, a customer arrives at 10 am, and the price for *charging*-**FLEX** is \$0.26/kWh – more than 51% discount than *charging*-**ASAP**. This incentivizes the customer to select *charging*-**FLEX**, which grants charging flexibility to the system operator to minimize power and consequently cost during the peak TOU period.

Figure 3.4 presents how the probability of choice alternatives varies over time. The users' utility functions are subject to factors like price variations, needed energy, stated duration, etc. Recall that the users are set to have the natural tendency toward *charging*-**ASAP** over *charging*-**FLEX**, whereas we observed in Fig. 3.4 that this tendency can be influenced using the controller's price incentives. Hence, more *charging*-**FLEX** choices are chosen, which provides the station operator with power management opportunities, in spite of the lower revenue from charging.

We also carry out a Pareto analysis to better understand how to set overstay penalty. This analysis also helps elucidate the relationship between the overstay penalty, the needed energy, and the stated parking duration (Fig. 3.5). The major finding here is the linear relationship (with $R^2 = 0.265$) between the overstay penalty and the combination of the needed energy and the stated duration. That is, when a small amount of energy is requested along with a short stated parking duration, the overstay penalty is relatively small. In contrast, when both the requested energy and the stated parking duration is high, the overstay penalty is relatively large. This is an interesting consequence that is aligned with what we can expect from the real world. When the user stays at a charging station for only a short period, it is more aware of the time, as the person needs to leave soon. Therefore, the overstay penalty is less powerful in incentivizing the user to leave on time.

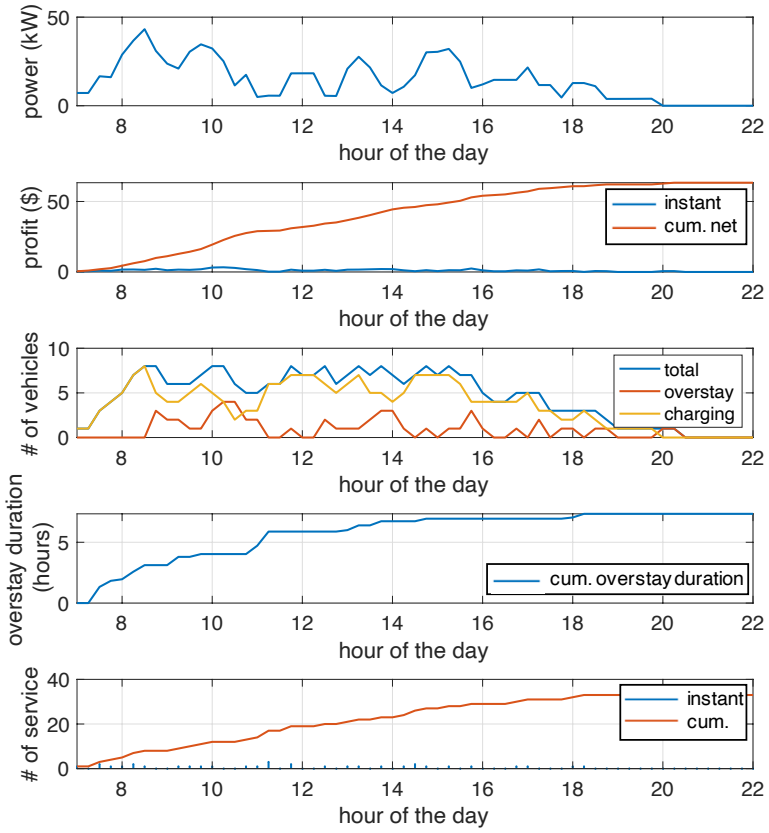

Figure 3.2: One-day operation result with the controller for eight charging poles. The profiles represent aggregate values over all charging poles.

We use a Monte Carlo simulation to quantitatively validate the performance of the proposed price control. Figure 3.6 reports that the overstay duration decreases by 41.08%, the net profit increases by 37.84%, and the number of served events (QoS) increases by 17.45%, compared to basecase which is without the pricing control [2]. Due to an adjusted overstay penalty, the users tend to leave soon after their charging session completes to avoid the penalty. The decrease in the overstay duration allows the charging station to accommodate more charging sessions and, consequently, yields the increase in net profit.

Lastly, we compare the effectiveness of the proposed station-wide optimization approach in power management compared to a single-charger optimization approach in [18], as shown in Fig. 3.7. We observed that power management across all charging poles (in which power

[2]Note that the choice option of ***leaving*** does not exist in the baseline. Hence, the baseline is inherently able to provide a charging service when a charging pole is empty.

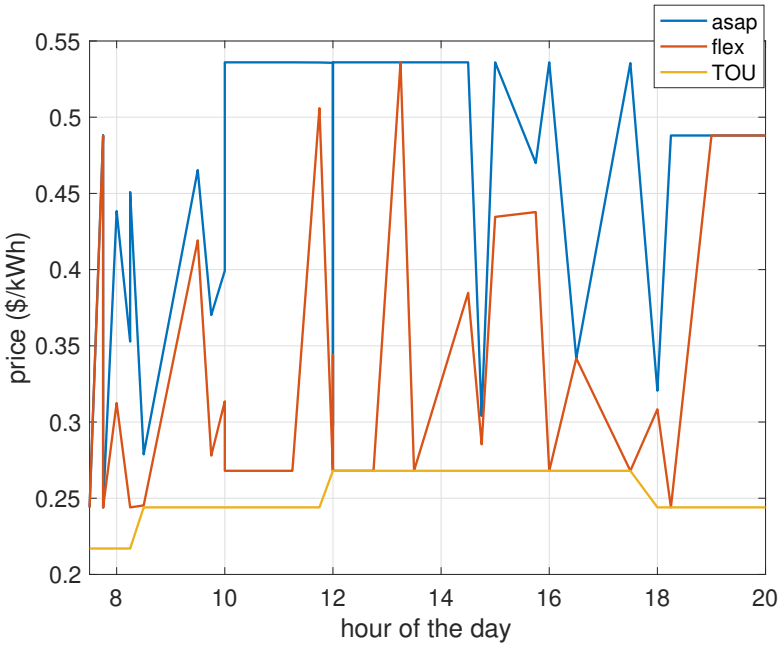

Figure 3.3: Optimal pricing policies over time and Time-of-Use price.

rate is controllable) results in reducing the peak power (24.6% against single-charger optimization approach), which yields a decrease in demand charge costs. It's interesting that the lowest peak power is actually observed in the baseline case (i.e., without the price controller). However, as a result, the profit made by the operator is minimal (Fig. 3.6), and higher costs may be translated to its customers. With the decrease in maximum power usage, the system operator can avoid investing in upgraded local transformers. That is, the capital cost of installing more charging poles and upgrading the station can be saved by managing the power profile.

3.6.3 Sensitivity Analysis

We conduct a sensitivity analysis on the total profit while varying the number of charging poles. Figure 3.8 illustrates how the total profit is segmented by charging service profit and overstay penalty (top) and how the quality of service varies (bottom).

There are two points to highlight from the top plots in Fig. 3.8. First, overstay revenue is greater with incentive control than without, since the controller is explicitly increasing the overstay penalty to turnover PEVs and increase utilization. Second, compare the total profits with and without incentive control. For a small number of poles, incentive control provides a greater profit. The reason is there exists more PEV charging demand than poles, creating congestion which is managed by incentive control. When a sufficient number of poles exist, there is no PEV charging demand congestion and thus pricing and charge scheduling does

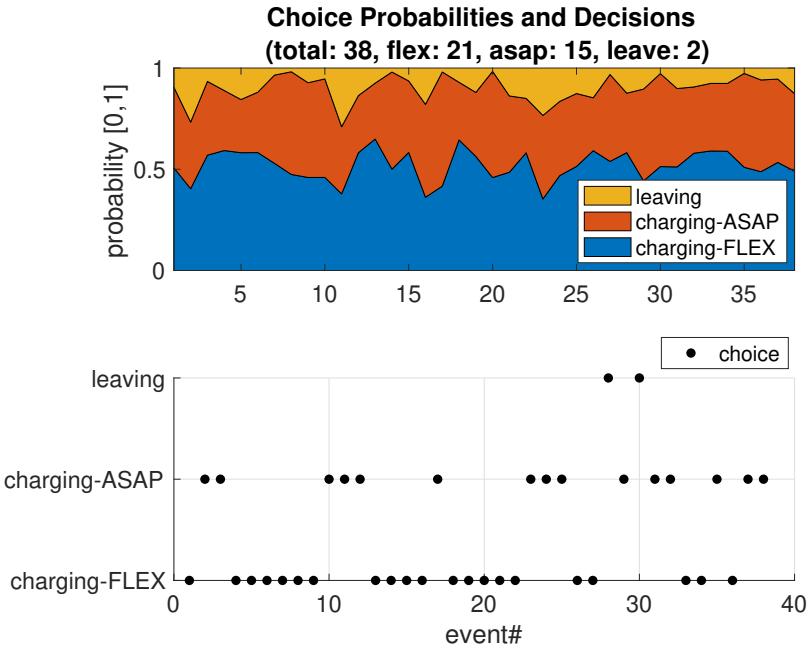

Figure 3.4: Probability distribution over choice alternatives over events (top) and corresponding choices (bottom). In top plot, each area represents the probability of choosing each alternative.

not increase profit. In fact, the overstay penalty can induce PEVs to leave, thus creating lost revenue.

Similarly, the bottom plot in Fig. 3.8 illustrates how the quality-of-service varies with a different number of charging poles. In general, the incentive control enables more charging services that a station can provide. The improvement mainly comes from the reduced overstay duration which frees the (formerly) occupied capacity to accommodate additional charging requests. However, as the number of poles reaches 17, the QoS is out-performed by the baseline. This is due to a saturation effect that most of the demands have been successfully fulfilled by the system operator (*leaving* is not considered as an option in the baseline). On the other hand, the benefit of proper management compensates the leaving loss by reducing overstay duration of existing customers and accepting new ones.

In summary, the qualitative and quantitative analyses show that (i) the incentive control has a strong potential in reducing overstay duration and securing additional profit as well as a curtailed peak power; (ii) incentive control achieves a higher level of quality-of-service. These benefits degrade as the number of poles increase relative to demand. Hence, we expect these findings to further help infrastructure operators at the network planning stage, e.g. smaller station configurations can avoid excessive capital investment costs.

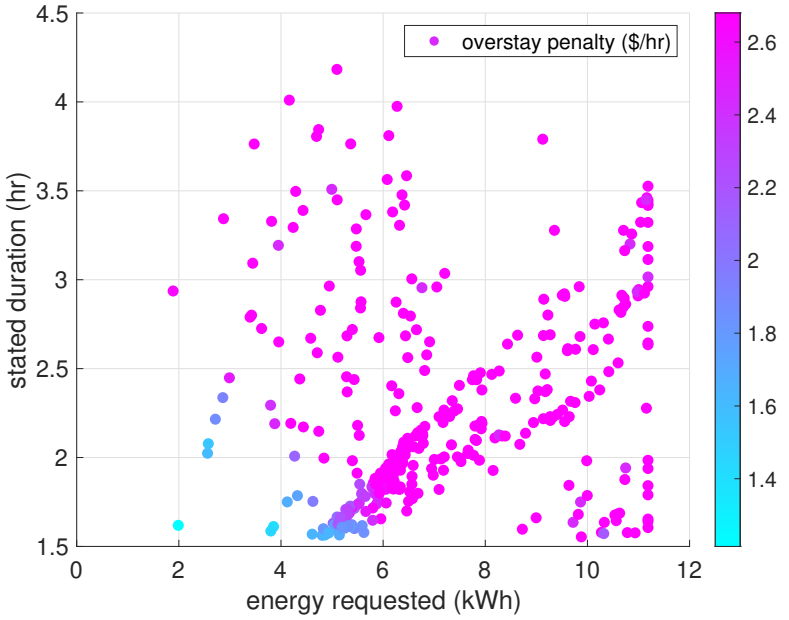

Figure 3.5: Overstay associated with (requested energy and stated parking duration). The color of dots indicates the magnitude of the overstay penalty.

3.7 Summary

This chapter explores a mathematical framework to optimally operate a charging station with distinguished charging service options. Due to the nonconvexity and complex problem structure, we reformulate an equivalent multi-block convex problem, which can be solved efficiently through the Block Coordinate Descent algorithm. The simulation results demonstrate high potential of the model for alleviating the overstay duration, increasing net profit, and providing additional charging services with a given number of charging poles.

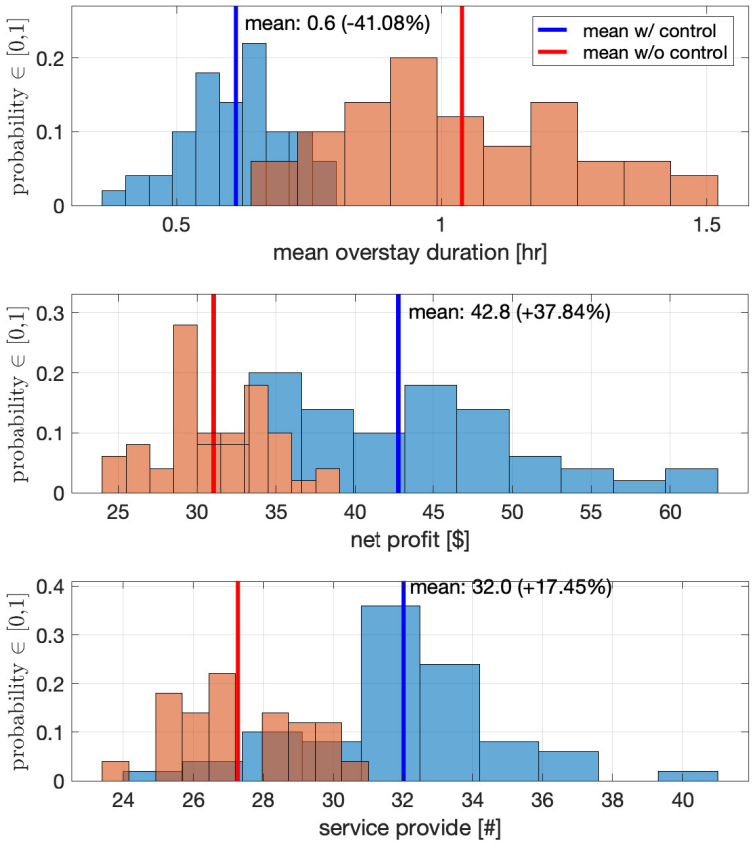

Figure 3.6: Monte Carlo simulation results with 30 samples. Each sample indicates each day. The total charging requests per day are set to 50. The values in parenthesis indicate relative improvements from using the proposed optimal policy compared to nominal policy without optimization. Since the overstay duration is targeted to reduce, negative improvements indicate a positive impact.

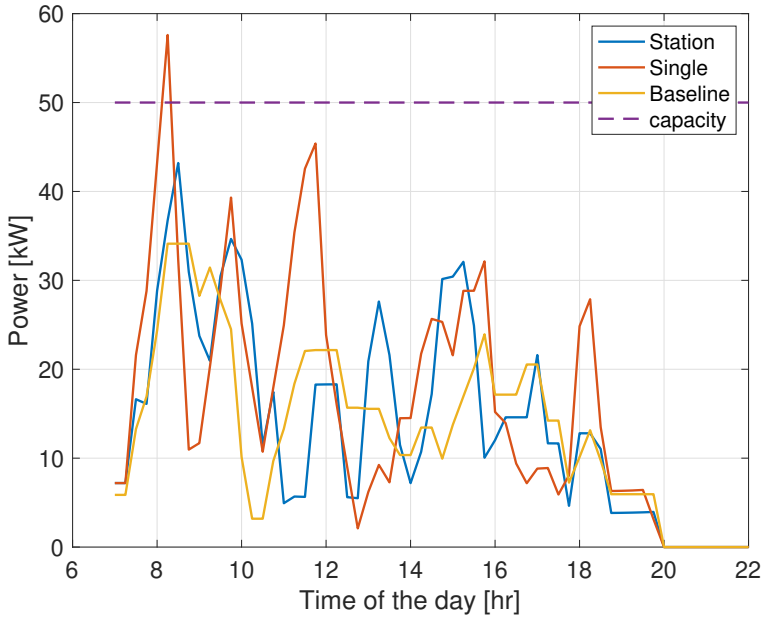

Figure 3.7: Power profile optimized by station-wide optimization (labeled as "station"), compared to single-charger optimization (labeled as "single"). The power profile optimized with the single-charger violates station power capacity (labeled as "capacity"), whereas the station-wide optimization successfully ensures power is bounded below the capacity.

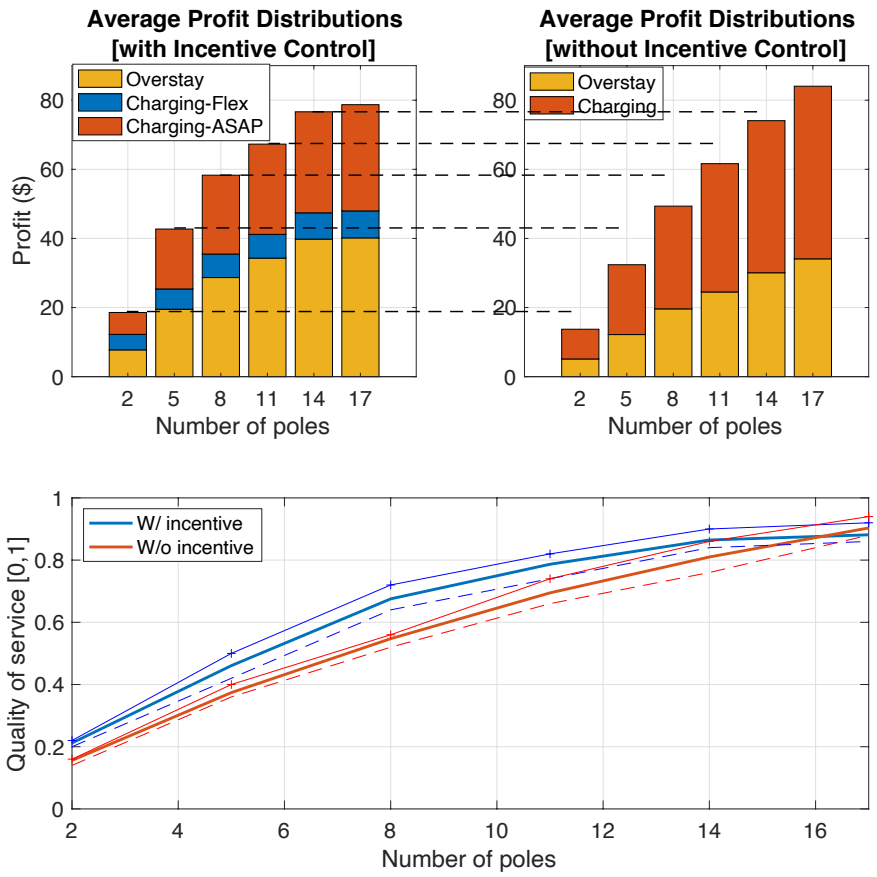

Figure 3.8: Sensitivity analysis by varying the number of charging poles: the composition of profit with incentive control (top left) and without (top right); the quality of service (bottom). Without incentive control, i.e., baseline, *charging*-**FLEX** is not available. In the bottom plot, the solid line with "+" indicates the upper error bound and the dashed line indicates the lower error bound.

Chapter 4

Charging Infrastructure Network and Mobility: Cargo Movement

4.1 Overview

This chapter proposes a new modeling framework for jointly optimizing the charging network design and the logistic mobility planning for an electric vehicle fleet. Existing literature commonly assumes the existence of a single entity – the social planner, as a powerful decision maker who manages all resources. However, this is often not the case in practice. Instead of making this assumption, we specifically examine the innate non-cooperative nature of two different entities involved in the planning problem. Namely, they are the charging service provider (CSP) and the fleet operator (FO). To address the strategic interaction between entities, a bi-level mixed integer program is formulated, with the CSP/FO's problem expressed in the upper/lower levels respectively, in a joint decision making process. These decisions involve the CSP's infrastructure siting, sizing, substation capacity upgrades, the FO's fleet composition, vehicle routing, charging, and delivery assignment. To solve the problem, an iterative fashion is adopted to solve and reach optimality. We conduct detailed numerical studies on a synthesized small network and the simulation results reveal the unique aspects of this two-entity framework. This modeling perspective can be generalized to other system design problems with two interacting agents planning and operating resources across networks.

This work originally appeared in the following publication:

Zhao, Yiqi*, Teng Zeng*, Zaid Allybokus, Ye Guo, and Scott Moura. "Joint Design for Electric Fleet Operator an Charging Service Provider: Understanding the Non-Cooperative Nature." Early access on *IEEE Transactions on Intelligent Transportation Systems*. (*equal)

4.2 Introduction

Decarbonization of the transportation sector is an important step toward alleviating climate change. In the U.S., about 28% of the total greenhouse gas emissions is contributed by transportation [154]. According to the California Air Resources Board (CARB), commercial trucks are responsible for 80% of the diesel soot emitted, leading the largest source of air pollution from vehicles [65]. Hence, a significant step to cut emissions is electric commercial vehicles, specifically E-trucks, as part of a sustainable supply chain. As a result, CARB has voted to rule out the sales of any fossil fuel trucks by 2045 and to force truck makers to begin the transition in 2024 [65].

Along with enforcing policy orders, many logistic and delivery companies (we refer to as fleet operators, FOs) and Charging Service Providers (CSPs) are committed to transportation electrification. To realize profit maximization, it is more important to have effective communications between these two entities. The CSPs, with knowledge of spatial-temporal charging demands, could strategically construct their charging network to accommodate the needs; whereas the FOs, whose electrified trucks are constrained by driving range, would consider charging en-route but with minimal detours.

4.3 Relevant Literature

In this section, we are going to review a body of literature that we have identified as not only relevant but also crucial to understand our problem. On one hand, to consider commercial E-trucks routing, a portfolio of attributes can be considered, including *homogeneous/heterogeneous fleet, range, partial/fully charging time, delivery time windows, etc.* On the other hand, to consider charging infrastructure planning, another set of attributes are considered, such as *the station locations, power constraints, etc.* The two entities, FO and CSP, are entangled through charging events and an extensive body of literature ([71, 72, 92, 93, 126–128, 166, 170]) has accounted for this interactions. In the field of Operation Research and Electrical Engineering, this is called the electric location routing problem (E-LRP), an extension to pure electric vehicle routing problem (E-VRP). For the classical vehicle/location routing problems, we refer interested readers to these two survey papers [120, 129].

In the aforementioned literature, each work varies focus slightly and considers a subset of the above entity-specific attributes. J. Yang and H. Sun [166] were the first to investigate the E-LRP, where the location of battery swapping stations (BSS) was jointly optimized together with the routing of a homogeneous E-trucks fleet. The computational results of the work were later improved by Hof, Schneider and Goeke [72]. M. Schiffer et al. conducted a series of research on E-LRPs. Each publication in this series has a different focus. For example, [126] incorporated real-world data to address the competitiveness between E-trucks and ICEVs, [92, 127] considered deployment of multiple types of facilities (replenishment, recharging, and combined type facilities), [93] addressed uncertainty using robust optimization , [128]

used different planning objectives. Authors in [170] further considered multiple types of charging facilities in E-LRP with time windows (E-LRPTW). Paper [71], on the other hand, investigated the effects of heterogeneous fleets on a similar E-VRPTW setting with a full recharge scheme. These works inevitably assume the existence of a powerful social planner, who is capable of coordinating all the tasks. However, this is often not possible in practice. Instead, the FO and the CSP are more likely to be separate organizations with misaligned incentives, leading to non-cooperative behavior. Such interactions exist in other domains, power system transmission expansion [187] , distribution system and demand response [15], food products supply chain [149], forestry and biofuel supply chain [172]. In the EV domain, a recently published paper [173] discussed a Stackelberg game setting for the private electric vehicles, in which charging facility locations, capacities and prices were the main focuses. However, the routing decisions for delivery, the charging schedule, the time windows are outside of their scope. Reference [6] included both the charging station siting and fleet sizing decisions, but a single planner was assumed. In this work, we specifically capture these dynamics and model it as a leader-follower Stackelberg Game, which to the authors' best knowledge, has never been studied.

Furthermore, the modeling approaches in the above works closely resemble each other and are the natural stems from the classic traveling salesman problem (TSP). The abstracted network is often called the customer-node based network, where customer nodes are the graph representatives and constrained to be visited once and exactly once. Additional features like range limits and charging speed for E-trucks are easily incorporated via supplemental constraints.

On the other hand, while the customer-node based network is classic and easy to adopt, the shortfall is prominent - lack of flexibility in tracking temporal events, such as charging. Since every node is associated with one specific set of entry and exit times for one vehicle, the temporal sense of simultaneous visits or queuing at a charging station node is dismissed. Adding trackers, e.g. indicator functions, is inevitable to address this issue. However, this makes the problem highly nonlinear and hence the solution quality cannot be guaranteed. Alternatively, references [90, 95] adopted the idea of layered graphs and proposed state-space-time/resource-space-time expanded networks to embed discretized resource values (energy consumption, time, etc.) when defining nodes. In this case, resource constraints are directly encoded in the expanded network model and time-dependent consumption patterns can be characterized. However, such modeling flexibility comes at a cost of significantly increased network size, and subsequently the problem scale. To plan a charging network, authors from [183] took a macroscopic point of view with traffic flow and designed another way to expand the transportation network. In this network, all reachable nodes are extended with hyper-arcs to model EVs' feasible routes. Then, a joint fleet sizing and charging system planning method for autonomous electric vehicles was proposed. However, the core, which is the extended network, requires full recharge and predefined homogeneous battery capacities. Recently, the authors of [81] introduced a novel mixed integer linear programming model for the E-VRP with load-dependent charging patterns. The proposed formulation allows multiple visits of charging stations without expanding the network into higher dimensions, thus helping

Table 4.1: Overview of considered aspects in existing literature

Ref.	View-point	Fleet Design	CS* Design	Charging Option	Logistic Cons.	TW*	CS Cons.
[71]	FO*	heter	×	Fully	✓	✓	×
[81]	FO	×	×	Partial	×	✓	×
[31]	FO	×	×	Fully	×	✓	✓
[93]	SP*	homo	site	Partial	✓	✓	×
[166]	SP	×	site	Fully	✓	×	×
[90]	SP	×	site	Partial	✓	✓	×
[183]	SP	homo	size	Fully	×	×	✓
Our	Multi-players	heter	site +size	Partial	✓	✓	✓

* CS: charging station; TW: time window at customer points; FO: fleet operator; SP: social planner.

to reduce the problem scale. Although this approach neatly relaxes the aforementioned restriction, it cannot be directly applied to a setting where locations of charging facilities are unknown. To conclude, though charging station location planning for E-trucks has been studied, incorporating station size and capacity upgrade remains as gap in this field of research.

We have reviewed a series of literature and identified the remaining gaps in the community. In Table 4.1, we summarize the aspects covered by some representative works and compare with ours.

4.4 Problem Definition and System Model

The overall goal of this paper is to optimally design the E-truck fleet composition and associated charging station network. Specifically, a charging service provider decides where to locate new CSs among candidate locations. Additionally, the number of charging ports and substation capacity upgrades (size configurations) are optimized. A fleet operator designs the portfolio of fleet vehicle types, and the optimal routing and charging strategies to deliver customer demands within given time windows while avoiding battery depletion. In this section, we define the problem and present the intuitive illustration to our proposed model.

4.4.1 Problem Description

The problem is defined on a directed graph $\mathcal{G} = \{\mathcal{E}, \mathcal{V}\}$, where $\mathcal{E}$ is the set of all edges[1] and $\mathcal{V}$ is the collection of all nodes. Specifically, nodes in $\mathcal{V}$ are categorized into three different types: a depot node D_0, customer nodes $\{C_1, C_2, ..., C_n\}$ in set $\mathcal{C}$, and candidate charging station (CS) nodes $\{F_1, F_2, ..., F_m\}$ in set $\mathcal{F}$. Successive visits of nodes are represented with chosen edges. This is the aforementioned *customer-node based network*. We assume the following common rules: [2]:

[**A1**] All customer nodes are visited once and only once by one vehicle during one duty cycle.

[**A2**] All E-trucks depart from the depot D_0 and return to the same depot after completing the assigned logistic tasks.

[**A3**] Customer demands are represented in the aggregate sense with real values and without specifications, e.g. weight, size, or shape.

An illustrative network and toy example is given in Fig.4.1. One depot D_0, two customer nodes C_1 and C_2, and one charging node F_1, dashed lines indicate feasible links. Assume there is an E-truck with a driving range of 4 units of length. One possible route is colored in red with arrow directing its trajectory: the E-truck will first make a stop at C_1 due to given time window [1,3], then recharge at F_1 and go to C_2, whose latest required arrival time is 5. Upon task completion, the E-truck will make a return to D_0. Alternatively, the feasible routing plan can be chosen as $D_0 - C_1 - D_0$ and $D_0 - C_2 - D_0$. Hence, recharging is not required, but two E-trucks are needed to fulfill the task.

In this model, every time index is inherently associated with the node. We loose information to concurrent charging sessions when multiple E-trucks are traversing on the graph. Hence, the model is unable to consider configurations of the charging infrastructure, i.e. the number of ports and transformer upgrades. A work-around is introducing indicator functions to determine specific charging periods; or full state-space-time layered graph is used (Section 4.3). Both approaches either impose nonlinearities or severe scaling issues (number of nodes and links explodes). In the next subsection, we propose a different graph expansion approach to capture the time information neatly.

4.4.2 Proposed Model: Partial Time Expanded Network Model

We propose to encode the time expansion solely on the charging station nodes, avoiding other unnecessarily added nodes. Namely, this is a partial time expansion. Each original candidate CS node $F_i \in \mathcal{F}$ is expanded across time and charging ports. A two-dimensional time-port graph (Fig.4.2) is introduced to represent a candidate CS node. Altogether, $|\mathcal{T}_i| \cdot |s_i|$

[1] We will use edge, link, and arc interchangeably.

[2] Background on the vehicle routing problem and its common formulations can be found in [58, 71, 72, 92, 93, 126–128, 166, 170].

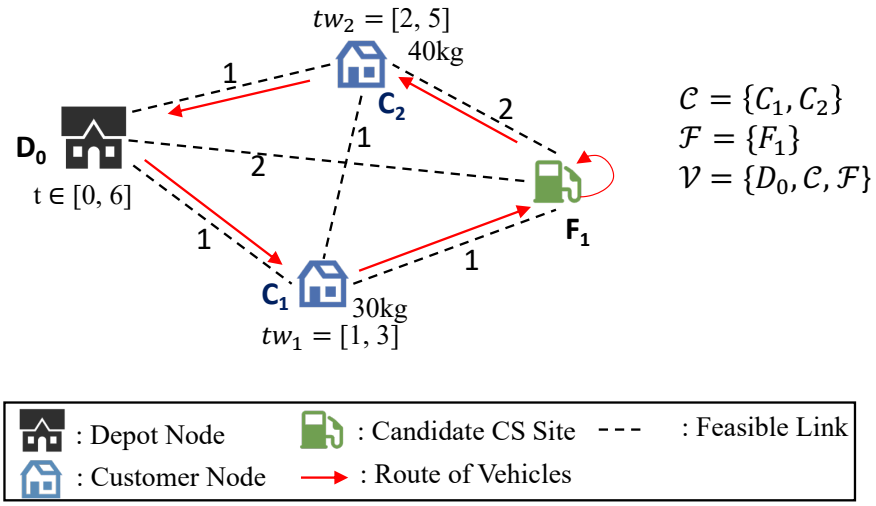

Figure 4.1: Illustrative network.

dummy nodes[3] are introduced to represent node F_i, where $|\mathcal{T}_i|$ is the time horizon (i.e. the number of feasible visiting time slots at F_i) and $|s_i|$ is the CS size (i.e. the number of charging ports). Each of these nodes, as shown in Fig.4.2, encodes two index trackers: the time availability index $t(\cdot)$ and the charging port index $p(\cdot)$. We denote a set $\mathcal{M}_i$ to represent these expanded nodes.

We have defined nodes and now will construct feasible links between nodes within this set $\mathcal{M}_i$. A link from node j to node m, $\{j, m \in \mathcal{M}_i\}$, is created if $t(m) - t(j) = \Delta t$ and $p(m) = p(j)$, indicating an E-truck charges at port $p(j)$ for one time step (Δt) starting at $t(j)$. We denote the set of all internal links at station node F_i as $\mathcal{A}_i$. A subset of time specific links is defined as $\mathcal{A}_i(t) = \{(j, m) \in \mathcal{A}_i \mid t(j) = t, t(m) = t + \Delta t\}$. The original links connecting between customer nodes and the station nodes are reconnected accordingly. With this expansion, real time charging power at station F_i can be easily computed by counting the number of traversed links in $\mathcal{A}_i(t)$. Take the case in Fig. 4.2 as an example, the connection represents that E-truck 1 charges during period $[2, 4]$ and E-truck 2 charges during $[3, 5]$. Hence, at least two chargers are needed as both E-trucks are present during time $[3, 4]$ (box color coded).

A copy of the depot node is also created as the sink node D_0' (due to assumption [**A1**], this is a common practice). A corresponding partial time expanded network is presented in Fig.4.3. The charging activity at F_1 is then modeled by the link $(F_1 - 1 - 2, F_1 - 1 - 3)$.

We will denote the expanded network as $\mathcal{G}^{PTE} = \{\mathcal{E}^{PTE}, \mathcal{V}^{PTE}\}$. Formal notations are summarized in Table 4.2, but relevant sets are also given in Fig.4.1 and Fig.4.3. We present

[3]We will use dummy nodes, dummies, and virtual nodes interchangeably.

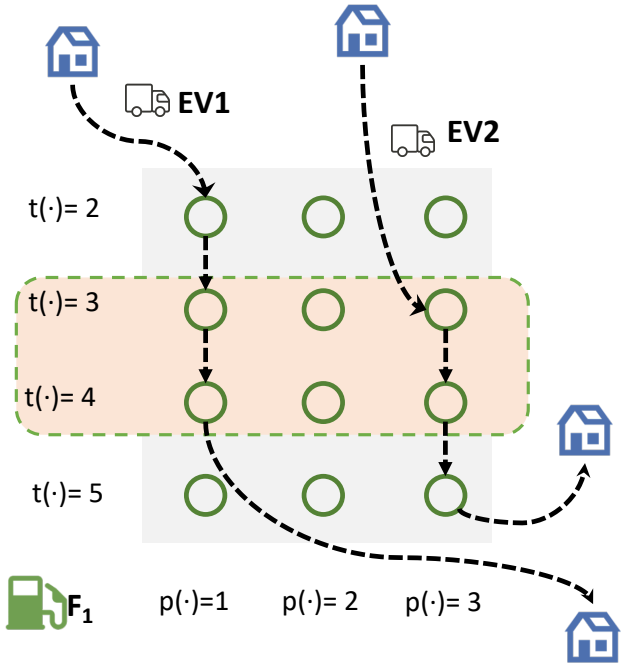

Figure 4.2: An example for a partial time expanded charging station.

the nomenclature in Table 4.3 and are now ready to formally introduce the planning problem formulation in the following section.

Table 4.2: Nodes and links before and after network expansion

Network	Nodes
$\mathcal{G}$	$\mathcal{V} = \{\mathcal{D}_0, \mathcal{C}, \mathcal{F}\}$
$\mathcal{G}^{PTE}$	$\mathcal{V}^{PTE} = \mathcal{V} \cup \mathcal{D}_0^{'} \cup \{\mathcal{F}' = \{\mathcal{M}_i \vert i \in \mathcal{F}\}\} \setminus \mathcal{F}$
	Arcs
$\mathcal{G}$	$\mathcal{E} = \{(i,j) \vert i,j \in \mathcal{V}, i \neq j\}$
$\mathcal{G}^{PTE}$	$\mathcal{E}^{PTE} = \{(i,j) \vert i,j \in \mathcal{V}^{PTE}, i \neq j\}$ $\setminus \{(i,j) \vert i,j \in \mathcal{F}_k^{'}, t(i) - t(j) \neq \Delta t\}$

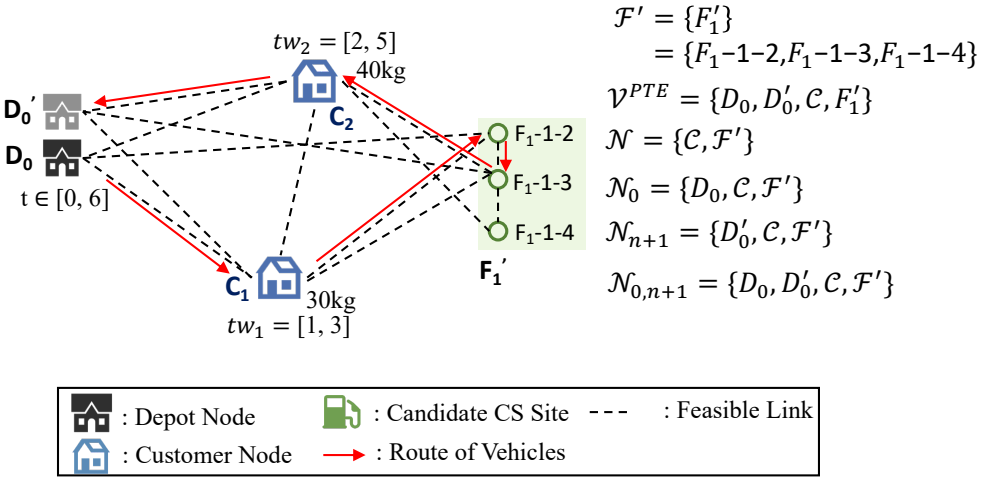

Figure 4.3: Expanded illustrative network. Here, the notation $F_1 - x - y$ represents the x^{th} charger and the corresponding time slot y.

4.5 Mathematical Formulation of the Problem as Bi-level Programming

As mentioned in previous sections, this study aims to capture the interactive dynamics between the charging service provider and the fleet operator. We do not assume cooperation between these two players and hence competition between the two entities is inevitable. Today, many transportation logistic companies are considering fleet electrification to reduce total cost of ownership, reduce greenhouse gas emissions, and satisfy upcoming regulations [33, 85, 141]. However, optimally designing the vehicle fleet, routing, and charging strategies remains as open questions. Fleet operators, as we observed, often seek consultation from charging service providers in practice. This naturally leads to a leader-follower setting, in which the charging service provider is the leader [4]. We assume leader is the CSP in this work and has complete information of the follower. Leader-follower games are also known as Stackelberg games [44].

The decision variables and notation for the problem are summarized in Table 4.3. Next, we detail the model for each player as well as for the complete problem.

[4]The leader knows the cost function mapping of the follower in this game. The follower, on the other hand, observes the strategies from the leader and always has to take them into account.

Table 4.3: Notation summary (Alphabetical order)

Variables	
b_i^k	Continuous variable, battery level (kWh) of type k vehicle when arrived at node i
ΔP_i	Continuous variable, upgrade capacity of the transformer connecting node i
q_i^k	Continuous variable, load level (kg) of type k vehicle when arrived at node i
s_i	Integer variable, number of charging ports installed in the charging station at node i
τ_i	Integer variable, time when a vehicle arrived at node i
x_{ij}^k	Binary variable, whether vehicle of type k visits node j after node i
y_i	Binary variable, whether a charging station is constructed at node i
Sets	
$\mathcal{E}^N$	Sets of links in the expanded network excluding the internal links within any CS, i.e. $\mathcal{E}^{PTE} \setminus (\cup \mathcal{A}_i)$
$\mathcal{F}'$	Set of all dummy CS nodes, i.e. $\{\mathcal{M}_i \vert i \in \mathcal{F}\}$
$\mathcal{K}$	Set of vehicle type index. The vehicle types are different in three aspects: their battery sizes (B^k), their load capacities (Q^k), and their costs (c^k)
$\mathcal{M}_i(t)$	Set of dummy nodes for CS i with whose time tracker equals t, i.e. $\{j \vert j \in \mathcal{M}_i, t(j) = t\}$
$\mathcal{N}$	Set of all dummy CS nodes and customer nodes, i.e. $C \cup \mathcal{F}'$
$\mathcal{N}_0$	Set of all nodes except the sink depot, i.e. $\mathcal{N} \cup \{D_0\}$
$\mathcal{N}_{n+1}$	Set of all nodes except the source depot, i.e. $\mathcal{N} \cup \{D_0'\}$
$\mathcal{N}_{0,n+1}$	Set of all nodes, i.e. $\mathcal{N} \cup \{D_0, D_0'\}$
Parameters	
B^k	Battery capacity of a type k truck, in [kWh]
c_i^p	Cost of one charging port at node i, in [$/port]
c_i^s	Cost of substation capacity upgrade at node i, in [$/kW]
c_i^e	Service fee charged by the charging station i, in [$/kWh]
c^k	Cost of vehicle type k, in [$]
c_{ij}^k	Cost of travel from node i to node j of type k, in [$]
d_i	Customer demand at node i
d_{ij}	Distance between node i and node j, in [km]
Δt	Time step
$\pi_{i,t}$	Electricity price at node i at time t, in [$/kWh]
p^{rated}	Charger rated power, in [kW]
$P_{i,t}$	Substation availability at time t, at node i, in [kW]
Q^k	Freight capacity of a type k truck, in [kg]
r^k	Energy consumption rate of type k, in [kWh/km]
t_i^e, t_i^l	Earliest arrival/Latest departure time at node i
t_i^s	Required service time of node i
t_{ij}	Travel time from node i to node j
$\zeta_{s/v}$	Capital recovery factors for the charging station and the vehicles respectively

4.5.1 CSP's Problem: Charging Network Design and Operation

The leader CSP aims to minimize its overall costs by optimally placing and sizing the new charging stations. The binary variable y_i is used to indicate the construction decision at the specific site F_i, and the integer variable s_i represents the number of chargers to be installed at F_i.

The overall cost g^L constitutes two parts. The first part is the capital expenditure (CAPEX), namely the costs for installing ports and for upgrading the local transformer if necessary. The second part is the operational profit introduced by providing charging service to E-trucks with the predetermined service fee c_i^e (\$/kWh). Mathematically, g^L is expressed as

$$g^L(\boldsymbol{y}, \boldsymbol{s}, \boldsymbol{\Delta P}) = \sum_{i \in \mathcal{F}} \{\zeta_s \cdot (c_i^s s_i + c_i^p \Delta P_i) - c_i^e E_i^{ch}\}. \tag{4.1}$$

Here, E_i^{ch} represents the total electricity delivered to E-trucks at station F_i. Based on the proposed PTEN model in Section 4.4.2, it is calculated as

$$E_i^{ch} = p^{\text{rated}} \Delta t \cdot \sum_k \sum_{(j,m) \in \mathcal{A}_i} x_{j,m}^k. \tag{4.2}$$

Factor ζ_s in g^L converts the life-cycle fixed cost into its annual equivalent level, which is calculated as

$$\zeta_s = \frac{r(1+r)^{Y_s}}{(1+r)^{Y_s} - 1}, \tag{4.3}$$

where r is the cash discount rate and Y_s is the service life of the charging station.

When building the charging stations, the CSP should ensure adequate chargers,

$$\sum_{k \in \mathcal{K}} \sum_{(j,m) \in \mathcal{A}_i(t)} x_{j,m}^k \leq s_i \quad \forall i \in \mathcal{F}, \forall t \in \mathcal{T}_i, \tag{4.4}$$

and sufficient transformer capacity to supply power to the visited vehicles. If at any point of time t, the total demanded power $s_i \cdot p^{\text{rated}}$ is higher than the available capacity $y_i \cdot P_{i,t}$, then the CSP would need to consider the transformer capacity upgrade cost,

$$s_i \cdot p^{\text{rated}} - y_i \cdot P_{i,t} \leq \Delta P_i \quad \forall i \in \mathcal{F}. \tag{4.5}$$

There are also constraints on the station size and variable domain constraints:

$$y_i s_i^{\min} \leq s_i \leq y_i s_i^{\max} \quad \forall i \in \mathcal{F}, \tag{4.6}$$

$$y_i \in \{0,1\}, s_i \in \mathbf{Z}^+, \Delta P_i \in \mathbf{R}^+, \quad \forall i \in \mathcal{F}. \tag{4.7}$$

4.5.2 FO's problem: Fleet Design and Operation

The FO's goal is to decide its E-truck fleet composition and routing plans so that its overall cost is minimized. The cost objective for the FO is

$$g^F(\boldsymbol{x}) = \zeta_v \sum_{k \in \mathcal{K}} \sum_{j \in \mathcal{N}} c^k x_{D_0 j}^k + \sum_{k \in \mathcal{K}} \sum_{i \in \mathcal{N}_0} \sum_{j \in \mathcal{N}_{n+1}} c_{ij}^k x_{ij}^k$$

$$+\sum_{i\in\mathcal{F}}\sum_{t\in\mathcal{T}_i}(\pi_{i,t}+c_i^e)\sum_{k}\sum_{(j,m)\in\mathcal{A}_i(t)}p^{\text{rated}}\Delta t\cdot x_{j,m}^k. \tag{4.8}$$

The first term in g^F represents the total E-truck purchase cost, which is converted into the equivalent annual level using ζ_v. The second term yields the traveling cost of the fleet. The last term calculates the cost of charging, where the per unit charging cost involves the electricity price $\pi_{i,t}$ plus the service fee c_i^e posed by the CSP.

Vehicle routing must respect resource constraints along the network, including time windows, payload capacity, energy, etc., which are given as follows.

Network flow constraints

$$\sum_{k\in\mathcal{K}}\sum_{j\in N_{n+1},j\neq i}x_{ij}^k=1\quad\forall i\in\mathcal{C}, \tag{4.9}$$

$$\sum_{k\in\mathcal{K}}\sum_{j\in N_{n+1},j\neq i}x_{ij}^k\leq 1\quad\forall i\in\mathcal{F}', \tag{4.10}$$

$$\sum_{j\in N_0,j\neq i}x_{ji}^k-\sum_{j\in N_{n+1},j\neq i}x_{ij}^k=0\quad\forall i\in N,\forall k\in\mathcal{K}, \tag{4.11}$$

Constraint (4.9) requires each customer to be visited once and only once, while for the expanded charging station nodes, this requirement is relaxed in (4.10). Flow conservation of each node, except the source and sink, is expressed by (4.11).

Time window constraints

$$t_i^e\leq\tau_i\leq t_i^l\quad\forall i\in\mathcal{C}\cup D_0,D_0^{'}, \tag{4.12}$$

$$\begin{aligned}\tau_j-\tau_i\geq(t_{ij}+t_i^s)\,x_{ij}^k-\left(1-x_{ij}^k\right)T\\ \forall i\in\mathcal{N}_0,\forall j\in\mathcal{N}_{n+1},\forall k\in\mathcal{K},j\neq i,\end{aligned} \tag{4.13}$$

$$\begin{aligned}t(j)-\tau_i\geq(t_{ij}+t_i^s)\,x_{ij}^k-\left(1-x_{ij}^k\right)T\\ \forall i\in\mathcal{N}_0,\forall j\in\mathcal{F}',\forall k\in\mathcal{K},j\neq i,\end{aligned} \tag{4.14}$$

$$\begin{aligned}t(j)-\tau_i\leq(t_{ij}+t_i^s)\,x_{ij}^k+\left(1-x_{ij}^k\right)T\\ \forall i\in\mathcal{N}_0,\forall j\in\mathcal{F}',\forall k\in\mathcal{K},j\neq i,\end{aligned} \tag{4.15}$$

$$\tau_j=\sum_{k\in\mathcal{K}}\sum_{i}x_{ij}^k\cdot t(j)\quad\forall i\in\mathcal{N}_0,\forall j\in\mathcal{F}' \tag{4.16}$$

The arrival time of a vehicle at a customer point i must respect the customer's service time window $\left[t_i^e,t_i^l\right]$ (4.12). For the depots, the time window is set as $[0,T]$. Constraint (4.13) expresses the relationship between two successive customer nodes i and j at their

respective visited times. When $x_{ij}^k = 1$, then E-truck k's arrival time at customer j depends on the traveling time between i, j and the service time at i. However, when $x_{ij}^k = 0$, i.e. j is not visited after i, then this constraint is relaxed.

Constraints (4.14)-(4.16) describe the evolution of visiting times when an E-truck is driving toward a charging station node. Since each dummy node is strictly associated with one specific time slot, the corresponding relation $x_{ij}^k = 1$ is true only if the arrival time τ_j at the charging node j matches $t(j)$, as shown in (4.14). Again, those constraints are relaxed if $x_{ij}^k = 0$.

Freight capacity constraints

$$q_j^k \leq q_i^k - d_i x_{ij}^k + \left(1 - x_{ij}^k\right) Q^k \quad \forall i \in \mathcal{N}_0, \forall k \in \mathcal{K}, \forall j \in \mathcal{N}_{n+1}, j \neq i, \tag{4.17}$$

$$0 \leq q_i^k \leq Q^k \quad \forall k \in \mathcal{K}, \forall i \in \mathcal{N}_{0,n+1}, \tag{4.18}$$

Following the same modeling philosophy from above, the available freight loads at each node along the route are tracked using (4.17). Constraint (4.18) ensures that the E-trucks are never overloaded.

Energy consumption/recharge constraints

$$b_j^k \leq b_i^k - r^k d_{ij} x_{ij}^k + \left(1 - x_{ij}^k\right) B^k \quad \forall (i,j) \in \mathcal{E}^N, \forall k \in \mathcal{K}, j \neq i \tag{4.19}$$

$$b_j^k \leq b_i^k + p^{\text{rated}} \cdot \Delta t \cdot x_{ij}^k + \left(1 - x_{ij}^k\right) B^k \quad \forall (i,j) \in \mathcal{A}_z, \forall z \in \mathcal{F}, \forall k \in \mathcal{K} \tag{4.20}$$

Given the limited range of E-trucks, it is crucial to track available battery energy while traveling, which is modeled by (4.19) and (4.20). These constraints are relaxed when $x_{ij}^k = 0$ by using the term $(1 - x_{ij}^k)B^k$. We assume a constant energy consumption rate while traversing to customers and a constant charging rate while traversing the charging links. Visiting consecutive charging nodes at one physical location represents charging for multiple time slots.

$$b_0^k = B^k \quad \forall k \in \mathcal{K}, \tag{4.21}$$

$$0 \leq b_i^k \leq B^k \quad \forall k \in \mathcal{K}, \forall i \in \mathcal{N}_{n+1}, \tag{4.22}$$

$$b_i^k + p^{\text{rated}} \cdot \Delta t \leq B^k \quad \forall k \in \mathcal{K}, \forall i \in \mathcal{F}', \tag{4.23}$$

We assume all E-trucks start fully charged at depot (4.21). The battery is never depleted nor overcharged as enforced by (4.22) and (4.23), respectively.

Simultaneous charging constraint

$$\sum_{k\in\mathcal{K}}\sum_{(j,m)\in\mathcal{A}_i(t)} x^k_{j,m} \le s_i \quad \forall i\in\mathcal{F}, \forall t\in\mathcal{T}_i. \tag{4.24}$$

The number of simultaneous charging E-trucks must respect the physical charging station size limit.

Additional variable domains

$$\begin{aligned} &x^k_{i,j}\in\{0,1\} \quad \forall i\in\mathcal{N}_0, \forall j\in\mathcal{N}_{n+1} \\ &\tau_i\in\mathbf{Z}^+, \quad q_i, b_i\in\mathbf{R}^+ \quad \forall i\in\mathcal{N}_{0,n+1}. \end{aligned} \tag{4.25}$$

4.5.3 Joint Problem as a Stackelberg Game

Given the CSP (leader) and FO (follower) optimization models above, we now integrate them to yield the complete joint planning problem:

$$\min_{\boldsymbol{y},\boldsymbol{s},\boldsymbol{\Delta P}} \quad g^L(\boldsymbol{y},\boldsymbol{s},\boldsymbol{\Delta P};\boldsymbol{x}^*) \tag{4.26a}$$

$$\text{s. to:} \quad h^L(\boldsymbol{y},\boldsymbol{s},\boldsymbol{\Delta P})\le 0 \tag{4.26b}$$

$$(\boldsymbol{x}^*,\boldsymbol{\tau}^*,\boldsymbol{b}^*,\boldsymbol{q}^*) = \arg\min_{\boldsymbol{x},\boldsymbol{\tau},\boldsymbol{b},\boldsymbol{q}} \quad g^F(\boldsymbol{x}) \tag{4.26c}$$

$$\text{s. to:} \quad h^F(\boldsymbol{s},\boldsymbol{x},\boldsymbol{\tau},\boldsymbol{b},\boldsymbol{q})\le 0.$$

The constraint set $h^L(\boldsymbol{y},\boldsymbol{s},\boldsymbol{\Delta P})$ contains (4.4)-(4.7) and $h^F(\boldsymbol{s},\boldsymbol{x},\boldsymbol{\tau},\boldsymbol{b},\boldsymbol{q})$ includes (4.9)-(4.25). For the reader's convenience, we have colored the leader's optimization variables blue and the follower's optimization variables red. Black bold variables are fixed optimization variables [5].

A key benefit of the proposed PTEN is the overall mathematical formulation (4.26) maintains a mixed integer linear programming structure. However, solving this model is still highly non-trivial. The main challenges are twofold: (i) The overall model is a bi-level mixed integer problem (Bi-MILP) and integer variables exist in both the upper and lower levels. In this case, the commonly-used KKT (Karush-Kuhn-Tucker)-based single-level reformulation method is not applicable. (ii) The electric vehicle routing problem, embedded as the essential part of the overall problem, is an NP-hard problem whose scale grows dramatically with the size of the network. This holds true even with the partial time expansion, which mitigates but does not eliminate the computational complexity.

[5] We would emphasize that although this is a fleet sizing, facility siting and sizing, and vehicle routing joint decisions, the model is also able to consider the current existing charging network. We simply convert the corresponding decision variables to input parameters. It is a degenerate case of our model.

4.6 Solution Algorithm Design

To solve this complex problem, the framework is broken down to be solved in an iterative fashion. A diagram flow in Fig.4.4 offers a more straightforward visualization of the overall architecture.

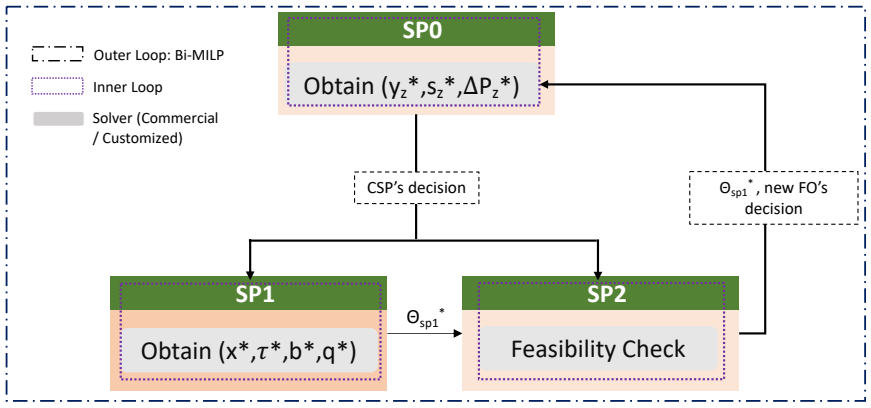

Figure 4.4: The overall solution architecture. Notice that (SP2) has been detailed in Section 4.6.1. It serves as a CSP feasibility check to evaluate the solution set from its successor (SP1). Its reformulation follows the exact same process from Section 4.6.2.

4.6.1 Outer-loop: Solving Bi-MILP with reformulation and decomposition

To address the first challenge (i), we facilitate the overall computation of the Bi-MILP with a reformulation and decomposition method [174]. We denote this as an outer loop design. The main idea of this approach and the problem-specific implementation are presented below and readers are referred to the original references for further theoretical details.

Reformulation

A key observation is that when all discrete variables in the lower-level FO problem are fixed, then the FO (4.26c) becomes a pure linear program with continuous decision variables. Then the optimal solution can be represented using KKT conditions. Given a specific realization for the z-indexed combination of the lower level discrete variables $\boldsymbol{x}^z, \boldsymbol{\tau}^z$, we denote the corresponding KKT conditions as $\Lambda(\boldsymbol{x}^z, \boldsymbol{\tau}^z)$. Therefore, if one enumerates all possible combinations of the follower's discrete decisions, we can denote their collection using index set $\mathcal{L}_{\text{full}} = \{1, \ldots, l^{\max}\}$ where $z \in \mathcal{L}_{\text{full}}$. Then the original problem can be equivalently

formulated as a single-level problem:

$$\textbf{(P0)} \quad \min \quad g^L(\boldsymbol{y}, \boldsymbol{s}, \boldsymbol{\Delta P}, \boldsymbol{x}^0) \tag{4.27}$$

$$\text{s. to:} \quad h^L(\boldsymbol{y}, \boldsymbol{s}, \boldsymbol{\Delta P}) \leq 0, \tag{4.28}$$

$$h^F(\boldsymbol{s}, \boldsymbol{x}^0, \boldsymbol{\tau}^0, \boldsymbol{b}^0, \boldsymbol{q}^0) \leq 0, \tag{4.29}$$

$$\forall z \in \mathcal{L}_{\text{full}}$$

$$g^F(\boldsymbol{x}^0) \leq g^F(\boldsymbol{x}^{\boldsymbol{z}}), \tag{4.30}$$

$$\boldsymbol{y}, \boldsymbol{s}, \boldsymbol{\Delta P}, \boldsymbol{b}^{\boldsymbol{z}}, \boldsymbol{q}^{\boldsymbol{z}} \in \Lambda(\boldsymbol{x}^{\boldsymbol{z}}, \boldsymbol{\tau}^{\boldsymbol{z}}). \tag{4.31}$$

Variables $\boldsymbol{x}^0, \boldsymbol{\tau}^0, \boldsymbol{b}^0, \boldsymbol{q}^0$ are duplications of the follower's decisions. Constraint (4.30) requires that the FO's objective is at least the same, if not improved, from the discrete (and previous as we shall see) realization $\boldsymbol{x}^{\boldsymbol{z}}$. Notably, in our case the discrete variables $\boldsymbol{x}, \boldsymbol{\tau}$ uniquely define the routes of the fleet. Once all routes are realized, then values of $\boldsymbol{b}, \boldsymbol{q}$ are implicitly determined. The complexity of (4.31) can thus be largely reduced.

Decomposition

Instead of directly solving the complete problem **(P0)** with all possible combinations of $\{\boldsymbol{x}, \boldsymbol{\tau}, \boldsymbol{b}\}$ enumerated, one may solve the problem with a subset $\mathcal{L}^{\text{sub}}$ of these combinations, i.e. $z \in \mathcal{L}_{\text{sub}} \subseteq \mathcal{L}_{\text{full}}$ and gradually enlarge the set. As explained in [174], the solution of **(P0)** can be obtained by iteratively solving the following decomposed parts,

- A restricted version of **(P0)** with the subset $\mathcal{L}_{\text{sub}} \subseteq \mathcal{L}_{\text{full}}$, denoted as **(SP0)**. Since only a subset of all the constraints are considered during each iteration (with fixed $\boldsymbol{x}^{\boldsymbol{z}}, \boldsymbol{\tau}^{\boldsymbol{z}}$ in (4.30)-(4.31)), **(SP0)** provides a lower bound to the original problem **(P0)**.

- Subproblem 1 **(SP1)** finds the follower's corresponding best response $\{\boldsymbol{x}^*, \boldsymbol{\tau}^*, \boldsymbol{b}^*, \boldsymbol{q}^*\}$ to the leader's decisions $\{\boldsymbol{y}^*, \boldsymbol{s},^* \boldsymbol{\Delta P}^*\}$ from **(SP0)**, i.e.

$$\textbf{(SP1)} \quad \min_{\boldsymbol{x}, \boldsymbol{\tau}, \boldsymbol{b}, \boldsymbol{q}} \quad g^F(\boldsymbol{x}) \tag{4.32}$$

$$\text{s. to:} \quad h^F(\boldsymbol{s}^*, \boldsymbol{x}, \boldsymbol{\tau}, \boldsymbol{b}, \boldsymbol{q}) \leq 0, \tag{4.33}$$

- Subproblem 2 **(SP2)** performs a feasibility check[6] and is defined as

$$\textbf{(SP2)} \quad \min_{\boldsymbol{x}, \boldsymbol{\tau}, \boldsymbol{b}, \boldsymbol{q}} \quad g^L(\boldsymbol{y}^*, \boldsymbol{s}^*, \boldsymbol{\Delta P}^*; \boldsymbol{x})$$

$$\text{s. to:} \quad g^F(\boldsymbol{x}) \leq \theta^*_{\text{sp1}}, \tag{4.34}$$

$$h^F(\boldsymbol{s}^*, \boldsymbol{x}, \boldsymbol{\tau}, \boldsymbol{b}, \boldsymbol{q}) \leq 0,$$

[6]Sometimes there may be multiple non-unique lower-level optimal solutions given the upper-level decision. By solving **(SP2)**, we select the follower solution that is most in favor of the leader.

where θ^*_{sp1} is the optimal value from **(SP1)**. When a solution is found feasible in **(SP2)**, then the decision set $\{\tilde{\boldsymbol{x}}^*, \tilde{\boldsymbol{\tau}}^*, \tilde{\boldsymbol{b}}^*, \tilde{\boldsymbol{q}}^*\}$ represents the most favorable follower action for the leader. We then add it into $\mathcal{L}_{\text{sub}}$ in **(SP0)** for the next round of iteration. **(SP2)** provides θ^*_{sp2} as an upper bound for **(P0)**, since it clearly finds a feasible solution.

The pseudo code is detailed in Algorithm 1.

Algorithm 1: Algorithm for the Joint Planning Bi-MILP

Input: model parameters and convergence margin ϵ

Output: optimal solution for both CSP and FO

- *Initialization* :

Set $LB = -\infty$, $UB = \infty$, and $l = 0$

- *Loop Process :*

while $UB - LB > \epsilon$ **do**

  Solve (SP0) with current combinations $z = 1, \ldots, l^{\text{sub}}$ and obtain $\{\boldsymbol{y}^*_{\boldsymbol{z}}, \boldsymbol{s}^*_{\boldsymbol{z}}, \boldsymbol{\Delta P}^*_{\boldsymbol{z}}\}$ and the optimal objective Θ^*_{RMP}, set $LB = \Theta^*_{\text{RMP}}$.

  Solve (SP1) given $\{\boldsymbol{y}^*_{\boldsymbol{z}}, \boldsymbol{s}^*_{\boldsymbol{z}}, \boldsymbol{\Delta P}^*_{\boldsymbol{z}}\}$ as fixed, and obtain $\{\boldsymbol{x}^*, \boldsymbol{\tau}^*, \boldsymbol{b}^*, \boldsymbol{q}^*\}$ and the optimal objective as θ^*_{sp1}

  Solve (SP2) with $\{\boldsymbol{y}^*_{\boldsymbol{z}}, \boldsymbol{s}^*_{\boldsymbol{z}}, \boldsymbol{\Delta P}^*_{\boldsymbol{z}}\}$ as fixed, and obtain $\{\tilde{\boldsymbol{x}}^*, \tilde{\boldsymbol{\tau}}^*, \tilde{\boldsymbol{b}}^*, \tilde{\boldsymbol{q}}^*\}$ and the optimal objective as θ^*_{sp2}

  if (SP2) is feasible **then**

    Set $\{\boldsymbol{x}^{\boldsymbol{z+1}}, \boldsymbol{\tau}^{\boldsymbol{z+1}}\}$ as $\{\tilde{\boldsymbol{x}}^*, \tilde{\boldsymbol{\tau}}^*\}$, $UB = \min\{UB, \theta^*_{\text{sp2}}\}$

  else

    Set $\{\boldsymbol{x}^{\boldsymbol{z+1}}, \boldsymbol{\tau}^{\boldsymbol{z+1}}\}$ as $\{\boldsymbol{x}^*, \boldsymbol{\tau}^*\}$

  end if

  Add the new optimal cut corresponding to $\{\boldsymbol{x}^{\boldsymbol{z+1}}, \boldsymbol{\tau}^{\boldsymbol{z+1}}\}$ to the (SP0), set $z = z + 1$.

end while

return $y^*_z, s^*_z, \Delta P^*_z, x^z, \tau^z, b^z$

4.6.2 Inner loop: Solving E-V/LRP

Notice that the three subproblems are structurally similar and the electric vehicle routing problem serves as the core in **(SP1)** and **(SP2)** and the location planning is encoded in **(SP0)**. Since novel computation algorithms are not the focus of this work, for the analysis in Section 4.7 we rely on a commercial solver (e.g. Gurobi) to solve these subproblems. However, one can reformulate these problems as generalized set-partitioning problems and subsequently solve them in an iterative fashion to reduce computational burden when the network size becomes very large, possibly sacrificing solution quality. We refer interested readers to [71] for set-partitioning reformulation.

Table 4.4: Parameters of candidate charging stations

Station ID	Available capacity (kW)	Charge rate (kW)	Cost of charger ($)	Substation upgrade cost ($/kW)	Electricity cost ($/kWh)
F_1	15	5	10000	788	0.1
F_2	30	10	10500	788	0.1

Table 4.5: Vehicle parameters

Vehicle ID	Freight capacity (kg)	Battery capacity (kWh)	Energy consumption (kW/unit length)	Vehicle cost ($)	Travel cost ($/unit length)
1	150	50	10	10000	0.5
2	200	60	10	18000	0.5

4.7 Numerical Studies

We have proposed an optimization modeling framework and iterative algorithm to solve this problem. To effectively demonstrate the model, we deliberately design a small but intuitive network. We will highlight some of the binding features, like the customer time windows and the charging rates.

The small network is presented in Fig. 4.5. It consists of 1 depot node D_0, 5 customer nodes $\mathcal{C} = \{A, B, C, D, E\}$ and 2 candidate charging station nodes $\mathcal{F} = \{F_1, F_2\}$. The dashed lines are the feasible links with adjacent numbers indicating the lengths. We summarize all relevant parameters for CSP in Table 4.4 [7] and for the FO in Table 4.5. Next, we will numerically demonstrate the necessity of the two-entity modeling. Then, we will study the cost breakdowns and the varying dynamics when stricter time windows are applied and charging rates are varied.

4.7.1 Base Case: Necessity of Considering Different Entities

We first focus on the different strategies when a social planner (single entity) or non co-operation (two entities) is considered. Simulations are performed for both scenarios with the service fee varying from 0 to 0.5($/kWh) [8]. The results obtained are given in Fig.4.6.

Consider the single entity scenario. To enable a fair comparison against the two-entity case, we plot the combined costs of electricity and service fee ($\pi_i + c_i^e$) for the single entity. Together they will jointly affect the vehicle routing, charging, as well as the infrastructure decisions. When the service fee is set to 0, the FO charges at the cost of electricity (π_i)

[7] We keep the station available capacity $P_{i,t}$ constant over time for convenience. It's not the main focus of this study.

[8] We leave customer time windows sufficiently wide in this case.

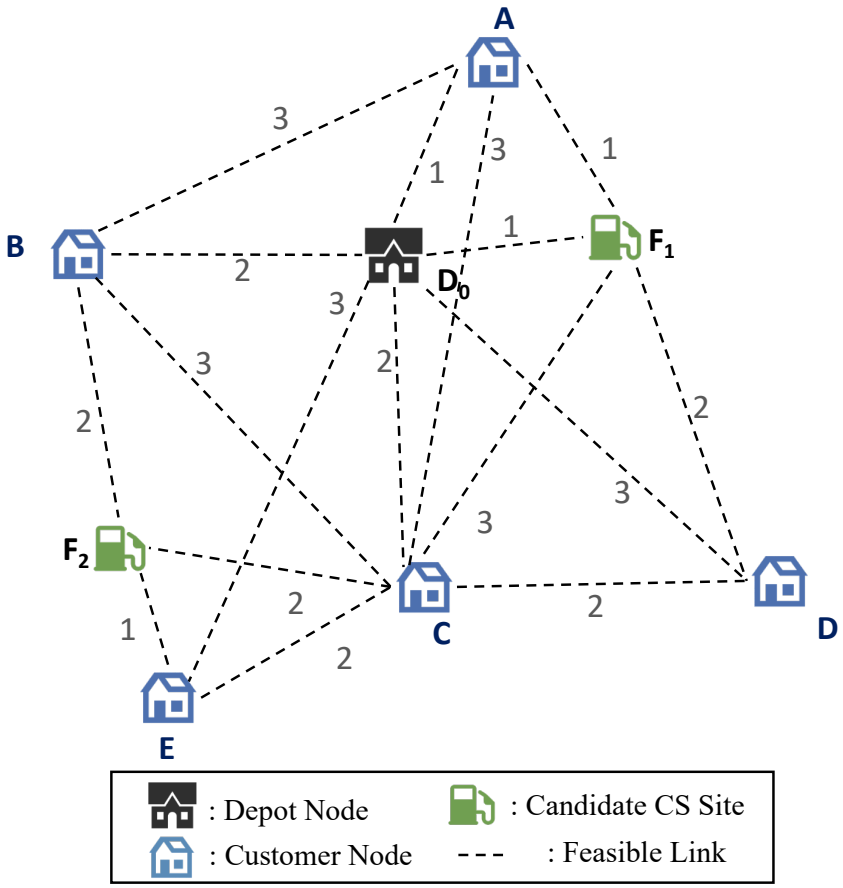

Figure 4.5: Small network (original)

purchased from the utility, i.e. with zero profit margin. Given the optimized planning results, we then split and plot the corresponding costs to the FO and CSP. In greater detail, the FO cost consists of the fleet investment, travel expenditure as well as the combined cost of electricity and service fee; on the other hand, the CSP cost is the infrastructure investment less the profits from providing service. The cost splits are presented by the dashed lines in Fig. 4.6 and the colored shape labels on the dashed line indicate the different optimal strategies corresponding (see Table VI) to each simulated price value. Note that when service fee is set at \$0/kWh, this is the case commonly known as to minimize the total cost of ownership (TCO) in literature. However, as shown in the left most in Fig.4.6, it actually induces the largest cost to the CSP.

For the two-entities scenario, we solve the problem with the proposed model. We superimpose the costs for the FO and CSP in Fig. 4.6 using solid lines. It is visually clear that the decisions under the two-entity scenario achieves lower net costs than the single entity sce-

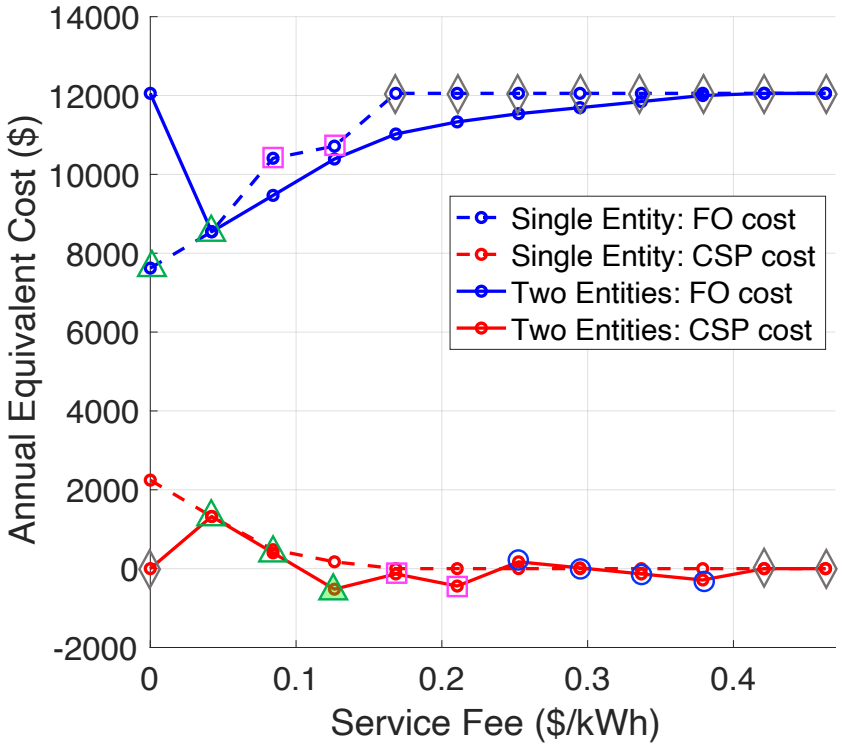

Figure 4.6: Cost of different players with respect to different service fee, without time windows. The colored marker shapes correspond to different strategies in Table VI. The markers on the upper dashed blue line correspond to the single entity case, whereas the markers on the lower solid red line correspond to the two-entity case.

nario most of the time, i.e. the FO achieves lower costs and the CSP generates more profit. The only exceptions happen when the service fees are extremely low (below \$0.05/kWh). Within this range, from a pure economic point of view, the CSP has little to no interest to invest and enter the market [9]. The CSP can be incentivized to participate by increasing the service fee. However, as the CSP becomes more "greedy," the FO will reject the option to charge at the facility. This then leads to a non-cooperative situation, as indicated by the grey rhombuses on the solid line in Fig. 4.6 (after service fee is more than \$0.421/kWh).

Since the CSP is the leader in the game, it will naturally take advantage of being the first-mover. The final decision for the CSP is to build charging stations at both locations with service fee set at 0.125 \$/kWh in this particular example (solid green triangle in Fig. 4.6). The corresponding fleet routes are shown in Fig. 4.7 (Plan 2). We denote the first/second

[9]Even if the CSP enters (the second green triangle), it is not at all cost-attractive. It experiences positive cost and no profit.

Table 4.6: Possible strategy-pairs in base case

Plan	FCS	Routing Plan
1(◊)	None	E-truck-1 of type 1: $D_0 \to B \to D_0$ E-truck-2 of type 2: $D_0 \to A \to C \to D_0$ E-truck-3 of type 2: $D_0 \to E \to D_0$ E-truck-4 of type 2: $D_0 \to D \to D_0$
2(△)	F_1, F_2	E-truck-1 of type 1: $D_0 \to D \to F_1 \to A \to D_0$ E-truck-2 of type 1: $D_0 \to B \to F_2 \to E \to C \to D_0$
3(□)	F_1	E-truck-1 of type 1: $D_0 \to B \to D_0$ E-truck-2 of type 2: $D_0 \to A \to F_1 \to D \to C \to D_0$ E-truck-3 of type 2: $D_0 \to E \to D_0$
4(◯)	F_1	E-truck-1 of type 2: $D_0 \to B \to A \to D_0$ E-truck-2 of type 2: $D_0 \to F_1 \to D \to C \to D_0$ E-truck-3 of type 2: $D_0 \to E \to D_0$

route chosen by E-truck-1/2 as route 0/1 for later reference. Indeed, it is the most efficient and straightforward to assume the existence of a powerful social planner. However, this common assumption in the literature is not always the case in real life. We further emphasize an important nuance here: only through rigorous and comprehensive cost analysis can we incentivize both entities to come up with an agreement that benefits both sides, even though the eventual outcome does not always lead to the social optimum as contests prevail [10].

4.7.2 The effects of customer time windows and charging rates

We are going to show how two of the binding features, time windows and charging rates, will influence optimal decisions. We set tighter delivery time windows for customer B, C and D as $[1, 4], [6, 9], [2, 3]$ respectively. First, we keep the charge rate as 10 kW as in the base case and the results are plotted in Fig. 4.8. In this case, the FO will reject charging service from the CSP when the price exceed 0.25 \$/kWh. This critical threshold was 0.421 \$/kWh in the base case (Section 4.7.1), where no time windows are set. The only profitable service fee for the CSP occurs 0.1684 \$/kWh, whereas all other services fees yield zero or negative

[10]Note that this is an one-to-one service scenario. More involved settings and further analysis can be extended to one-to-many or many-to-one scenarios. This is out of scope and we will leave it for future work.

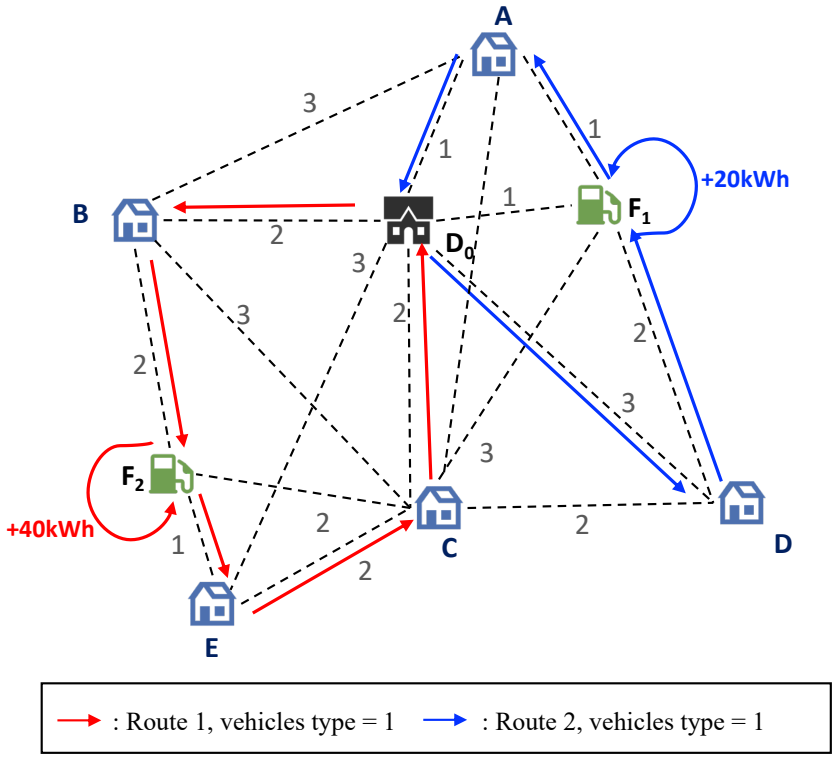

Figure 4.7: Optimal routes of FO.

Table 4.7: Selected strategy when tighter time windows are applied

Plan	FCS	Routing Plan
1(★)	F_1	E-truck-1 of type 1: $D_0 \to B \to D_0$ E-truck-2 of type 1: $D_0 \to C \to D_0$ E-truck-3 of type 1: $D_0 \to E \to D_0$ E-truck-4 of type 2: $D_0 \to D \to F_1 \to A \to D_0$

profit. Note, in the base case, there were six profitable service fees. However, the profit now is 74.23% lower than that in the base case.

In this example, some tightened time windows significantly reduced the number of feasible routes for the FO. It becomes a tougher decision to balance both time spent for charging and time to meet customers. The previously selected route 1 ($D_0 \to B \to F_2 \to E \to C \to D_0$) becomes infeasible as the E-trucks need 4 units of time to charge (to complete the trip) but

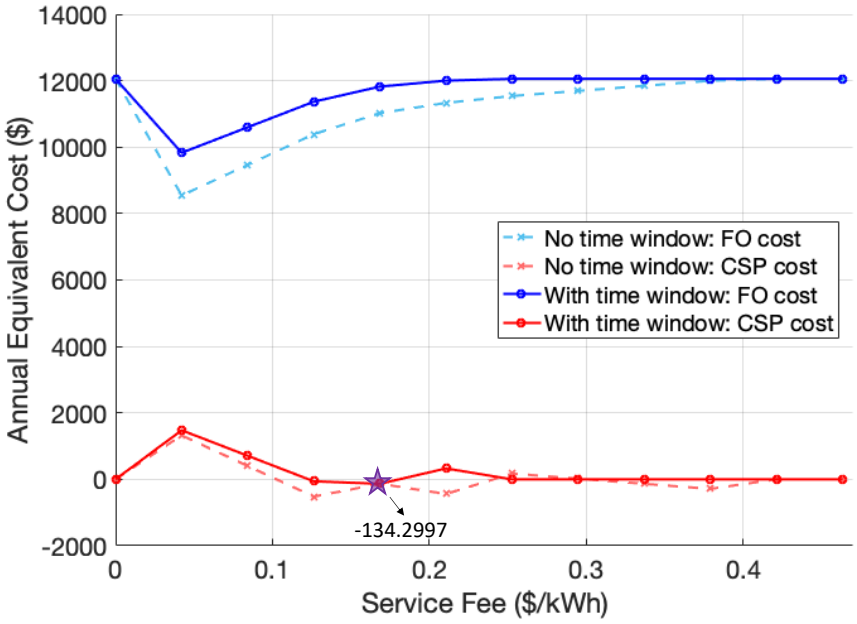

Figure 4.8: With time windows, cost of different players with respect to different service fee. The two upper curves correspond to the FO costs; the lower two are the CSPs'.

will miss customer C. As a result, three separate E-trucks are purchased instead to serve customer B, C and E respectively. The detailed plan is given in Table VII. This increases the final cost of the FO by 13.8%.

One alternative solution that may realize benefits to both sides is to increase the chargers' charging rate. The cost breakdowns over the variations of rate are shown in Fig. 4.9. They are plotted with respect to the two entities – the FO on the left and the CSP on the right. Black dashed lines indicate the CSP's overall net cost/profit (for positive/negative values resp.). The corresponding strategies are also listed in Table VIII. We see that when the rate increases from 10 kW to 15 kW, the previously selected route 1 can again be assigned to a larger E-truck, whereas when the rate is doubled, the smaller E-truck may be used. Although more charging energy is needed, the trucks still meet all the delivery time windows. As a result, reductions in E-truck fleet investment and travel cost compensate the extra charging expenditure and lead to overall FO cost savings. From the CSP's perspective, although more infrastructure investment is required[11] up-front, it also realizes more profit gains. The increased revenues from energy service cover the increased capital costs.

[11]The cost for a single port is assumed to increase with the charging rate. Indeed the infrastructure investments at 15 and 20 kW are subtly different.

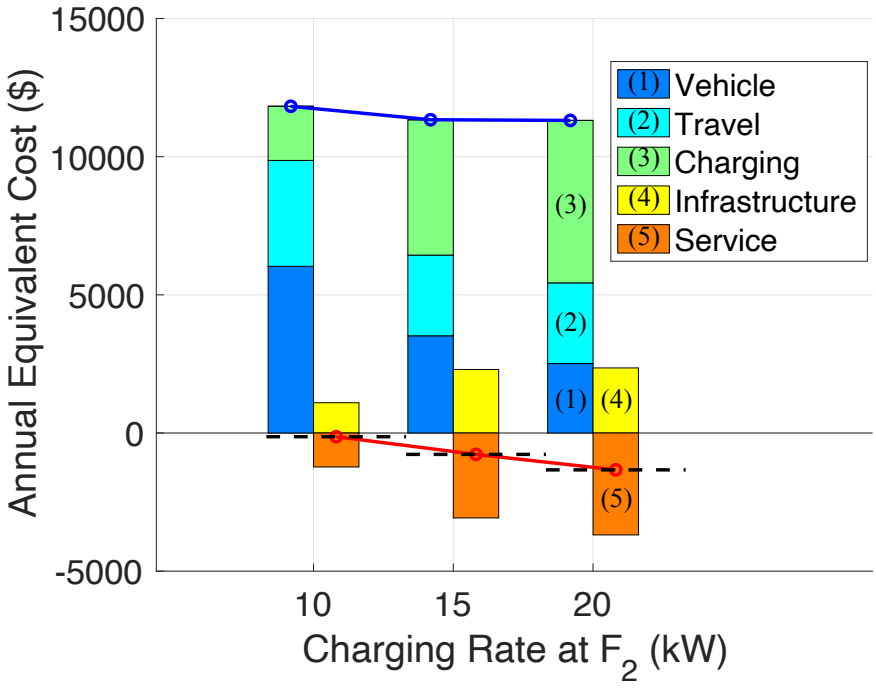

Figure 4.9: Costs of different players with different charging rate at F_2. Upper solid line is the net annual equivalent costs of the FO and the lower dashed line is the net profits of the CSP.

Table 4.8: Players' strategies with different charging rates

Rate	CSP's Strategy	FO's Strategy
10kW	F_1	Number of E-truck of type 1: 2 Number of E-truck of type 2: 2 Enroute charging: 20kWh
15kW	F_1, F_2	Number of E-truck of type 1: 1 Number of E-truck of type 2: 1 Enroute charging: 50kWh
20kW	F_1, F_2	Number of E-truck of type 1: 2 Number of E-truck of type 2: 0 Enroute charging: 60kWh

We have illustrated two of the binding features along with the dynamic interactions between the two entities. This is indeed a complex but more realistic situation, as opposed to existing work that considers a single entity only. We have demonstrated that without assuming the existence of a powerful social planner, careful analysis is needed to contemplate and incentivize both parties to collaborate. With our framework, the FOs and the CSPs can now look for their operation "sweet spots" and be more committed to transportation electrification.

4.7.3 Complex Network Study

For this work, we highlight the modeling contribution, rather than any algorithmic superiority. However, to analyze the computational burden and results as network size grows, we synthetically generated three larger instances. There are 12, 15, 20 nodes in the instances respectively. Each instance has three candidate charging station nodes. The total number of nodes and edges are calculated after partial time expansion at the three candidate sites. These are fully connected graphs and the networks after expansion contain thousands of edges (summarized in Table 4.9). Since the commercial solver is not able to handle the latter two instances, we reformulated the subproblems as a set-partitioning problem and solve iteratively. The computational times are summarized in Fig. 4.10

The parameters used in these instances are summarized in Table 4.10 and Table 4.11. These parameters are adopted to reflect practice: customers are more spatially distributed, the E-truck ranges and energy consumption are taken from vehicle specifications announced by the manufacturers, and all cost parameters are adopted from References [50, 54, 142, 175, 183]. We demonstrate that the outer-loop algorithm from Section 4.6.1 empirically converged in much fewer iterations as compared to the enormous set $\mathcal{L}_{\text{full}}$ (Table 4.9). Our results align with the findings in [172]. In fact, these iterations may be interpreted as a negotiation process between the leader (CSP) and the follower (FO). While solving the leader problem in **(SP0)**, (4.30) upper bounds the follower's objective and ensures it decreases (or stays the same) at each iteration. With this (follower's response) in mind, the leader proposes a design and operational plan until an optimal proposal is accepted by both entities.

The non-cooperative nature of the two entities holds for these larger instances. We will share N12 as an example in Fig. 4.11. There are four possible strategy pairs for the leader (CSP) and follower (FO) detailed in Table 4.12, corresponding to different service fees imposed by the CSP. With smaller service fees, such as Plan 1, the CSP is not willing to open more than one charging station to provide service; on the other hand, when the service fee is high, such as Plan 4, the CSP will invest heavily and open all stations. In Plan 4, however, the CSP faces the risk that the FO deploys more E-trucks to accommodate customer demand yet reduce charging needs, which increases the FO's cost but decreases the CSP's revenue. As Fig. 4.11 demonstrates, the best strategy for the CSP is actually Plan 3, where the CSP finds the most profitable action is to open 2 charging stations and the FO deploys 5 E-trucks to fulfill customer demand.

Table 4.9: Configurations of instances

Instance Name	Number of Nodes	Number of Candidate Charging Station Nodes	Number of Nodes (Expanded)	Number of Edges	Iterations to Converge
N12	12	3	201	3,712	4
N15	15	3	204	4,924	2
N20	20	3	209	6,984	3

Table 4.10: Vehicle Parameters

Vehicle Type [50]	Freight Capacity (kg)	Battery Capacity (kWh) [50]	Energy Consumption (kWh/km) [54]	Cost of Vehicle ($) [183]
1	250	350	1.44	100000
2	180	260	1.44	66000

Table 4.11: Miscellaneous Parameters

Name (unit) [Source]	Value
Capital Recovery Factor [[175]]	0.10
Charge Rate (kW)	200
Cost of Charger ($/port) [183]	185000
Cost of capacity upgrade ($/kW) [183]	788
Discount factor [175]	0.06
Life year [183]	15
Road length range (km)	[70, 140]
Speed (km/h) [142]	88
Time horizon (hour)	12
Time steps	24

Table 4.12: POSSIBLE STRATEGY-PAIRS FOR N12

Plan	CSP Decisions	FO Decisions
1	open 1 station	4 Type 1 E-truck
2	open 2 stations	4 Type 1 E-truck
3 (□)	open 2 stations	5 Type 1 E-truck
4	open 3 stations	6 Type 1 E-truck

4.7.4 One-to-multiple Generalization

This work studies in depth the non-cooperative nature between the charging service provider (CSP) and the truck fleet operator (FO), a one-to-one interactive setting. However, this framework can also be generalized to a one-to-multiple setting, where multiple fleet

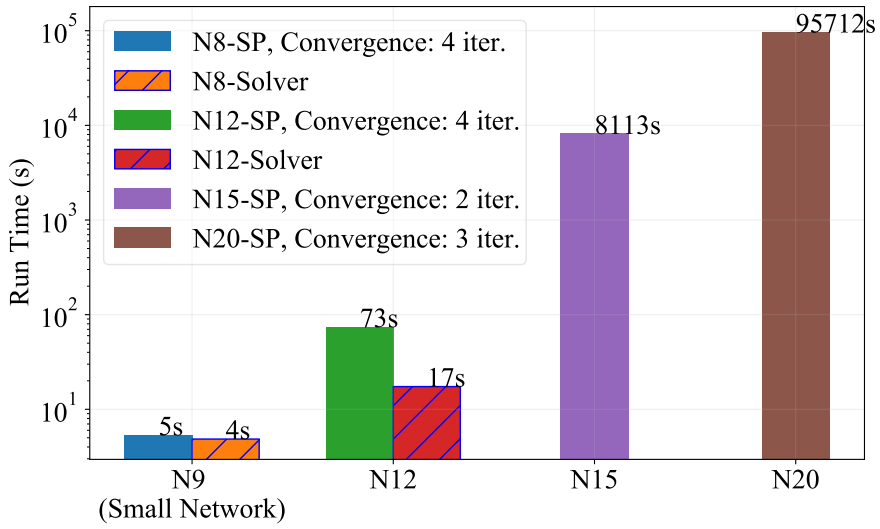

Figure 4.10: Computation Time for 4 Different Instances. Since the commercial solver (denoted "-Solver") is not able to handle the latter two instances (freezes over 100,000s), we have reformulated the problem as a set-partitioning (SP) problem and solved.

operators charge through a single service provider. In reality, logistic companies provide delivery services through bilateral contracts with individual customers. This is unlike an open market, where different suppliers compete for customers with bid offers. In fact, about 80% of this market is based on long-term contractual agreements. Each truck fleet operator has pre-determined the specific portfolio of customer locations and demands. Hence, to model multiple FOs in the problem, we consolidate these fleet operators and simply introduce the idea of a "Super FO". Relevant constraints like (4.4) (the charger constraint) can be extended to the following,

$$\sum_{\phi\in\Phi}\sum_{k\in\mathcal{K}_\phi}\sum_{(j,m)\in\mathcal{A}_i(t)} x_{j,m}^{k_\phi} \le s_i \quad \forall i\in\mathcal{F}, \forall t\in\mathcal{T}_i, \tag{4.35}$$

where notation Φ represent the set of fleet operators. On the other hand, we would like to point out that if competition prevails among the fleet operators to use the chargers (i.e. charging demand exceeds supply), then the notion of "Super FO" may not exist. A study of market equilibrium becomes necessary. However, this is out of the scope of this work.

4.8 Summary

This chapter proposes a new modeling framework to capture the non-cooperative interactions between a charging service provider (CSP) and fleet operator (FO) in the joint charging network design and mobility planning problem. This reflects reality, in which the two entities

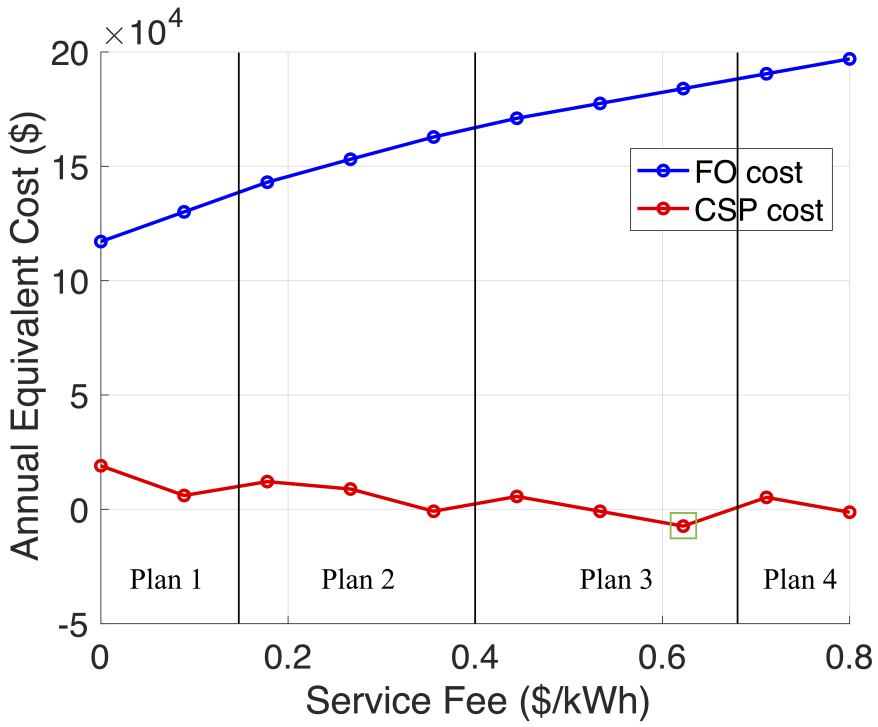

Figure 4.11: Cost of different players with respect to different service fees. The green rectangle in the figure indicates the best action of CSP, which yields the most profits.

are separate self-optimizing organizations. To consider the charging station capacity, this work also proposes, for the first time, a partial time expanded network. It enables jointly optimizing the size of the charging infrastructure in the classic location routing problem regime. The non-cooperative interaction is formulated in a Stackelberg game framework as a Bi-MILP problem. The solution frame work was broken down to be solved in an iterative fashion.

We find that non-cooperation between these two entities can lead to lower total costs than a single entity scenario. Detailed numerical studies demonstrate the effects of binding features and provide insights to interested players. The nature of the solutions with a single social planner and two non-cooperative entities can be dramatically different. Our framework examines these distinct aspects and hence provide more reliable results to the case in real life. In the end, we have also included a discussion about the generalization from one to multiple FOs setting.

Chapter 5

Charging Infrastructure Network and Mobility: Human Movement

5.1 Overview

Feasibility studies on autonomous robotaxi ride-hailing services have revealed a clear initial market for autonomous electric vehicles (AEVs) because of the high daily vehicle utilization and low operational costs of EVs. However, range and charging-time constraints limit the adoption of electric vehicles. A reliable and reachable charging network is necessary for a sustainable business. Herein, we propose a computationally efficient and scalable framework to size an AEV fleet, match vehicles with mobility demands, and design facilities in New York City. We observe that strategic management can reduce fleet size and unnecessary cruising mileage by up to 40% and 70%, respectively. This reduces traffic congestion, increases vehicular movement, reduces travel time, and further reduce fleet sizes. However, access to infrastructure is the prerequisite for these results. Contrary to current market trends, the results of this study reveal that neither large-battery-size AEVs nor high-power charging infrastructure is necessary to achieve efficient service. This effectively alleviates financial and operational burdens on fleet operators and power systems. Furthermore, strategic fleet management results in low mileage, reducing emissions detrimental to human health. In this study, the reduced emissions were quantified and evaluated according to the economic effect on healthcare costs. Furthermore, the reduced travel time and emissions resulting from efficient fleet management create an economic value that exceeds the total capital investment and operational costs of fleet services.

This work has been submitted for peer-review:

Zeng, Teng*, Hongcai Zhang*, Max Z.J. Shen, and Scott J. Moura. "Enhancing the Environmental and Economic Benefits of Automated Electric Vehicle Ride-Hailing Fleets in New York City." *completed 1st round revision at Nature Communications.* (*equal)

5.2 Introduction

In this study, a precise, scalable, and computationally efficient mathematical framework is proposed for region-wide autonomous electric vehicle (AEV) fleet management and charging infrastructure planning decisions. The results of the study provide three major insights: (i) large battery size and high-power charging are not necessary for efficient service; (ii) small fleets reduce congestion, which decreases travel time and enables further fleet reduction – a feedback effect not previously understood; (iii) societal healthcare benefits from reduced particulate matter (PM) 2.5 emissions may dominate investment costs in this sector.

In the past five years, electrification is dominating global transportation trends. The average annual electrification growth rate from 2014-2019 reached 60%, with more than 7.2 million plug-in electric vehicles (PEVs) on roads. However, this number was only approximately 17,000 in 2010 [3]. In 2020, despite lockdowns and manufacturing delays due to COVID-19 in the first half of the year, the annual growth of the electric vehicle market was 40% [4]. The total electric vehicle fleet size is expected to hit 50 million by 2025 and 140 million by 2030 [3]. With the emergence of PEVs, considerable technological and commercial breakthroughs have been achieved in autonomous driving. Many PEV manufacturers are equipping new car models with these technologies, e.g. Tesla's "Full Self Driving", BAIC Arcfox's autonomous driving, and Volvo's autonomous highway pilot. Furthermore, many autonomous driving software solution companies, such as Waymo and Aptiv in the U.S., Baidu and Pony.ai in China, and Ravin in Europe, are testing autonomous technologies on roads. Transportation electrification and autonomous driving are two major technologies that are expected to reshape urban mobility systems in the future. A prominent initial market is ride-hailing services with AEVs[145]. A study revealed that worldwide penetration of ride-hailing services was 8.3% in 2017, generating 44 billion USD of revenue and expected to increase by almost 5 times in 5 years [55, 143]. According to a market research, the global autonomous mobility market is expected to increase from 5 billion USD to 556 billion USD from 2019 to 2026 [79, 112]. Vehicle automation reduces the operation expenditure of fleet companies by cutting labor costs considerably [28, 75, 103]. Furthermore, as advanced eco-driving technologies are designed and deployed, AEVs are expected to achieve high energy efficiency, which further reduces operating costs [66, 94, 98, 169].

Therefore, the system design and its potential effect on society should be studied [83]. Determining the number of AEVs required in this ride-hailing market and supporting infrastructure is critical. The results are consequential for not just researchers but also city planners and policy makers [80]. The optimum number of AEVs and the supporting infrastructure are referred to as fleet management and charging infrastructure planning problems. Many studies have examined a holistic planning and management framework from the perspective of an urban system. Studies can be categorized into two approaches, namely simulation-based and operations research approaches. With the use of simulation tools, studies have focused on congestion pricing [67, 137], fleet re-balancing [38, 134], charging behaviors, and infrastructure siting and sizing [20, 21, 89, 134, 135, 156]. In the operations research approach, in addition to similar factors [132, 181], vehicle routing [78, 93, 120], fleet

sizing [71, 93, 183], pickup and delivery [71, 129], power and transportation network interactions [185] are considered. However, the two approaches exhibit distinct advantages and trade-offs. The simulation-based approach is designed for complex systems, but optimality and deterministic results are difficult to achieve [133]. The operations research approach can be used to compute the social optimum with defined metrics, but it is constrained by the network size. Among these studies, perhaps the most critical breakthrough was proposed in Alonso-Mora et al.[10] and Vazifeh et al.[155]. In these studies, a graph-theory-based operation approach was adopted, referred to as the minimal path covering problem on a vehicle-shareability network. This method demonstrated a precise approach to intelligently match conventional vehicles with trips and determine the size of a ride-hailing fleet. The approach proved to be computationally effective in a mobility dataset (150M+ trips) from a large network, in the New York Manhattan area. This method is the first that preserves both of the aforementioned advantages and, therefore, can be used as the foundation of this study.

In this study, we adopt and apply a tractable mathematical framework to simultaneously address the AEV fleet and charging infrastructure design and management problems in the context of a large urban mobility system. We expand the network to the entire New York Area (four out of five boroughs), where trips are more widely spread geo-spatially. In a previous study [155], dense mobility demands within only the Manhattan area shortened the inter-trip connection time. However, any vehicle could be matched with a request quickly. Consequently, the effect of fleet size reduction because of vehicle automation within a large area was overestimated. Furthermore, range anxiety from human driver and charging time constraints limit the adoption of electric vehicles [117]. Although range anxiety can be easily addressed with autonomy, the charging downtime of AEVs is considerable. It is critical to account for additional AEVs required to accommodate the loss of service capacity due to charging. In this paper, we provide insights into the optimal composition of the fleet size, battery size, infrastructure location, and charger capacity. The results of the study reveal that the dynamic interaction between fleet size and traffic congestion are critical. Finally, a techno-economic analysis is introduced not only to calculate the societal costs but also to quantify health benefits resulting from reduced PM2.5 emissions.

5.3 Methods

5.3.1 Data

We evaluated various datasets, including the raw mobility data recorded by the New York taxicabs, the transportation network open-sourced by the OpenStreetMap, the electricity generation fuels breakdown by the New York Independent System Operator.

Mobility data

The dataset we used contains data of more than 175 million trips a year, or 485,000 a day, for the New York City yellow taxi fleet during 2013. Yellow taxicabs licensed with the *medallions* are the only vehicles authorized to provide mobility services. A total of 13,437 medallions were issued in year 2013.

Four attributes, such as pickup date and time, dropoff date and time, pickup latitude and longitude, and dropoff latitude and longitude, were used to construct trips in this study. A trip T_i is formally defined by an array of four elements, (t_i^p, t_i^d, l_i^p, l_i^d), namely the pickup and dropoff times (capitalized T for trip and lower case t for time), the pickup and dropoff locations. However, additional post-processing and calculations were required to detail the transportation system conditions, such as the link (from physical intersection to intersection) travel time.

Travel time estimation

The mobility dataset provided only the pickup and dropoff locations. The exact path and segment speeds remain unknown. Because the link travel time information is key to the vehicle-shareability network, a large-scale heuristic method was developed [10, 49, 155] to compute the estimated link travel time for each traversed road segment $\{t_{ud} \mid \forall (u,d) \in \mathcal{S}\}$, where u and d denote the upstream and downstream intersections of a physical street and $\mathcal{S}$ is the set of all streets. The evaluation criteria was selected such that the average relative error between all estimated and actual trip travel times was minimized. The same method was extended and applied to every hour of the day to determine hourly traffic fluctuations, $\mathcal{T}^{\text{travel}} = \{t_{ud,t} \mid \forall (u,d) \in \mathcal{S}, \forall t \in \mathcal{T}^{24}\}$. An averaged hourly system speed profile is illustrated in Fig. 5.1. When $\mathcal{T}^{\text{travel}}$ is captured, the travel time between any two intersections u and d on the map $\mathcal{S}$ at a given time t can be determined using a defined routing algorithm, such as the shortest path/time routing. The details of the algorithm and the computation results are provided in Alonso-Mora et al.[10] and Donovan et al.[49], respectively.

Secondary traffic impact

The proposed framework considerably reduced the number of AEVs required to satisfy given mobility demands. Proper trip assignments and vehicle matching reduced not only the fleet size but also the deadheading mileage. Theses reduced mileage would induce traffic improvement and hence a secondary effect on fleet sizing. Therefore, we proposed Proposition 1. To analyze the secondary traffic effect induced by fleet optimization, we assumed that the change to traffic volume is proportional to the ratio change of the total societal vehicle mileage travelled. However, various types of vehicles contribute differently to the total VMT; this ratio among the private vehicles, taxis, trucks, and others are detailed in Blasio et al.[26]. In 2014, the VMTs of two key sectors, private and taxi vehicles, had a ratio of roughly 5 to 2; and other VMTs were negligible. We leveraged the NYC open source data, the road link volume data, and compared them with the estimated link travel time. Figure 5.2 shares

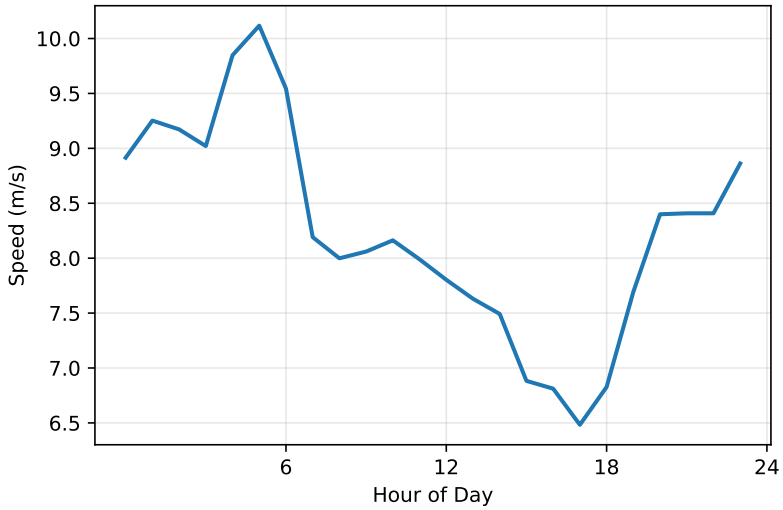

Figure 5.1: Averaged hourly system speed.

an example of the volume-time relationship, which is then fitted by a polynomial regression model.

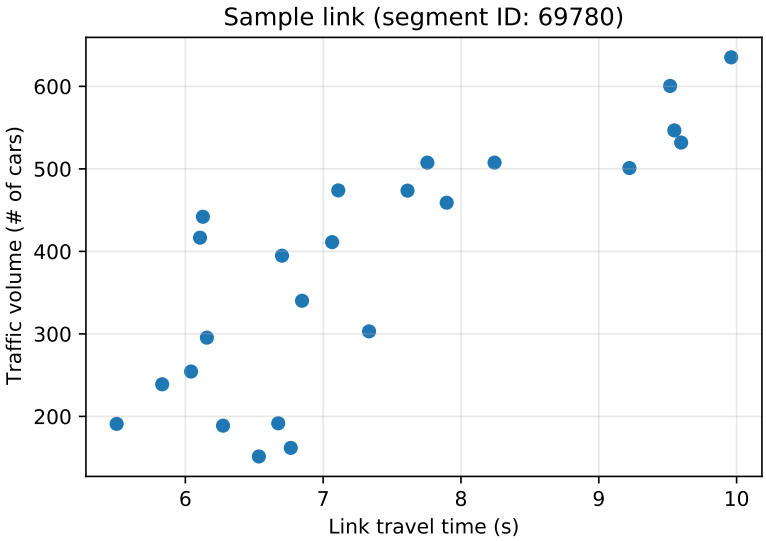

Figure 5.2: Cross-matched link volume-travel time graph.

We detailed the process in Fig.5.9b and specified the link travel time re-estimation as follows:

1. Calculate percentage of VMT change to the total taxi mobility VMT, δ_{VMT};
2. Calculate updated taxi mobility VMT ratio to the system, $\text{VMT}_{\text{taxi}}^{\text{updated}} = 2*(1-\delta_{\text{VMT}})$;
3. Calculate volume change ratio based on Assumption 1, $\delta_{\text{vol}} = 2/7 - \text{VMT}_{\text{taxi}}^{\text{updated}}/(\text{VMT}_{\text{taxi}}^{\text{updated}} + 5)$.

Given the output volume impact ratio, δ_{vol}, we identified and updated all link travel times based on the fitted regression model.

Proposition 1: Reduced unnecessary cruising reduces VMT and alleviates traffic congestion. The resulting traffic conditions further affect the fleet size planning strategies (closed-loop feedback).

Assumption 1: The ratio change to traffic volume is proportional to the ratio change to total VMT.

Electricity generation profile

AEVs emit zero carbon emission at the end-user level. Thus, the use of AEVs can considerably reduce the carbon footprint of the transportation sector. We traced the energy sources used to generate electricity [114] and calculated the carbon emission rates associated with various fuels at the hourly basis. The AEV fleet carbon intensity was then calculated according to the hourly fleet-level energy charging demands (Fig.5.14).

5.3.2 Key parameters of the model

The key parameters used to calculate the AEV upfront capital investment costs as well as the fleet management operation costs are summarized in Table 5.1. Environmental and health-related parameters, which are used for quantifying emission and health effects, are included.

5.3.3 Fleet sizing algorithm

The contributions from Vazifeh et al. [155] were considered in this study. The shareability network it proposed discussed the sharing of vehicles to connect and complete multiple trips. Our network methodology expanded this model but was more comprehensive and customized toward the AEV operations. The model considers the electric vehicle range constraints and downtime effect of the autonomous machines, both of which are essential for AEV fleet analysis.

Vehicle-shareability network

The vehicle-shareability network is based on a directed acyclic graph $V = (\mathcal{N}, \mathcal{E})$ to describe the relationships among trips $\mathcal{T}$. As illustrated in Fig. 5.3, a vertex $n_i \in \mathcal{N}$ in

Input Names	Values	References
Annual discount factor	0.06	[179]
Battery cost	\$200/kWh plus 30% fleet discount	[20]
CO2 emission (Well-to-wheel)	2.59 gCO2/mile	[138]
CO2 lifecycle emission - Hydro gas	26 tonne CO2e/GWh	[57]
CO2 lifecycle emission - Natural gas	499 tonne CO2e/GWh	[57]
CO2 lifecycle emission - Nuclear	29 tonne CO2e/GWh	[57]
CO2 lifecycle emission - Wind	26 tonne CO2e/GWh	[57]
Cost of charger	\$700/charger/kW + \$15/charger/kW/year	[20]
Cost of station	\$10 000 per location	[20]
Cost of electricity	\$0.12/kWh	[20]
Cost of vehicle automation	\$10 000 per vehicle	[20]
Cost of vehicle maintenance	\$0.04/mi	[20]
Cost of vehicle purchase	\$20 000 per vehicle	[20]
Effect Factor (EF)	290 DALY/kg PM2.5 inhaled	[64]
Emission Factor - brake (urban)	4.7 mg PM2.5/km-vehicle	[23]
Emission Factor - road abrasion (urban)	4.2mg PM2.5/km-vehicle	[23]
Emission Factor - tyre (urban)	6.1 mg PM2.5/km-vehicle	[23]
Emission Factor - tailpipe (light duty vehicle)	1.86 mg PM2.5/km-vehicle	[5]
Fuel efficiency	0.25 kWh/mi + 0.0006 kWh/mi per kWh battery capacity	[20]
Intake fraction	48 ppm	[13]
System horizon	20 years	[20]
Value of Statistical Life [1] (VSL)	location = 0, scale = 7.75, shape = 1.51 (million USD)	[99]

Table 5.1: Key parameters used in this work.

the graph represents a ride-hail/mobility request $T_i \in \mathcal{T}$, and an edge represents a feasible connection between two trips performed by the same vehicle in time sequence. Formally, considering two consecutive trips T_a and T_j with given dropoff and pickup time (t_a^d, t_j^p) and the travel time between (l_a^d, l_j^p), t_{aj}^{conn}, an edge can be connected on the graph only if $t_j^p - t_a^d \geq t_{aj}^{\text{conn}}$. Therefore, the edges indicate feasible paths for subsequent trips. A chain of connected nodes indicates the trip chain to be traveled by a vehicle. The minimum fleet size problem can then be translated into a minimum path cover problem. Studies have revealed that this problem is equivalent to the maximum matching problem on bipartite graphs, which can be solved by the Hopcroft–Kap algorithm in polynomial time $O(|\mathcal{E}||\mathcal{N}|^{1/2})$ [74]. This approach enabled computational efficient algorithms to realize precise and optimal solutions. More details are provided in previous studies [10, 124, 155].

Fleet size without range constraints

First, we started with AEVs of sufficiently large battery capacity. An ideal scenario without range constraints in mobility service was considered. This assumption is an equivalent scenario to operate the autonomous vehicles with convention internal combustion engines.

Stage 1. Limiting trip connection time

To reduce model complexity, the intertrip travel time t_δ was introduced. This more stringent connection time reduced the number of graph edges in Fig. 5.3. It has practical implications. When t_δ becomes infinitely large, the sequenced trips that are distant (in

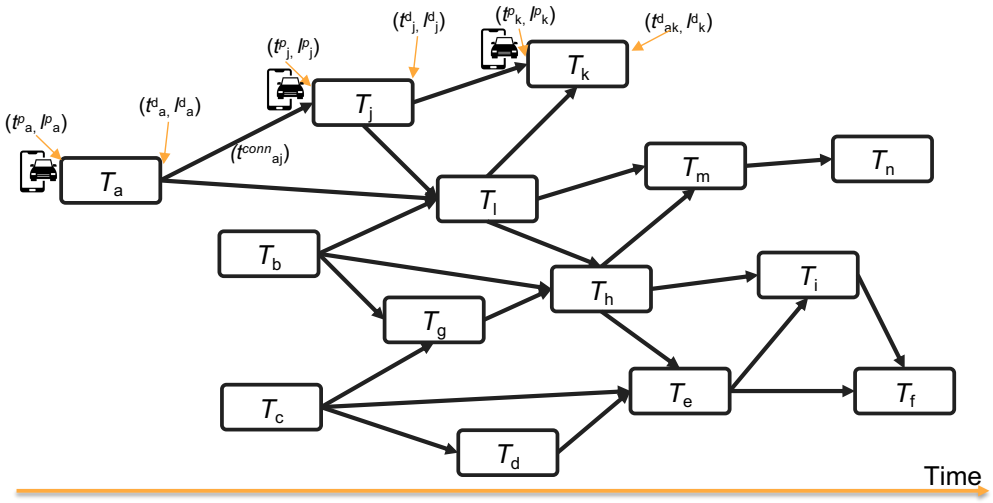

Figure 5.3: Vehicle Shareability Network: a directed acyclic graph.

space and/or in time) can be connected. However, it wouldn't be ideal to construct such a trip chain. It leads to long and unnecessary travel-to-pickup distances, results in worse emissions and exacerbates the traffic congestion. A candidate solution like this becomes trivial. Hence, in our setting, two trips are connected only if two conditions are satisfied, namely $t_\delta \geq t^p_j - t^d_a \geq t^{\text{conn}}_{aj}$ (Fig. 5.4). In our experiment, t_δ was set to 15 min (It was shown from the previous study [155] such that for allowable connection time t_δ more than 15 min, the effects on the fleet size and mobility service were negligible).

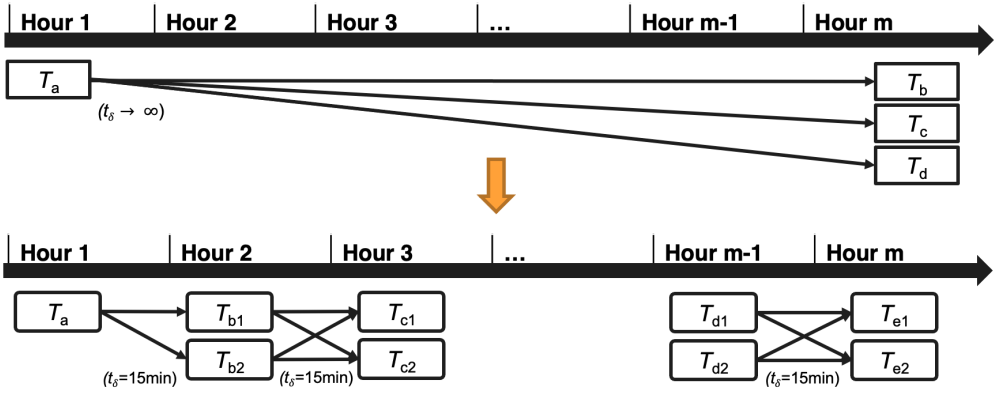

Figure 5.4: Stage 1 complexity control: Limit trip connect time to 15 min so that only neighboring trips are connected, both spatially and temporally.

Stage 2. Relaxing waiting time

To enable a further stage complexity control, we detailed the main behavioral difference between an AEV and a human-driven taxi as follows: allowing an AEV wait has lower economic burden than that of a human driver, who is paid hourly wage ($21.07/hour for Uber driver [42] and $14.77/hour for New York taxi driver [77]). The typical daily mobility demand patterns correspond to two peaks, one early in the morning (before work) and the other late in the afternoon (after work). Therefore, we first combined solved trip chains from Stage 1 as the pseudo-trips and introduced another parameter of time limit t^{down} (we set to 600 min, any long enough horizon should suffice) to reconstruct the shareability network (Fig. 5.5). An edge can be connected only if $t_\delta + t^{\text{down}} \geq t_j^p - t_a^d \geq t_{aj}^{\text{conn}}$. Thus, some AEVs can be parked and deactivated into the "sleep" mode during the period of demand trough and then be reactivated to when the second demand peaks (Fig. 5.6). Therefore, a further minimization of the fleet size can be achieved.

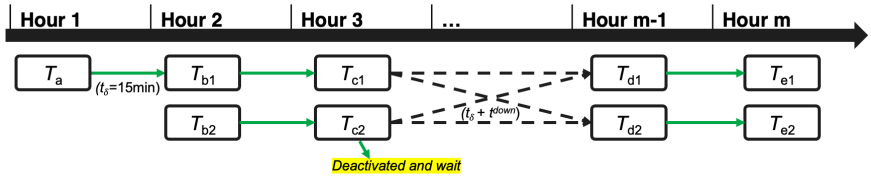

Figure 5.5: Stage 2 complexity control: deactivate AEVs to sleep and allow large time window to enable trips service that are temporally distant.

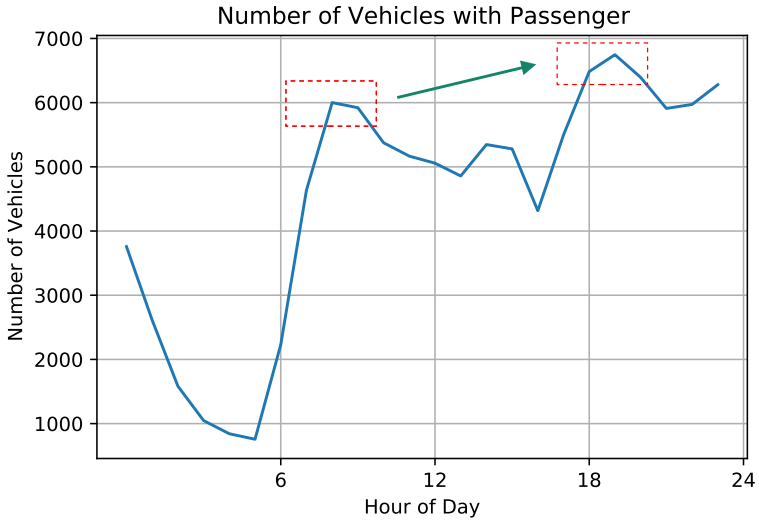

Figure 5.6: Daily dual demand peaks.

Fleet size with range constraints

We introduced the range constraint to the AEV fleet by introducing the AEV battery capacity limit B.

Step 1. Warm start without range constraints

This is the same step as mentioned previously. The outputs were the chains of trips $\mathcal{T}^{\text{chains}}$, each to be served by a conventional autonomous vehicle.

Step 2. Identify charging events in trip chains

We consider the given battery capacity B, energy efficiency η, and convert it to the effective driving range L^{DR} using the following formula:

$$L^{\text{DR}} = \frac{B}{\eta}. \tag{5.1}$$

By considering the identified trip chains T_i^{chain} in $\mathcal{T}^{\text{chains}}$, we identified the exact times and locations the charging events occur. The AEVs charge in three scenarios. First, when an AEV does not contain sufficient energy to perform the next trip or travel to the next charging station. The second is the "smart heuristic" scenario when an AEV has a considerably large time window until the next upcoming trip. Mathematically, $t_j^p - t_a^d \geq t^{\text{down-charging}}$ ($t^{\text{down-charging}}$ is set at 30 min) is satisfied between two trips T_j and T_a. Notably, $t^{\text{down-charging}} > t_{aj}^{\text{conn}}$, namely the period until the AEV needs to travel to the next pickup location is sufficiently long and is flexible to charge. The final situation is the "recovery" scenario in which by the end of the vehicle trip chain, the AEV is dispatched to recover its consumed energy, for the next-day mobility service.

Step 3. Reconstruct vehicle-shareability network

After Step 2 identification for each AEV i, we combined all upstream trips before the first identified charging event at t_i^{charge} as one super pseudo trip, $T_i^{\text{S-pseudo}} = \{T_i \mid t_i^d \leq t_i^{\text{charge}}, \forall T_i \in \mathcal{T}_i^{\text{chain}}\}$ (Fig. 5.5). We could re-chain all beforehand trips because any newly identified charging event at any time t^{charge} does not affect the upstream trips that already occurred. Thus, a novel vehicle-shareability network was constructed and all the subsequent trips were reset and re-optimized.

Step 4. Re-solve the fleet sizing problem

We re-solved the problem to determine a new set of trip chains, $\mathcal{T}^{\text{chains}}$. Next, a $T_i^{\text{chains}} \in \mathcal{T}^{\text{chains}}$ may look like: $\{T_i^{\text{S-pseudo}}, T_{i,x}, T_{i,y}, T_{i,z}, \dots\}$, where $t_i^{\text{S-pseudo},d}$, $t_{i,x}^p$, etc. respect the relevant conditions (Fig. 5.7).

Model complexity and convergence guarantee

We summarized the overall algorithmic flowchart in Fig.5.9a. This iterative algorithm can still be solved using the polynomial expression, with complexity $O(|T||\mathcal{E}||\mathcal{N}|^{1/2})$. Recall that the Hopcroft–Karp algorithm preserves a complexity of $O(|\mathcal{E}||\mathcal{N}|^{1/2})$ for solving the maximum matching problems in bipartite graphs [74]. The key of our algorithm is that only $O(|T|)$ iterations are required to combine and re-solve trips. Therefore, this algorithm guarantees termination. Furthermore, the algorithm typically converges considerably faster

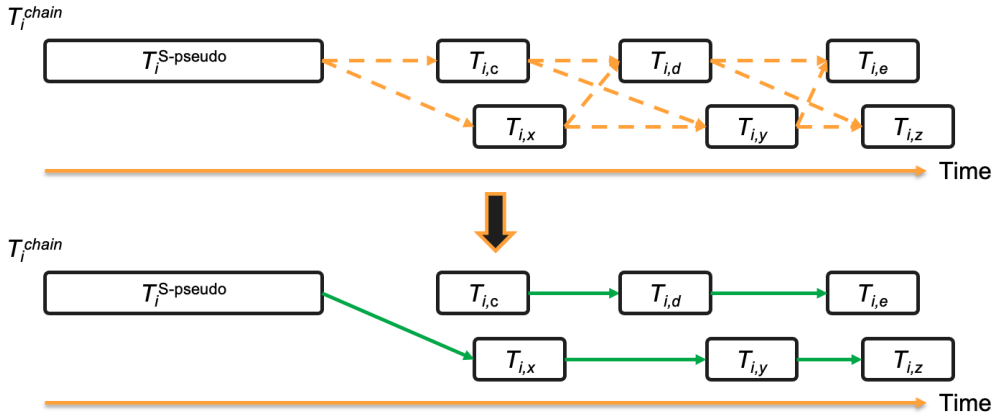

Figure 5.7: Re-optimize the newly constructed vehicle-shareability network. Green solid lines represent the new determined trip chain.

than the total number of time steps (Fig. 5.8). The intuition behind is AEV fleet charging need does not incur in every iteration. Only when a charging need is detected, would the algorithm reconstruct the vehicle shareability network and introduce new AEVs to dispatch. Secondly, the fleet size generally stabilizes after the peak hours. Hence, the algorithm converges much faster than the total number of time steps. The program may be pre-maturely terminated to accelerate the process as the number of the newly identified charging events yield an upper bound to the additionally required AEVs and the total fleet size.

5.3.4 Charging infrastructure planning

The output results of the aforementioned algorithm include all spatial and temporal information of the charging events. We adopted the classic K-means clustering method to determine the locations where charging infrastructure could be placed. This methods proved to be meaningful and computationally efficient [181]. We applied a probabilistic constraint to determine the number of required chargers at each charging station. This constrained programming embedded a service-level model [180, 181], which is subject to a tunable quality of service parameter α. Thus, the model guaranteed that under $(\alpha \times 100)\%$ of the time, an AEV was charged immediately upon arrival. Given the average charging requests λ_{tk} at location k during hour t, the minimum number of chargers n_k, was constrained as follows:

$$n_k \geq t^{\text{charge}}\lambda_k + \Phi^{-1}(\alpha)\sqrt{t^{\text{charge}}\lambda_k}, \tag{5.2}$$

$$\lambda_k = \max_t \lambda_{tk}, \tag{5.3}$$

where t^{charge} is the charging duration to full and $\Phi^{-1}(\cdot)$ is the inverse of the cumulative distribution function of the standard normal distribution. As Eqn.(5.2) indicates, the number of chargers is dictated by the expected peak hour charging demands and the arrival rate λ_k

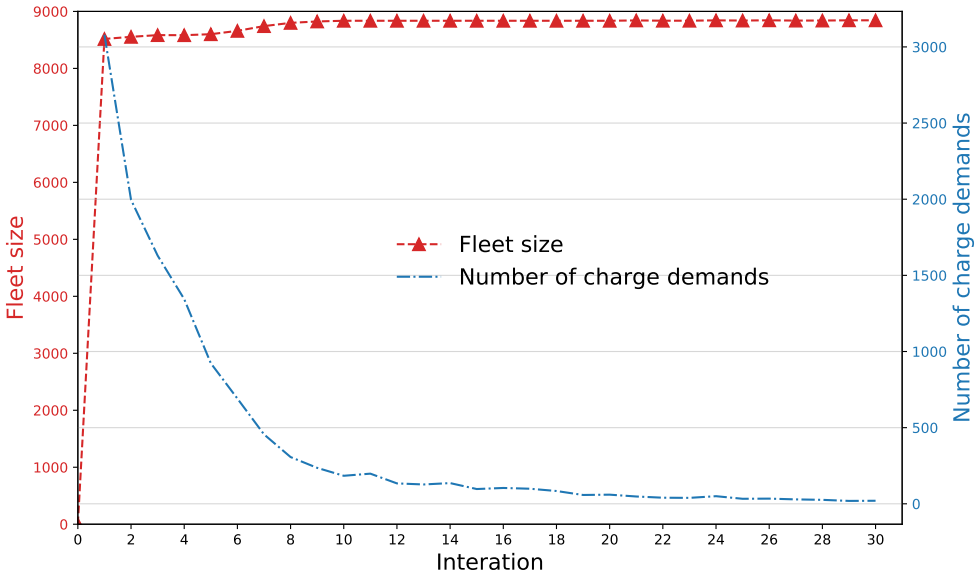

Figure 5.8: Convergence analysis, it is guaranteed to converge in $O(|T||\mathcal{E}||\mathcal{N}|^{1/2})$.

(first term); it is additionally affected by the excessive demands over the mean (second term). This phenomenon is covered in detail in previous studies[180, 181].

5.3.5 Calculating the capital recovery factor

The capital recovery factor (CRF) is calculated according to Eqn.(5.4), where n is the number of years and i is the discount factor. To incorporate the battery degradation cost in our financial assessment, we group the AEVs based on their daily charging frequencies. Essentially, for each group, there is a different n, which follows Eqn.(5.5). Finally, the battery degradation cost is proportional to each CRF.

$$CRF = \frac{i(1+i)^n}{(1+i)^n - 1}, \tag{5.4}$$

$$n^{\text{batt}} = \frac{\text{cycle life}}{\text{daily charging frequency} * 365 \text{ days/year}}. \tag{5.5}$$

5.3.6 Total cost calculation

$$C^{\text{total}} = \underbrace{\underbrace{\underbrace{CRF^{\text{veh}} * C^{\text{veh}} + CRF^{\text{batt}} * C^{\text{batt}}}_{\text{Fleet Cost in Fig.5.15}a} + \underbrace{CRF^{\text{infra}} * C^{\text{infra}}}_{\text{Infrastructure Cost in Fig.5.15}b}}_{\text{CAPEX in Fig.5.15}c} + \underbrace{C^{\text{oper}}}_{\text{OPEX in Fig.5.15}d}}, \tag{5.6}$$

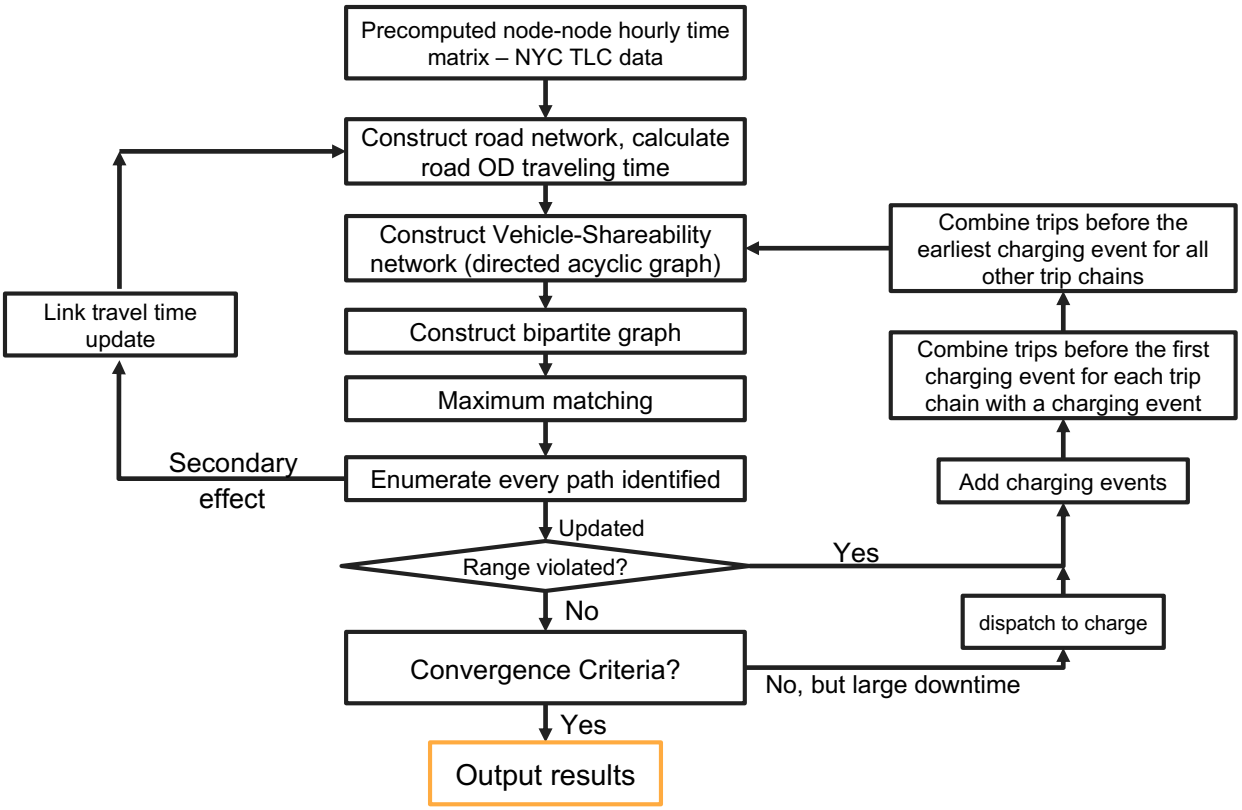

(a) Overall algorithmic flowchart, solvable in polynomial time $O(|T||\mathcal{E}||\mathcal{N}|^{1/2})$

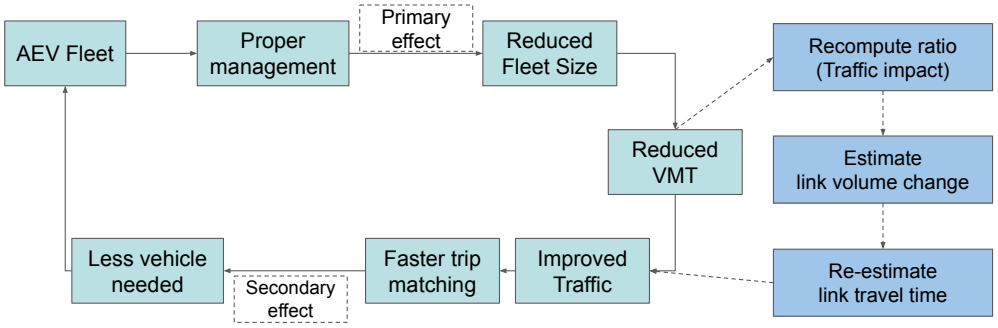

(b) Secondary traffic effect and link travel time update flowchart (expands from the left loop in Fig.5.9a above).

Figure 5.9: Algorithmic flowchart

where all CRFs follows the above Eqn.(5.4) calculation. For CRF^{veh} and CRF^{infra}, the time horizon spans 20 years (Table 5.1); whereas for CRF^{batt}, it follows the calculation done previously.

5.4 Results

5.4.1 Autonomous vehicle utilization

Fleet size reduction

The fleet had 13,437 authorized yellow taxicabs and covers all five boroughs, namely Manhattan, Bronx, Brooklyn, Queens, and Staten Island, including two airports, JFK and LGA [27]. Approximately 90.3% of the pickup events occur within the Manhattan area. The previous study [155] has revealed that a considerable fleet size reduction (down to 4,627 taxicabs) can be achieved with appropriate fleet management within the region. However, approximately 10% of the mobility demands are outside of this highly concentrated area, which results in long trip connections and increased vehicle deadheading travel. This study [155] does not recognize that trips within the Manhattan area are close and a vehicle can perform more trips within the Manhattan borough than in other boroughs. Therefore, the results tend to be overpromising for an integrated urban area. We adopted a novel fleet sizing methodology to the entire New York City area to addresses this limitation. The operational status of the fleet across a week is visualized in Fig.5.10. From the current 13,437, the fleet size can be reduced to 8,100 during peak demands, which is a 40% reduction.

Effect of fleet automation on traffic congestion

Studies have revealed that since the advent of ride-hailing services from 2010, traffic congestion and VMT have increased [47, 59, 121, 125]. Major cities and regions across the world, such as New York City (U.S.) [47, 121, 125], the San Francisco Bay Area (U.S.) [47, 59, 121], Shenzhen (China) [110], Mumbai, New Delhi, and Bangalore (India) [1] have been covered in these studies. The results revealed a global concern for increased traffic congestion from ride-hailing services. According to the projected growth of this market, VMT will increase drastically, further exacerbating congestion.

This study highlighted the necessity of proper fleet management, which can potentially reduce traffic congestion. During demand lulls, autonomous vehicles can be rested instead of futile cruising on roads, circumventing deadheading behaviors [47]. This effectively reduced the number of vehicles on the road. Therefore, traffic congestion caused by ride-hailing services can be alleviated through fleet automation. To determine the effect of fleet sizes on the traffic system, we adopted a novel approach to quantify the reduction of the VMT and presented it on the system network. Because VMT dominates the traffic conditions [51, 62], it was used to quantify traffic volume changes. The improvement of traffic congestion resulting from fleet management optimization was quantified and revealed to reduce traffic volume by 10%. This also increased the average system traffic speed from 8.91 to 9.25 m/s, which is a 4% improvement (spatial changes detailed in Fig.5.11). As a direct result, we found a non-trivial economic effect on societal travel time savings, quantified in the next section. Furthermore, speed increase enabled better vehicle and customer connectivity, that is less vehicles needed for the same demands. Another iteration of fleet size optimization

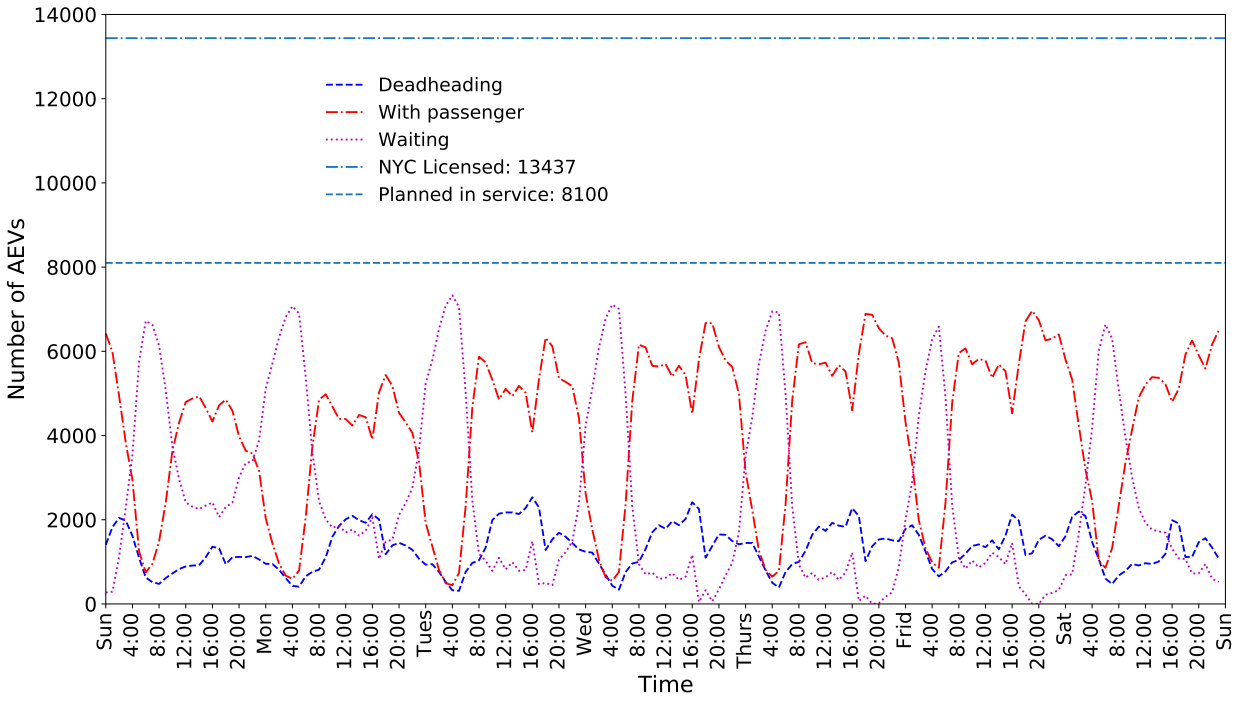

Figure 5.10: Autonomous conventional vehicle (AV) fleet operation status across a 7-day week. "In service" denotes AVs in service on the road; "Deadhead" is AVs driving to next pickup locations; "With passenger" denotes AVs driving on road with passengers; "Waiting" denotes AVs resting to avoid unnecessary cruising. "NYC Licensed" indicates the total number of licensed taxi (Medallions) in New York City (year 2013), 13,437, whereas with proper fleet management the fleet size can be reduced to 8100, which is approximately a 40% reduction.

was conducted and we achieved further reduction in fleet sizes (see Fig.5.11). On average, 62 vehicles (about 1% of the entire fleet) were eliminated (difference between the green and black curve). This overall finding is particularly relevant to social planners and policy makers.

Traffic economic analysis

To quantify the economic effect of reduced traffic congestion, we computed the product of total travel time saved by the cost of travel time. A common method in literature to measure the cost of travel time is presented in Gwilliam[68] and Litman[87]. The hourly cost of travel time is equal to 30% of a household income per hour. The median value of New York household annual income is reported to be $53,843 [46]. We then converted the value to an hourly basis and multiplied it with the estimated total amount of time saved. The

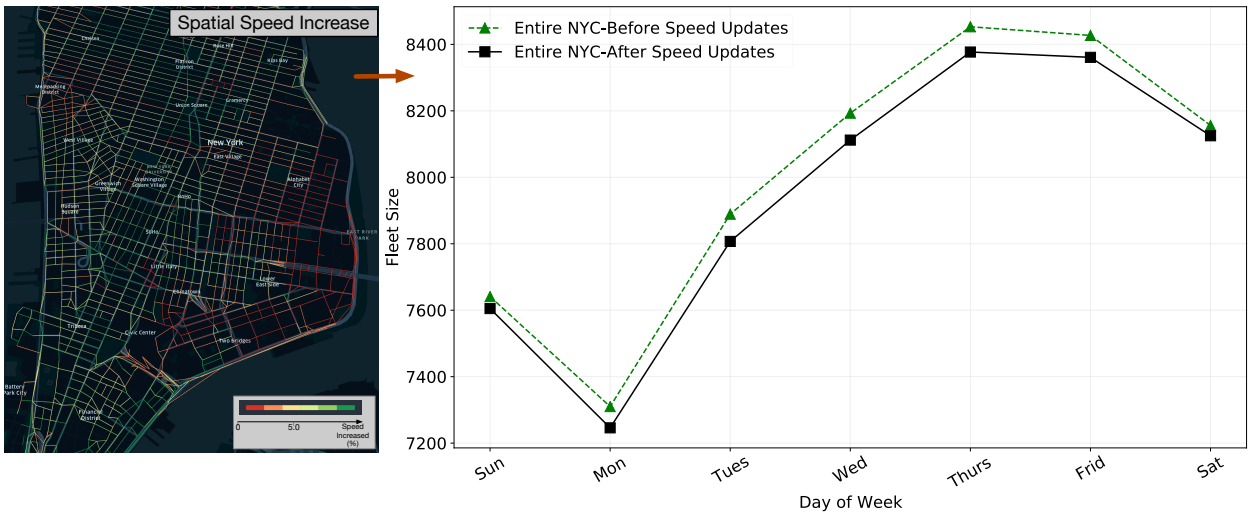

Figure 5.11: Fleet size reduction on proper fleet management. The reduced deadheading VMT alleviated traffic congestion. Because of increased average speed, the fleet size could be reduced further. The speed increase across different links in space is detailed on the left hand side.

formulas to estimate the total economic effect is as follows:

$$\text{Total time saved} = \text{Total VMT/speed before} - \text{Total VMT/speed after} \approx 35\text{Million hours}, \tag{5.7}$$

$$\text{Societal savings} = \text{Total time saved} \times 30\% \text{ household hourly income} \approx \$255\text{Million}. \tag{5.8}$$

The annual total vehicle mileage travelled data is from the New York State Department of Transportation Office of Technical Services. The value increases from 18,759 million miles in 2016 to 18,944 miles in 2019, less than 0.1% increment. We assume annual travel pattern of this society remain the same level. Therefore, on average economic savings of more than $255 million a year can be achieved in New York City. Furthermore, we conduct a sensitivity analysis on the levels of the household income, detailed in Fig. 5.12. Namely, these scenarios are $53,843 (2013 median household income) [46], $71,117 (2020 median household income) [76], $93,196 (2013 mean household income) [122], and $105,304 (2020 mean household income) [76]. As we expect the annual household incomes to grow from year to year, the economic benefits of an improved traffic system will be more and more profound. As calculated in the "2020 Mean" scenario, the cost saving is estimated to be 500 million USD. Comparing the total value saved to the total annual equivalent financial burden, appropriate fleet management can benefit the entire community.

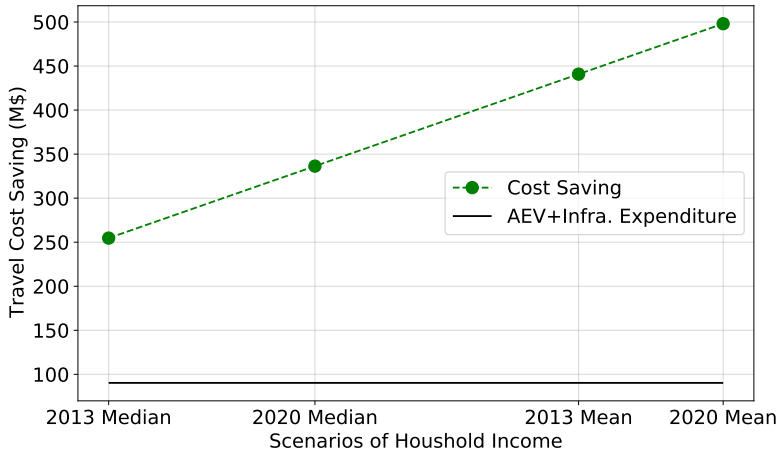

Figure 5.12: Cost savings estimated from reduced travel time (Million USD) in four scenarios. Namely, these scenarios are based on different levels of household income. The value we extracted from [46, 76, 122] are $53,843 (2013 median household income), $71,117 (2020 median household income), $93,196 (2013 mean household income), and $105,304 (2020 mean household income). The calculated values from these scenarios are reported to be at least 250 million USD. As we expect the annual household incomes to grow from year to year, the economic benefits of an improved traffic system will be more and more profound. As calculated in the "2020 Mean" scenario, the cost saving is estimated to be 500 million USD, far dominating the expected annual costs to deploy an AEV fleet for New York City (black solid line).

5.4.2 Effect of the driving range, charging infrastructure, and charging behaviors

In this section, we investigate the effect of charging behavior on effective fleet management. Charging may lead to considerable down times, preventing AEVs from providing mobility services. Therefore, more AEVs are required to satisfy demand [34]. Two factors, namely battery capacity (i.e., driving range) and charging power, simultaneously affect AEV mobility patterns. Specifically, a smaller battery and slower charging speed result in a higher downtime and deteriorates the service capability (if the number of chargers is fixed). The societal cost of AEVs with large batteries and fast charging speeds is substantially higher. Therefore, social planners should meticulously examine and identify the financial "sweet spot".

Effect of battery size and charging speed on AEV charging behaviors

We conducted geo-spatial and cross-sensitivity analysis with the following parameter settings. The battery size ranged from 50 kWh (Tesla Model 3, Nissan Leaf, VW ID.3) to 175 kWh (NIO ET7, Rivian, other future models),[2] and the charging speed varied from 25 kW (regular fast charging) to 175kW (Tesla Supercharger V2). A visualization of an example for the geo-spatial distribution of chargers is presented in Fig.5.13.

The average travel distance to the charging sites was capped at 1 mile, to ensure the chargers were conveniently accessible to most AEVs. In addition, a probabilistic constraint was adopted to ensure that 95% of the charging events may reach a station within 2 miles. Next, another probabilistic constraint was introduced to control station queuing. In this particular scenario (Fig.5.13), a total of 3,665 chargers were required to satisfy all AEV charging demands such that 80% of the time an AEV arrives to an available charger without waiting.

We conducted a cross-sensitivity study of various power levels and AEV battery sizes. The AEV fleet was set at full energy level as the initial condition. A vehicle was dispatched to charge when there was no sufficient energy to complete the next trip and route to the nearest charging station. When an AEV completed its daily service, it was dispatched to charge back up to the full level, but at a much slower rate ("rest and charge" mode) in preparation for the next day service. The temporal energy demands are plotted in Fig.5.14. As displayed, the power level did not affect the vehicles' charging patterns across the day, but vehicle battery size was influential. As the charging speed varied (same column), obvious changes in charging energy delivered were not observed when peak demands occurred. However, as the battery sizes of the AEVs varied (same row), both the quantity and time at which peaks occurred varied. For small battery sizes, bulk and high charging demands peaked in the afternoon. As the battery size increased, the bulk demands shifted to later in the day. Eventually, with high-energy AEVs, charging sessions only occurred at night.

Range anxiety and downtime due to charging are the two major factors that affect human mobility behaviors. The former influences drivers' decisions to charge, and the latter induces pure labor cost. It is expensive to leave a driver idle! Whereas for AEVs, who solely comply with control signals, range anxiety and downtime are alleviated.

Societal economic analysis

Economic cross-sensitivity analysis with regard to both the battery size and charging power were performed. From the perspective of charger powers, some of the resulting charging C-rates[3] may induce considerable damages or degradation effects to the battery packs. Detailing the battery model and quantifying the degradation cost are beyond the scope of this

[2]We assume energy-efficient computing and aerodynamic sensor stacks are implemented, meaning that there is negligible energy consumption trade-off between automation and electrification [101].

[3]C-rate is a normalized unit of battery charging speed, enabling comparison across battery's with different capacities [157]. Specifically, C-rate = (Power [kW])/(Energy Capacity [kWh]). For example, a 50 kWh battery charging at 100 kW will charge at a C-rate of 2C.

Figure 5.13: Geo-spatial distribution of charging infrastructure with parameter settings: 50 kWh battery AEVs and 50 kW chargers. Each green pin icon represents a sited charging station at the centroid of a cluster. The colored / clustered dots indicate locations where AEVs were signaled to route to a charging station. The number of required chargers were placed according to the peak charging demands to ensure quality of service.

study. The common approach to preserve battery life is to charge at less than 2C-rate [104]. Hence, we intentionally greyed out these (power, battery) combinations: (100kW, 50kWh), (125kW, 50kWh), (150kW, 50kWh), (175kW, 50kWh), (150kW, 75kWh), (175kW,75kWh). Nonetheless, small battery fleet tends to charge more frequent in a day and hence degrade quicker. We consider the cycle life of the lithium-iron phosphate (LFP) batteries in our

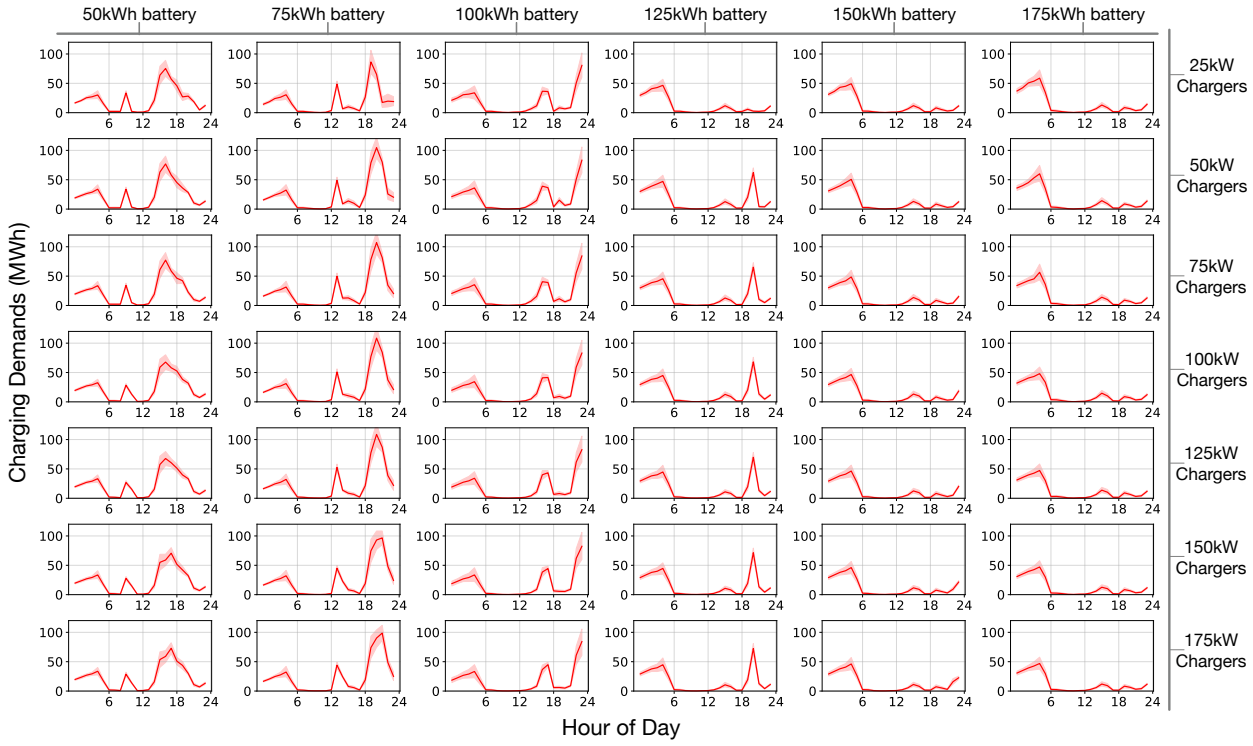

Figure 5.14: Temporal charging profile variation for combinations of AEV battery size and infrastructure power. Profiles under the same power setting are plotted on one horizontal level; vertical direction varies battery sizes.

calculation [130]. [4] These batteries are widely adopted in the current electric vehicle models. For each operation scenario (power, battery combination), we group the AEVs based on their daily charging frequencies. The annual battery degradation cost for each group is proportional to its corresponding capital recovery factor (CRF).

The investment cost consists of the capital cost to deploy an AEV fleet of a certain size (Fig.5.15a) and to place charging equipment across geo-locations (Fig.5.15b). A clear gradient is observed in Fig.5.15a. When the AEV fleet is equipped with large batteries (175kWh), the recommended fleet size is similar to the number required for AVs. This is intuitive since AEVs with large batteries rarely charge over the course of one day operation. In a scenario with smaller battery AEVs, more charging events happen during the day, resulting more AEVs needed. This is economical since the increased fleet purchase cost outpaced that of fleet size reduction. As a result, the capital investment cost of the fleet increased accordingly. On the other hand, in Fig.5.15b, the trend of the cost of infrastructure placement differed considerably because vehicle battery size dominated the fleet charging

[4] In our calculation, we conservatively estimate the battery degradation cost by assuming at worst case 1,700 cycles. This corresponds to the LFP batteries performing at 0 temperature [130].

pattern. Therefore, for 75- and 100-kWh AEVs, the charging demands were concentrated, which resulted in high peak demands (second and third columns in Fig.5.14). Therefore, more chargers are required to accommodate peak demand.

Considering hardware life, the total investment cost is converted to an annual equivalent value through the capital recovery factor and summarized in Fig.5.15c. In Fig.5.15d, the operational cost is the total annual energy charging cost plus maintenance posed to the AEV fleet. The total annual cost is summed and presented in Fig.5.15e. These combinations (50kW, 50kWh), (75kW, 50kWh) were found to be the most cost-attractive in the planning investment cost analysis (Fig.5.15c). In the operational cost analysis after deployment, the smallest battery fleet (50 kWh) was also the most appealing (Fig.5.15d). The net effect in Fig.5.15e revealed that an AEV fleet of (50kW, 50kWh) was the most cost-effective solution.[5] The total AEV fleet size is recommended to be 9,517, which is 15% higher than the AV fleet size.

This result is compelling and non-intuitively. We find that an AEV fleet with smaller battery capacity and a charging network with relatively low charging power minimizes total cost of ownership (TCO). This result flies counter to the trend of developing and deploying chargers with power 250 kW and higher [52, 152]. Meanwhile, high power chargers are concerning for grid operators since their peak power imposes stringent requirements on the local electrical infrastructure.

5.4.3 Environmental and health analysis

Implementation of an AEV fleet for ride-hailing services can provide multiple social benefits in addition to the aforementioned transportation time saving. Converting conventional vehicles to EVs circumvents the use of gasoline fuel and considerably reduces transportation carbon emission. In the next step, autonomous vehicles can be centrally optimized and operated. Unlike AEVs, human drivers purposely drive on road to search for customers, which results in unnecessary VMT and particular matter emissions. These particles are emitted from vehicle braking, tires, and road abrasion in the urban environment [23]. Avoiding unnecessary VMT hence reduces these particle emissions, which cause damage to human body and are potentially life threatening. In the following sections, we studied the two social benefits from the perspective of environment (CO2 emissions) and human body health (PM2.5 emissions).

Effect on environment

Unless complete transition to renewable energy is achieved, the use of an AEV fleet will still inevitably be associated with carbon emissions. In New York State, more than 40% of the electricity is generated from fossil fuels [113]. We matched the temporal charging profiles with the sources of electricity generation [114] during a particular time and calculated the

[5]This combination is the absolute total cost minimum in Fig.5.15e.

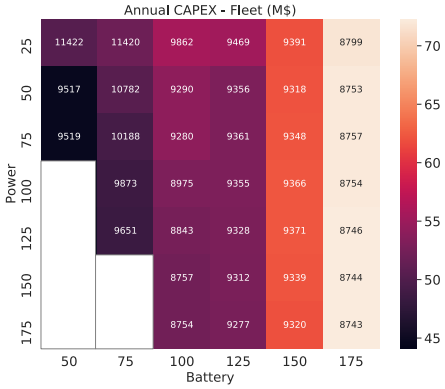

(a) Fleet purchase costs.

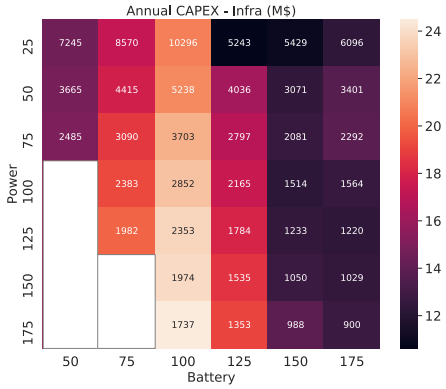

(b) Infrastructure placement costs.

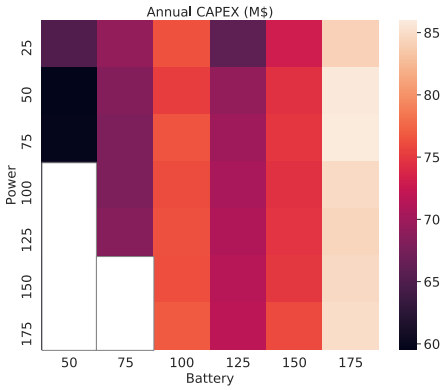

(c) Investment costs

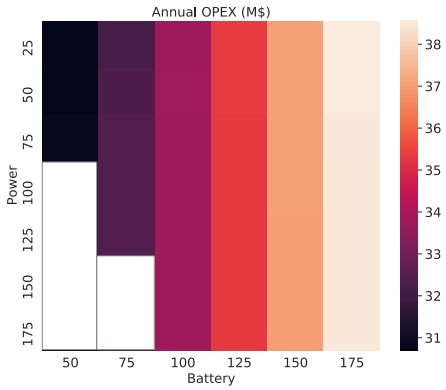

(d) Operational costs

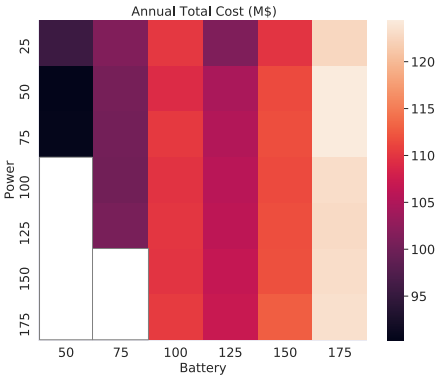

(e) Total costs

Figure 5.15: Summary of annual equivalent cost heat map. Top two heat maps (5.15a), (5.15b) are breakdown of the annual equivalent investment costs (CAPEX, (5.15c)). Annotation on each block in (5.15a) indicates the number of required AEVs and in (5.15b) indicates the number of required chargers. The operation costs in (5.15d) include the electricity and maintenance costs posed to the AEV fleet. The summation of (5.15a), (5.15b) is (5.15c) and the summation of (5.15c) and (5.15d) becomes (5.15e).

fleet temporal carbon emissions due to energy consumption. These temporal profiles under various combined settings of power and battery are displayed in Fig.5.16a. We focused on three prominent scenarios, namely the pre-electrification with conventional vehicles (ICEV), the least total cost of ownership (TCO), and the least CO2(eq) cases, and plotted them in Fig.5.16b. For the pre-electrification case, the total CO2 emissions were calculated based on the estimated Well-to-Wheel carbon intensity of gasoline [138]. For the least TCO case, it is identified from the power and battery cross-sensitivity analysis enlisted in Fig.5.15e. The optimal combination falls under the setting with 50kW charging infrastructure and 50kWh battery AEV fleet. This is a low power and small battery fleet setting. For the least CO2 emitting case, 25kW charging network and 125kWh battery fleet, it is identified from the calculations conducted in Fig.5.16a. It does not coincide with the previously identified least TCO case, particularly due to the differences in the AEV fleet charging patterns. The results revealed that natural gas and dual fuel[6] generation dominate the emission profile because they are two of the most carbon-intensive generation fuels and constitute more than 39% of the entire generation. Nonetheless, the substitution of an AEV fleet for the ride-hailing mobility service already eliminates 90% of carbon emissions (Fig.5.16b). This is achieved primarily via electrification, where internal combustion emissions are replaced by electricity generated from New York's electric grid.

Notably, in the small-battery fleet, EVs have to be charged multiple times during the day. Fossil fuel generation predominates during the charging down time and thus causes high carbon emissions. However, the penetration of renewable energies, such as solar [148], is expected to continue and rapidly grow. The New York State Energy Research and Development Authority (NYSERDA) announced plans to achieve 70% renewable and a zero-emission electricity by 2030 and 2040, respectively [146]. In the near future, carbon emissions resulting specifically from day charging can be considerably alleviated. Therefore, the most economic beneficial case (middle case in Fig.5.16b) may be more environment-friendly than the scenario portrayed in this study.

Effect on health

We adopted the "effect factor" (EF) [64, 73] as a measure of the relationship between the population intake of pollutants, like PM2.5, and the associated health effects. It describes the correlation between the change in mortality to the change in mass of PM 2.5 inhaled. The change in mortality is then converted to an economic measure by multiplying with the value of statistical life-year (VSLY). VSLY, converted from the value of statistical life, is the annual monetary amount that people are willing to pay for small reductions in their mortality risks [6]. The numeric values used in the study are recorded on Table 5.1.

The population economic impact of emissions due to PM2.5 is calculated as follows:

$$\text{Total PM2.5 emission} = \text{Total VMT} \times \text{PM2.5 emission/mile},$$

[6]Dual-fuel generators, which are primarily fueled by natural gas, but with capabilities to use other fuels, such as oil[114].

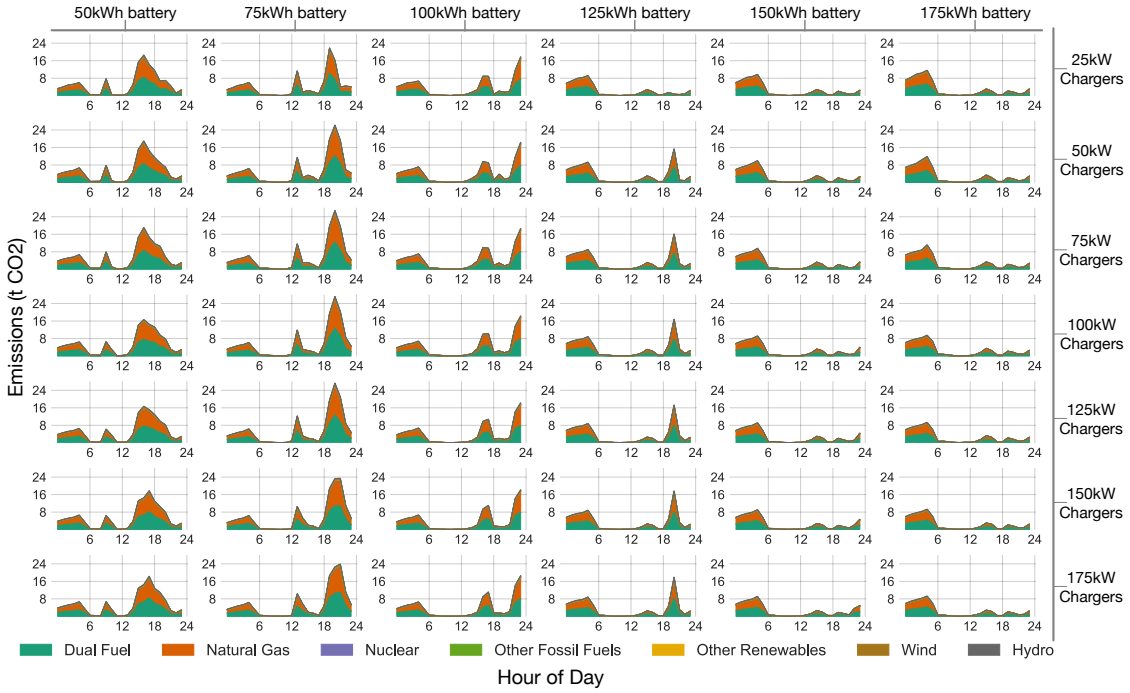

(a) Temporal CO2-equivalent emission profile for various combinations of AEV battery sizes and infrastructure powers. Profiles under the same power setting are plotted on one horizontal level; and the vertical direction denotes the battery sizes.

Figure 5.16: Details of CO2 and PM2.5 emissions. Note that CO2 emission tightly couples with the fleet's charging pattern, hence we differentiate two separate scenarios under the "Managed AEV", namely the "least TCO" and the "least CO2" (Fig.6b). The "least TCO" scenario does not coincide with the "lease CO2" scenario under current grid structure in New York State. Whereas PM2.5 emission tightly couples with the vehicle mileage travelled and thus no case separation is made.

$$\begin{aligned} \text{Population Intake (PI)} &= \text{Intake fraction (IF)} \times \text{Total PM2.5 emission}, \\ \text{Population economic impact} &= \text{PI} \times \text{EF} \times \text{VSLY}. \end{aligned} \tag{5.9}$$

We summarized the annual PM2.5 emissions particularly due to braking, tires, and road abrasion in Table 5.2 and visualized in Fig. 5.16c.[7] For the pre-electrified case, PM2.5 emission from the tailpipe was incorporated to the calculation (unit values were summarized in Table 5.1).[8] The resulted economic effect on population health was also analyzed, according

[7] A different view in Fig. 5.17.

[8] The U.S. Environmental Protection Agency imposes strict emission regulations on all types of vehicles. It has lowered the amount of pollution light duty vehicles can emit multiple times since the first standards were set in 1970 [5]. As a result, the unit PM2.5 emission from tailpipe alone contributes to only 11% of the total emission per kilometer. The majority nowadays comes from braking, tires, and road abrasion.

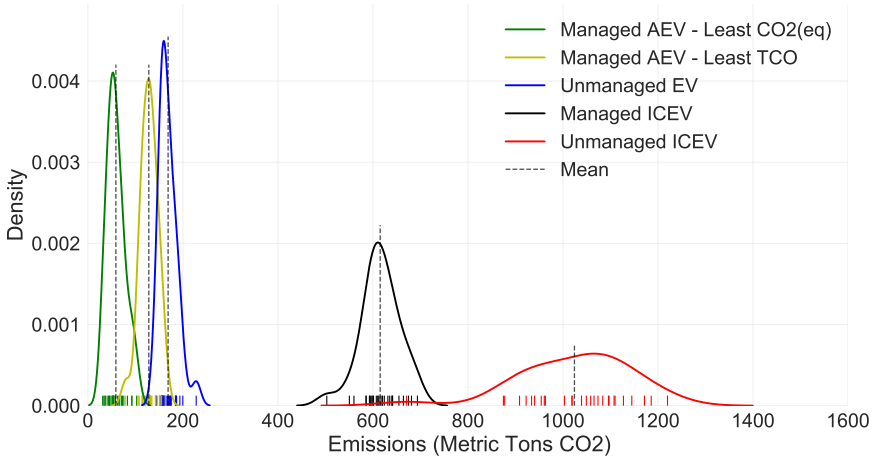

(b) Comparative impacts on fleet CO2 emissions due to electrification and management. Comparing the "Managed ICEV" and "Unmanaged ICEV" cases, we observe 40% CO2 emission reductions simply by introducing the fleet management strategy. Whereas, comparing the "Unmanaged EV" and "Unmanaged ICEV" cases, we observe about 84% changes. Electrification is the primary factor to cut down the greenhouse gas emission. Furthermore, fleet electrification and management together save over 90% CO2 emissions ("Unmanaged ICEV" vs. "Managed AEV").

Figure 5.16: Details of CO2 and PM2.5 emissions. Note that CO2 emission tightly couples with the fleet's charging pattern, hence we differentiate two separate scenarios under the "Managed AEV", namely the "least TCO" and the "least CO2" (Fig.6b). The "least TCO" scenario does not coincide with the "lease CO2" scenario under current grid structure in New York State. Whereas PM2.5 emission tightly couples with the vehicle mileage travelled and thus no case separation is made. (Cont.)

to the above Eqn.(5.9). As a result, simply electrifying the fleet of vehicles neither mitigates miles wasted for cruising nor reduces PM2.5 emissions by significant amount (first and second column of Table 5.2). The key is to introduce fleet management and a boost of progress is observed. By deploying a fleet of managed AEVs, over 45% of PM2.5 emission can be saved a year for the New York City. This translates to up to 250 million USD of NYC residence health condition improvement per year. More details can be found in Fig. 5.18, where we conducted a Monte-Carlo simulation to measure the economic impacts from the health improvements. The values of statistical life follow a Weibull distribution, estimated from 26 related studies recommended by the U.S. Environmental Protection Agency [6]. These values were converted to current values through an inflation calculator and subsequently to an equivalent value of statistical life-year following Eqn.(5.11). We acknowledge that we haven't accounted for secondary emissions, nor other emissions that cause respiratory health problems, so these calculations are underestimating health impacts. Nonetheless, this analysis provides a compelling reason for social planners and policy makers to transition ride-hailing vehicles to AEV fleets, even with the added infrastructure.

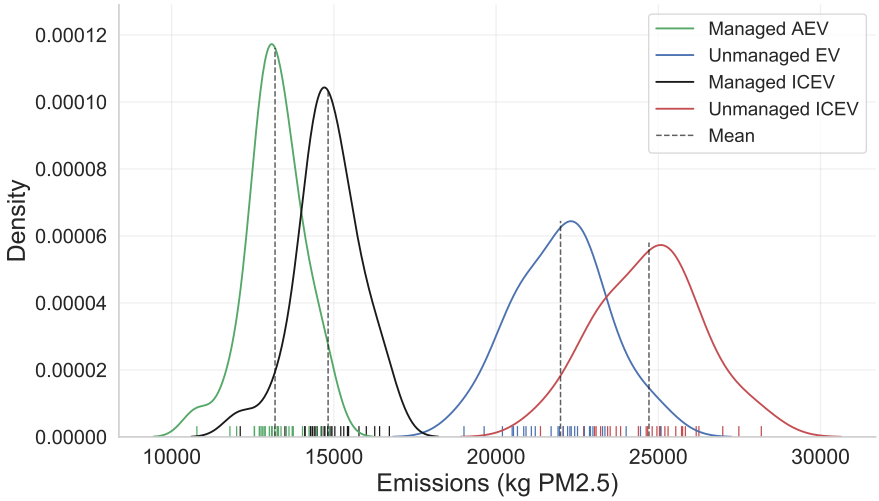

(c) The statistical distributions of the annual PM2.5 emissions particularly due to braking, tires, and road abrasion. For the ICEV fleet, PM2.5 emitted from the tailpipe is also accounted for. We observe that fleet management dominates the reduction effect on PM2.5 emission. Electrification contributes only 11% to PM2.5 reduction. Whereas together with management, 47% of the PM2.5 reduction can be achieved.

Figure 5.16: Details of CO2 and PM2.5 emissions. Note that CO2 emission tightly couples with the fleet's charging pattern, hence we differentiate two separate scenarios under the "Managed AEV", namely the "least TCO" and the "least CO2" (Fig.6b). The "least TCO" scenario does not coincide with the "lease CO2" scenario under current grid structure in New York State. Whereas PM2.5 emission tightly couples with the vehicle mileage travelled and thus no case separation is made. (Cont.)

5.5 Discussion, Policy Implication and Summary

The AEV fleet sizing results with management presented in this work are more practically implied. Comparing to the agent-based simulation approach, these results are more reliable. The optimal fleet sizing and infrastructure placement decisions are deterministic and recommputable. Comparing to the operations research approach, this work first stretches the geographic region. Vehicles tend to serve more trips in the denser area. Our approach not only recognizes the short trips in the denser area (Manhattan), but also account for the longer trips in the more sparse regions (outside Manhattan). This is more geospatially comprehensive. Secondly, this work considers the range constraints and charging downtime, two critical properties to an electric mobility service fleet. The fleet size requirement of a fleet with autonomous conventional vehicles is 15% smaller than the recommended size of an AEV fleet. This demonstrates that the two aforementioned behaviors tightly couple with the AEV fleet's service capability and hence heavily impact our fleet sizing result. Furthermore, we quantify the secondary traffic impact as a result of our fleet management strategy. This

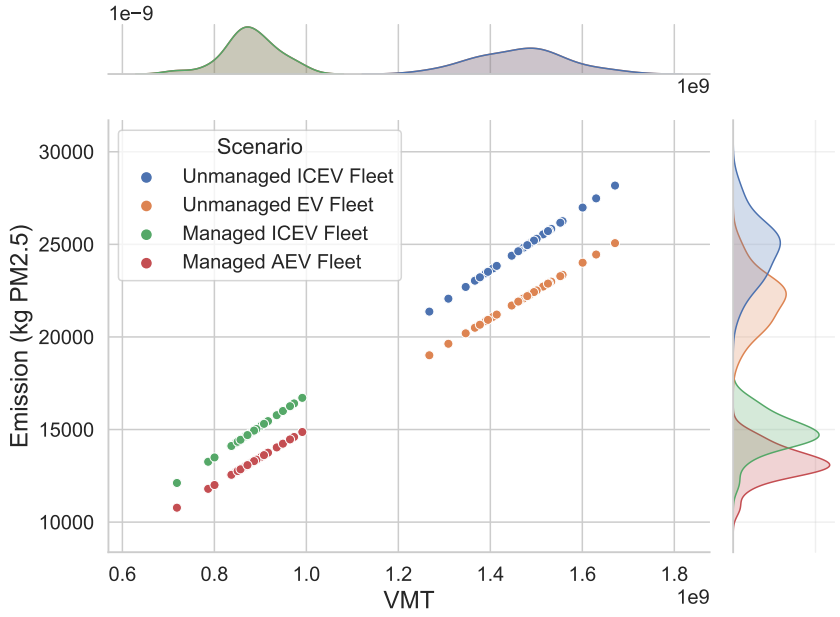

Figure 5.17: Annual PM2.5 emissions particularly due to braking, tires, and road abrasion. For internal combustion engine taxi fleet, PM2.5 emitted from the tailpipe is also accounted for.

Vehicle Type	Unmanaged ICEV Fleet	Unmanaged EV Fleet	Managed ICEV Fleet	Managed AEV Fleet
Total VMT (miles, 5%-95% CI)	916,110,061 (818,851,590 - 1,016,689,156)		549,487,373 (476,396,342 - 616,159,393)	
VMT with Passengers	416,884,181 (360,489,184 - 465,763,980)			
VMT for Deadheading	499,225,880 (458,362,406 - 550,925,176)		132,603,192 (115,907,158 - 150,395,413)	
CO2 Emission (Metric Tons CO2(eq))	1024.18 (875.59 - 1180.80)	168.85 (146.57 - 197.62)	615.28 (553.78 - 678.98)	58.92 (34.31 - 92.62)
PM2.5 Emission (kg)	24712.99 (22288.09 - 27309.31)	21986.64 (19829.27 - 24296.54)	14822.97 (13341.39 - 16357.72)	13187.70 (11869.56 -14553.14)

Table 5.2: Total vehicle miles travelled for mobility service and for deadheading (to pick up or relocate) are summarized in the second and third row. We see more than 70% deadheading mileage reduction with managed fleet. Together we summarize the annual CO2 and PM2.5 emission. We have also analyzed the 5- and 95- percentile impact, and given the confidence intervals. To view from left to right, two factors have changed, electrification and fleet management. The former is in particular beneficial to reduce the CO2 emission, whereas the latter contributes most to cut down PM2.5 emission.

perspective, to the authors best knowledge, has not been discussed elsewhere. The AEV fleet can be minimally sized to meet demand, thereby reducing traffic congestion, which

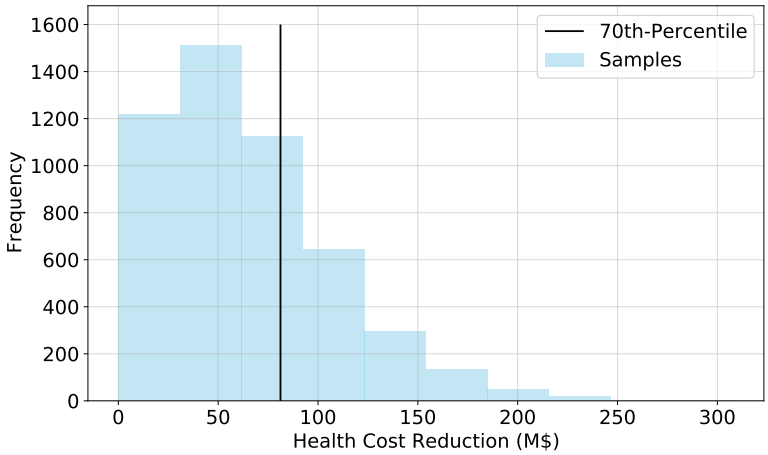

Figure 5.18: Health cost reduction (Million USD) based on the converted Value of Statistical Life Year (VSLY) sampled from EPA's Weibull Distribution [48]. At 70-percentile of the samples, the health cost is around 81 Million USD, which compensates the cost to deploy the AEV fleet completely. Under certain scenarios as we expect the value of statistical life to grow, the value to health improvement dominates the basic costs. This provides another compelling reason to the AEV fleet and the charging infrastructure deployment. To convert from Value of Statistical Life (VSL) to Value of Statistical Life Year (VSLY), we adopt from [41],

$$VSLY = \frac{rVSL}{1-(1+r)^{-L_{\bar{a}}}}, \tag{5.11}$$

where $-L_{\bar{a}}$ is the average number of remaining life years for the average person in the sample and r represents the discount rate. Note that this approach, however, fails to capture the underlying heterogeneity of the willingness to pay by different age groups. It is beyond the scope of this work to further discuss in depth, we refer interested readers to [41].

produces a feedback loop by increasing traffic speed and enabling further reduction in the AEV fleet size. By optimally designing the AEV fleet size, one can reduce travel times and costs throughout NYC. It's important to note that we are not considering every societal impact in this work, in particular the automation on labor and workforce development. The introduction of low cost AEV will undoubtedly reduce the number of driver jobs, but may also increase other opportunities, such as the remote assistance operators, mapping data collectors, etc. [43]. We don't anticipate forecasting the societal impact on this aspect. Although we do not endeavor in this work, here are some references [43, 45, 115] to this topic.

The infrastructure planning results also draw important insights. Since AEVs do not experience range anxiety nor time costs, it is not recommended to deploy large battery fleet and super high power charging infrastructure. This counter the current market hypes. In our analysis, we demonstrate that the scenario with large battery fleet and high power chargers may even deteriorate the societal economic benefits. In the most economic viable

scenario, the results assume deployment of 3,665 DC fast chargers throughout the NYC boroughs. To put into context, New York City has 339 public charging stations, in total 1000 electric vehicle supply equipment (EVSE) ports[9] according to the Alternative Fueling Station Locator[105].[10] Therefore, to efficiently deploy a fleet of AEVs, it will nearly triple the current size of the charging network. Although there are many incentives to purchase EVs (e.g. state and federal rebates), there are comparatively fewer incentives for deploying charging infrastructure. The recently passed Bipartisan Infrastructure Law will provide $7.5 billion to charging infrastructure development national wide, significantly offsetting the financial burden to stakeholders [119]. Nonetheless, to facilitate widespread deployment of charging infrastructure, we may need incentives that enable shared land use, and increased electrical capacity, in addition to financial assistance. Incorporating the availability and the value of lands and power capacity remains a challenge for conducting relevant studies. These information are important issues that need to be considered by policy makers.

Electrification and automation of ride-hailing vehicle fleets provide substantial environmental and health benefits. First, converting New York City's taxi fleet to AEVs can cut greenhouse gas emissions by over 90%. This is achieved primarily via electrification, where internal combustion emissions are replaced by electricity generated from New York's electric grid. As the NYISO further decarbonizes their electric generator fleet, the CO2 equivalent emissions will continue to reduce. Second, optimally dispatching a NYC AEV ride-hailing fleet reduces PM2.5 emissions by over 45%. The primary reason is not electrification, but rather automating dispatch to substantially reduce vehicle miles travelled. Reduced vehicle miles travelled results in less fine particulate emissions from tires, brakes, and road wear. The reduced PM2.5 emissions has direct impacts on respiratory health, thereby decreasing health care costs by up to 250 million USD per year in NYC. Policies that support electric mobility to reduce air pollution and their health impacts (e.g. PM2.5) should measure progress by electric vehicle miles traveled, not just the number of EVs sold. As we have seen, reduced vehicle miles travelled is critical to reducing PM2.5 emissions, since it reduces fine particulate emissions from tires, brakes, and road wear. Third, to reduce vehicle miles travelled ride-hailing vehicles should park and wait when demand is low. However, increasing parking spaces in NYC for ride-hailing vehicles comes in conflict with other productive uses of land. Further studies should be conducted to evaluate dramatically different city planning designs with transportation infrastructure optimized for ride-hailing AEVs that can park and wait, without consuming otherwise valuable space.

[9] This is as of September 2022.

[10] Alternative Fuels Data Center is a data center setup by the U.S. Department of Energy and the Alternative Fueling Station Locator is a database hosted by the center.

Chapter 6

Conclusion

6.1 Dissertation Summary

In this dissertation, four studies are presented to advance our understanding of optimally planning and operating the PEV charging stations, from atomic to network level. These works are carefully selected. They intend to demonstrate that optimization, control, and data analytics for transportation electrification are crucial to help reduce both the economic and infrastructural hurdles to widespread EV adoption at the consumer and industrial level. The summarized intellectual contributions are discussed in Section 1.2. The other related works can be referred to Section 1.3. This chapter finalizes with a discussion on the opportunities for future work.

6.2 Potential Directions for Interested Researchers

6.2.1 Human Decision Factors at Single Charging Station

One important assumption behind the case study in Chapter 3 is: the behavior model in the optimization well represents the generated choices in the simulations. This assumption is critical and can be validated if the DCM model accurately represents the actual choice behaviors. However, the validation requires an empirical research with human subjects in each specific application (since a generalizability is not guaranteed). We have physically constructed three sites, including on the campus of UC Berkeley and UC San Diego [1], that hold full functionalities of the described mechanism. Therefore, we will further calibrate and validate the model accuracy with the collected revealed preference data. In addition, we see the potential of the parking data in [167] to enhance the behavioral choice modeling accuracy, by integrating a temporal parking demand into the model. We also consider it for future work. Nevertheless, we have the intention to publicize the collected dataset (referred to [J3] in Section 1.3). It will enrich the community with the understanding of PEV drivers'

[1] the SlrpEV project, https://sites.google.com/berkeley.edu/slrpev

sensitivity to charging prices and schedules. It would also have a broader impact beyond the scope of workplace charging station. For utilities and game players involved in charging demand response service, the flexibility of users' time, energy and price need to be clearly identified [7, 40, 63, 136, 157]. This dataset can also be used by energy modeling research [69, 100, 182], system operations research [8, 184, 190], life cycle analytic [56, 107], PEV policy research [144, 150], etc.

6.2.2 The Non-Cooperative Nature Among Players and Vehicle Routing Problem

Two suggested aspects for future direction are extended from Chapter 4. Notice that a "one-to-multiple" generalization is provided in Section 4.7.4, it refers to multiple fleet operators charge through a single service provider. As the systems evolve and the interplay among entities become more complex, multiple fleet operators and multiple service providers may compete in the market at the same time. It's inevitable to extend the generalization to the "multiple-to-multiple" scenario. Furthermore, when different fleet operators compete for customers with bid offers, the Nash Game [108] shall be considered accordingly. This results a Stackelberg-Nash structure, which significantly increases the complexity of the problem. On the other hand, in the context of the trucking logistics, the daily customer cargo demands, time windows, electricity consumption along routes fluctuate. Many literature have incorporated the uncertainties in time and payloads [9, 109, 151]. Yet, incorporating the accurate energy consumption of electric trucks, and more importantly to validate the results, remain a clear gap.

6.2.3 Ride-hailing Fleet Management

In Chapter 5, we adopt a weighted graph to determine matching among vehicles and trips. The weights solely depend on the estimated travel time. However, it's recommended to have finer modeling, incorporating various factors such as road grades, energy consumption, etc. The enhanced weighted graph can be tailored to different routing strategies, such as the most energy conserved or the least polluting matching. As a future research direction, we recommend studying the online optimal dispatch for AEV recharging. Rather than recharge upon battery depletion, AEVs can be pre-dispatched to recharge at non-busy hours and be fully prepared for the peak period to secure high profits. They can also be pre-commanded to recharge in a manner that minimizes system-wide peak power demand.

Appendix A

Nomenclature

Definitions/Abbreviations

PEV Plug-in electric vehicle

SoC Battery state of charge

Indices/Sets

ω/Ω Index/set of charging demand scenarios

i/I Index/set of PEVs

$i/\mathcal{A}_m$ User set with service option m

$i/\mathcal{I}$ User set at charging station, $\mathcal{I} = \mathcal{A}_{\text{flex}} \bigcup \mathcal{A}_{\text{asap}}$

$m/\mathcal{M}$ Alternative/option set available at charging station. $\mathcal{M} = \{\text{flex, asap, leave}\}$

$t, \tau/T$ Index/set of specific time interval of a day

Parameters

Δt Duration of each sub-hourly time interval (hour)

Δt_i^{itc} i^{th} PEV's interchange time (hour)

E_i^{req} Desired needed energy of user i, in [kWh]

η Charger efficiency

η Efficiency during charging

$\text{p}^{\max}$ maximum charging power rate, in [kW]

π_ω Probability of occurrence of scenario ω

T_i Planned departure time of user i

ξ_i Fixed overstay penalty for existing customer i, in [\$/h]

ζ_i Fixed charging price for existing customer i, in [\$/kWh]

B_i i^{th} PEV's battery capacity

c^{ch} Per-unit cost for charger (\$)

c^{ed} Per-unit electricity demand charge cost ($/kWh)

c^{loss} Per-unit cost for load shedding ($/kWh)

c_D Utility rate for demand charge, in [$/kW]

c_t Utility rate for electricity at time t, in [$/kWh]

c_t^{e} Per-unit cost for electricity consumption at time interval t ($/kWh)

$c_{\text{oper}}^{\text{itc}}$ Per-unit cost for interchange ($/operation)

$c_{\text{plan}}^{\text{itc}}$ Per-unit cost for plug-in energy demand interchange ($/kWh)

$e_i^{\max}$ i^{th} PEV's maximum energy possibly acquired by its battery

e_i^{need} i^{th} PEV's required energy when departs

e_i^{pmax} i^{th} PEV's maximum plug-in energy

e_i^{pneed} i^{th} PEV's minimum (required) plug-in consumption

$e_{i,\tau}^{\text{p}+/-}$ i^{th} PEV's plug in energy upper/lower bound at time τ

p^{rated} Charger's rated charging power

$p_{\max/\min}^{\text{tran}}$ Local transformer power upper/lower bound

$p_{i,\tau}^{\text{p}+/-}$ i^{th} PEV's plug in power upper/lower boundary at time interval τ

SoC_i^{d} i^{th} PEV's expected departure SoC

$t_i^{\text{a/d}}$ i^{th} PEV's arrival/expected departure time

Variables

T^{overstay} Overstay duration, in [h]

$D_{\tau/t}$ Station peak power at control horizon time-step τ or global time t, in [kW]

$e_{i,t}$ Accumulative added energy level for user i at time t, in [kWh]

$G_{\tau/t}$ Station charging load at control horizon time-step τ or global time t, in [kW]

P_t PEVs aggregate power profile at time interval t

P_t^{grid} Net grid power at time interval t

P_t^{loss} PEVs unsatisfied aggregate power demand at time t

P_t^{pitc}	PEV's aggregate plug-in power demand shed due to interchange at time t
P_t^{p}	PEVs aggregate plug-in power demand at time t
$p_{i,t}$	Charging power for user i at time t, in [kW]
$S_{i,t}$	i^{th} PEV plug in status at time interval t, 1 for plugged in, 0 otherwise
$S_{i,t}^{\text{itc}}$	i^{th} PEV interchange status at time interval t, 1 for interchange, 0 otherwise
X	Number of chargers
y_i^{m}	Per-unit overstay penalty for option m for user i, in [\$/h]
z_i^{m}	Per-unit price for option m for user i, in [\$/kWh]

Appendix B

Supplementary Information for Chapter 2

B.1 Cost Calculation of Interchange in Real Life

In practice, Tesla has implemented a penalty policy to disincentivize the overstaying issue. Tesla charging facility users are penalized by the "idle fee." For detailed rates, refer to [84]. Here, we simply adopt the pricing policy \$1/minute for the supercharger and perform conversion as follows to obtain the cost of interchange for our public level-2 charging station planning model:

- It's assumed that the delay for a human to interchange for the charger is half an hour.
- The level-2 AC charger to DC supercharger cost ratio is simply $\frac{\$4000}{\$60{,}000} = 0.067$ [2];
- $c^{\text{itc}}_{\text{oper}} = \$1/\text{minute} \times 30\text{minute/time} \times 0.067 = \$2.01$;
- According to Eqn.(B.2),
  $c^{\text{itc}}_{\text{plan}} = \frac{c^{\text{itc}}_{\text{oper}}}{p^{\text{rated}} \cdot (\Delta t^{\text{overstay}} - \Delta t^{\text{itc}})} \approx \$0.3/\text{kWh}.$

B.2 Cost Calculation of Interchange with Robot

Since to the authors' best knowledge, there has not been a work addressing the cost of the interchange issue, an estimation of the interchange costs via automation (e.g. robots) is as follows:

- We assume automatic machines (robots) exist to perform the interchange during real time operation. As a cost reference, a commercial house cleaning robot that is capable of self-navigating and avoiding barriers is sold at around \$300 on the market [12]. In order for a robot to perform plug-in/unplug operation, more advance mechanical

controls are involved. Thus, we quintupled the price and assumed the cost of an interchange robot is at \$1500.

- For the robots, we assume 2000 cycles of battery lifetime, each of which supplies up to 6 hours of usage. We also assume that the machine is able to perform interchange operation 12 times per hour (5 minutes for one operation). Therefore, over the span of the machine lifetime, it is able to perform 60,000 interchange operations and on average, $c^{\text{itc}}_{\text{plan}} = \$0.003/\text{kWh}$.

B.3 Simulation Model

In this section, we use a simulator to validate our planning results. That is, we examine the station performance with the optimal number of chargers, X, during real time operation. We formulate an optimization model with interchange mechanism for real time control. Note that during the planning stage, it is unreasonable to model all individual interchange events of the chargers, as they are affected by the real time status of the charging station, including the operation status, customers actual arrival and departure profiles, etc. Therefore, an aggregate model is applied. However, in the simulator, the controller will see the actual demand as the PEVs arrive. It will then provide real time decisions on when to interchange and how many interchanges to be performed at each time stamp.

The operational objective is to minimize the annual operation cost associating with the delivered electricity, penalty resulted from unsatisfied demand, interchange operation cost, and demand charge. To conduct a simulation in a practical sense, we assume the station operator can only perform charging operations on the existing PEVs at the station, and future demand remains unknown until new PEVs arrive. Therefore, the charging operation is based on a rolling horizon optimization simulation procedure [178][19][189]. The system operator optimizes the energy allocation to the connected PEVs on a 15-minute basis; the time horizon length is 7.5 hours, which help address the overnight charging PEVs. We seek to provide optimal coordinating charging service but acknowledge the trade-off of computation complexity and optimality. In addition, the interchange mechanism is incorporated into the model, and the resulting optimal solution will decide whether interchange occurs on any specific PEV. The model is formulated as a mixed integer programming as follows:

$$\min_{\substack{P_{i,t},P^{\text{loss}}_{i,t},\\ S_{i,t},S^{\text{itc}}_{i,t},P^{\text{grid}}_{\max}}} \sum_t \sum_i \left(c^{\text{e}}_t P_{i,t} + c^{\text{loss}} P^{\text{loss}}_{i,t} + c^{\text{itc}}_{\text{oper}} S^{\text{itc}}_{i,t}\right) \Delta t + \frac{1}{30} c^{\text{ed}} P^{\text{grid}}_{\max} \tag{B.1a}$$

subject to:

$$0 \le P_{i,t} + P^{\text{loss}}_{i,t} \le p^{\text{rated}}, \quad \forall i, \forall t, \tag{B.1b}$$

$$0 \leq P_{i,t} \leq p^{\text{rated}} S_{i,t}, \quad \forall i, \forall t, \tag{B.1c}$$

$$\sum_{\tau=t_i^{\text{a}}}^{t_i^{\text{d}}} \left(P_{i,\tau} + P_{i,\tau}^{\text{loss}}\right) \eta \Delta t \geq e_i^{\text{need}}, \quad \forall i, \tag{B.1d}$$

$$S_{i,t} = \begin{cases} 0, & \text{PEV disconnected} \\ 1, & \text{PEV plugged in to charger,} \end{cases} \tag{B.1e}$$

$$S_{i,t}^{\text{itc}} = \begin{cases} 0, & \forall i, \forall t \notin \left(t^{\text{a}}, t^{\text{d}}\right] \\ |S_{i,t} - S_{i,t-1}|, & \forall i, \forall t \in \left(t^{\text{a}}, t^{\text{d}}\right] \end{cases}, \tag{B.1f}$$

$$\sum_i S_{i,t} \leq X, \quad \forall t, \tag{B.1g}$$

$$P_t^{\text{grid}} = \sum_i P_{i,t} + p_t^{\text{base}} \leq P_{\text{max}}^{\text{grid}}, \quad \forall t, \tag{B.1h}$$

$$P_t^{\text{grid}} \leq p_{\text{max}}^{\text{tran}}, \quad \forall t, \tag{B.1i}$$

$$P_{i,t} \geq 0, \quad P_{i,t}^{\text{loss}} \geq 0, \quad \forall t, \tag{B.1j}$$

$$S_{i,t} \in \{0,1\}, \quad S_{i,t}^{\text{itc}} \in \{0,1\}, \quad \forall t. \tag{B.1k}$$

where f$P_{i,t}$ is the charging power of PEV i during time interval t; $P_{i,t}^{\text{loss}}$ is the unsatisfied power demand. Variable $S_{i,t}$ denotes the plug-in status of PEV i during time interval i and $S_{i,t}^{\text{itc}}$ denotes whether an interchange event occurs. Similar to the planning model, there is a cost trade off between the number of times interchange is performed, and the number of chargers. The more chargers are installed, the less interchange operations are needed. Constraints (B.1b) and (B.1d) describe the power and energy lower and upper bounds at individual PEV level. Constraint (B.1e) specifies the plug-in status binary variable $S_{i,t}$, and consequently (B.1c) restricts the power delivered to the each PEV. Further, the total number of plug-in PEVs is upper bounded by the available chargers - Constraint (B.1g). Constraint (B.1f) indicates one interchange operation, which is associated with costs to be accounted for in the objective function. Constraints (B.1h) and (B.1i) are local distribution system and transformer limits. Lastly, (B.1j) and (B.1k) are the domain constraints.

Remark 2: In operation, the per-unit interchange cost, $c_{\text{oper}}^{\text{itc}}$ (USD/operation) is different from the one at the planning stage, $c_{\text{plan}}^{\text{itc}}$ (USD/kWh). However, they are correlated through the following formula:

$$c_{\text{plan}}^{\text{itc}} = \frac{c_{\text{oper}}^{\text{itc}}}{p^{\text{rated}} \cdot \left(\Delta t^{\text{overstay}} - \Delta t^{\text{itc}}\right)}, \quad \text{where } \Delta t^{\text{overstay}} > \Delta t^{\text{itc}} \tag{B.2}$$

where $\Delta t^{\text{overstay}}$ is the average overstay time and Δt^{itc} is the average interchange time. This means the PEV on average will overstay $\Delta t^{\text{overstay}}$ without interchange, but Δt^{itc} with interchange after being fully charged.

B.3.1 Simulation Results

A summary of simulation results is presented in Table.B.1. The simulation runs over 336 days, in which a total of 11932 charging sessions take place. All charging requests information is real data and comes from Cal Poly San Luis Obispo campus. The station controller with interchange successfully deliver sufficient charging to 11235 sessions and fail to the rest 697. The overall success rate is around 94%. This results corresponds well with our planning initiative, reliability factor $\epsilon = 0.1$. Moreover, the operation performance is more robust could be due to the fact that our controller runs on real time, constantly adjusts and re-optimizes through a feedback loop.

Table B.1: Simulation Summary over a Year

Total Number Sessions	Success	Failure	Success Rate
11932	11235	697	$\geq$94.1%

An example of simulation result in Fig.B.1. During peak hours, which in this case is around 8am to 4pm (typical school hours, there are at most 40 EVs come to the station/park at the station at the same time requesting charging service. Without proper management, the station operator will need to install at least 40 chargers on site to satisfy the demands. However, we satisfy all the demands with only 18 chargers when overstay issue is taken into account during planning and interchange during real time operation.

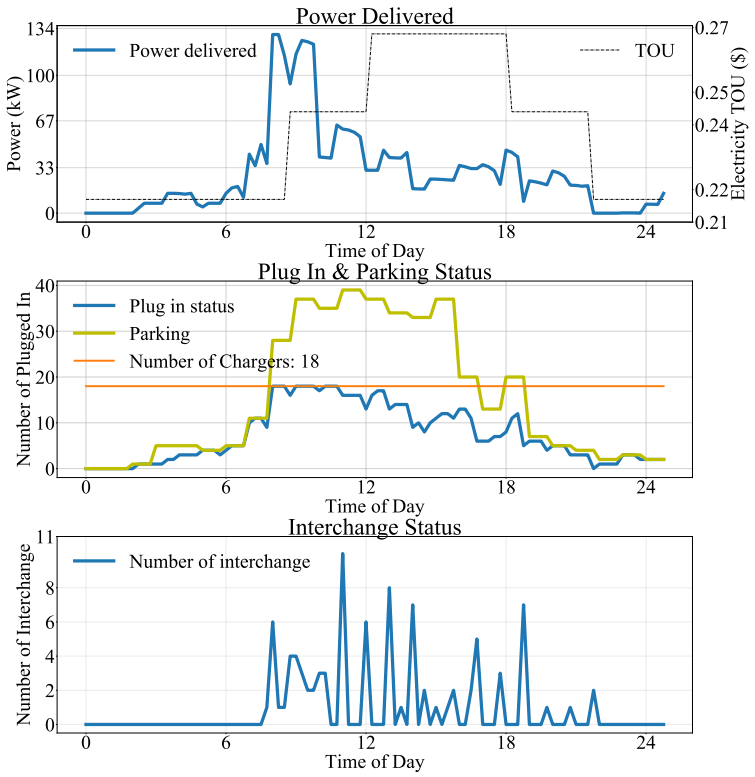

Figure B.1: Simulation result on Dec. 6th.

Appendix C

Supplementary Information for Chapter 3

C.1 Reformulation Process and Proof

C.1.1 Compact Form Representation

To describe formulations in the compact form, we would denote a long array x, which consists of new and existing customers charging profile, p and the corresponding energy profile e. We then rewrite the objective function (3.17) as

$$\begin{aligned}
&\min_{z\in\mathcal{Z}} \ \mathrm{sm}(\Theta z)_{\mathrm{flex}} \cdot (\min_{x\in\mathcal{X}} \ f_{\mathrm{flex}}(z,x)) \\
&\qquad + \mathrm{sm}(\Theta z)_{\mathrm{asap}} \cdot (\min_{x\in\mathcal{X}} \ f_{\mathrm{asap}}(z,x)) && \text{(C.1)}\\
&\qquad + \mathrm{sm}(\Theta z)_{\ell} \cdot f_{\ell}(z) && \text{(C.2)}\\
&= \min_{z\in\mathcal{Z},x\in\mathcal{X}} \ \mathrm{sm}(\Theta z)^{\top} h(z,x), && \text{(C.3)}
\end{aligned}$$

where

$$\mathrm{sm}(\Theta z)_j = \frac{\exp\theta_j^{\top} z}{\sum_{i\in\mathcal{M}} \exp\theta_i^{\top} z}, \ \ \forall j \in \mathcal{A}, \tag{C.4}$$

$$h(z,x) = \begin{bmatrix} f_{\mathrm{flex}}(z,x) \\ f_{\mathrm{asap}}(z,x) \\ f_{\ell}(z) \end{bmatrix} \tag{C.5}$$

$$z = \begin{bmatrix} z_{\mathrm{flex}} & z_{\mathrm{asap}} & y & 1 \end{bmatrix}^{\top}, \tag{C.6}$$

$$\Theta = \begin{bmatrix} \theta_{\mathrm{flex}} & \theta_{\mathrm{asap}} & \theta_{\ell} \end{bmatrix}^{\top}, \tag{C.7}$$

$$\mathcal{Z} \text{ is the domain of } z, \tag{C.8}$$

$$\mathcal{X} \text{ is the domain of } x, \text{ satisfying (3.1)-(3.6).} \tag{C.9}$$

C.1.2 Reformulation to Multi-block Convex Problem

Note that the softmax function is a non-linear and non-convex function, and hence the problem (C.3) is non-convex. We reformulate the problem into a *multi-block* convex problem by investigating the problem structure and applying the Fenchel-Young inequality theorem.

First, by introducing variable v, we rewrite the problem (C.3) as

$$\min_{z\in\mathcal{Z},x\in\mathcal{X}} \quad v^\top f(z,x), \tag{C.10a}$$

$$\text{where } \; v = \mathrm{sm}(\Theta z). \tag{C.10b}$$

Note that the objective function in Eqn. (C.10a) is a three-block *multi-convex* with respect to z, x, and v. However, the non-convex equality (C.10b) is added and we will reformulate it as a bi-convex constraint in the following section.

Bi-convex Representation of Eqn. (C.10b)

Consider the Log-Sum-Exponential function

$$\mathrm{lse}(u) = \ln\left(\sum_{j\in\mathcal{A}} \exp(u_j)\right). \tag{C.11}$$

Given $u \in \mathbb{R}^n$,

$$\mathrm{lse}(u) = \ln(1^\top \exp(u)), \tag{C.12}$$

$$\nabla \mathrm{lse}(u) = \mathrm{sm}(u), \tag{C.13}$$

$$\text{where } \; \exp(u) = [\exp(u_1)\dots\exp(u_n)].$$

The convex conjugate (a.k.a. Legendre-Fenchel transformation) of Log-Sum-Exponential is defined as

$$\mathrm{lse}^\star(v) \triangleq \max_u u^\top v - \mathrm{lse}(u). \tag{C.14}$$

From [29], the convex conjugate of LSE reads

$$\mathrm{lse}^\star(v) = \begin{cases} v^\top \ln(v) & \text{if } v \geq 0 \quad \text{and } 1^\top v = 1, \\ \infty & \text{otherwise} \end{cases} \tag{C.15}$$

Let $\mathcal{V} \triangleq \{v \| \; v \geq 0, \quad 1^\top v = 1\}$ denote a set of finite discrete probability distributions. The Fenchel-Young inequality reads

$$\mathrm{lse}^\star(v) - u^\top v + \mathrm{lse}(u) \geq 0, \; \forall u, \; \forall v \in \mathcal{V}. \tag{C.16}$$

The equality in Eqn. (C.16) is true *if and only if*

$$u_\star = \text{argmax}_u u^\top v - \text{lse}(u). \tag{C.17}$$

$u_\star$ is a maximizer since Log-Sum-Exponential is convex and differentiable for all u. The first-order optimality condition for Eqn. (C.17) derives

$$v = \nabla \text{lse}(u_\star) = \text{sm}(u_\star). \tag{C.18}$$

Hence, the following suffices

$$\text{lse}^\star(v) - u_\star^\top v + \text{lse}(u_\star) \leq 0 \iff v = \text{sm}(u_\star). \tag{C.19}$$

Now, we can replace the inequality constraint in Eqn. (C.19) with the equality in Eqn. (C.10b).

Then, replace $u_\star$ with Θz in Eqn. (C.19), i.e.,

$$\text{lse}^\star(v) - v^\top(\Theta z) + \text{lse}(\Theta z) \leq 0. \tag{C.20}$$

We relax the above inequality by introducing a precision parameter ε as $\text{lse}^\star(v) - v^\top(\Theta z) + \text{lse}(\Theta z) \leq \varepsilon$. This inequality represents a *bi-convex* set w.r.t. (z, v).

Reformulation of Eqn. (C.10) **into Multi-block Convex Problem**

Eventually, the original problem (C.10) is reformulated and relaxed as

$$\begin{aligned} \min_{z\in\mathcal{Z}, x\in\mathcal{X}, v\in\mathcal{V}} \quad & v^\top f(z, x) \\ \text{subject to:} \quad & \text{lse}^\star(v) - v^\top(\Theta z) + \text{lse}(\Theta z) \leq \varepsilon, \end{aligned} \tag{C.21}$$

which is *three-block* convex w.r.t. (z, x, v).

C.1.3 Block Coordinate Descent (BCD) Algorithm

The Block Coordinate Descent algorithm [162] is effectively solves a multi-convex problem and we apply it to solve the problem in Eqn. (C.21). An update of each variable (z, x, v) solves a convex problem. Details of the algorithm are presented in Algorithm 2.

Note that each update of the variables solves a strongly convex problem where the objective function (C.10a) is differentiable with a Lipschitz continuous gradient. Hence, the BCD algorithm has a linear convergence rate [22]. As a result, there is high practical value since it enables real-time implementation.

Algorithm 2: Block Coordinate Descent Algorithm

Init : $z^{(0)} = z_0, x^{(0)} = x_0, v^{(0)} = \mathrm{sm}(\Theta z_0)$
$F^{(0)} = v^{(0)\top} f(z^{(0)}, x^{(0)})$

while $\|F^{(i+1)} - F^{(i)}\| > \epsilon$ **do**
  $x^{(i+1)} = \mathrm{argmin}_{x \in \mathcal{X}} \quad v^{(i)\top} f(z^{(i)}, x)$
  $z^{(i+1)} = \mathrm{argmin}_{z \in \mathcal{Z}} \quad v^{(i)\top} f(z, x^{(i+1)}) + \mu(\mathrm{lse}(\Theta z) - (\Theta z)^\top v^{(i)})$
  $v^{(i+1)} = \mathrm{argmin}_{v \in \mathcal{V}} \quad v^\top f(z^{(i+1)}, x^{(i+1)}) + \mu(\mathrm{lse}^\star(v) - (\Theta z^{(i+1)})^\top v)$
end

Bibliography

[1] Saharsh Agarwal, Deepa Mani, and Rahul Telang. "The impact of ride-hailing services on congestion: Evidence from indian cities". In: *Indian School of Business* (2019).

[2] Josh Agenbroad and Ben Holland. *Pulling Back the Veil on EV Charging Station Costs*. 2018. URL: https://rmi.org/pulling-back-veil-ev-charging-station-costs/.

[3] International Energy Agency. *Global EV Outlook 2020*. 2021. URL: https://webstore.iea.org/download/direct/3007 (visited on 05/01/2021).

[4] International Energy Agency. *How global electric car sales defied Covid-19 in 2020*. https://www.iea.org/commentaries/how-global-electric-car-sales-defied-covid-19-in-2020 Accessed: 2021-05-01. 2021. URL: https://www.iea.org/commentaries/how-global-electric-car-sales-defied-covid-19-in-2020 (visited on 05/01/2021).

[5] United States Environmental Protection Agency. *Light Duty Vehicle Emissions*. 2017.

[6] United States Environmental Protection Agency. *Mortality Risk Valuation*. 2020. URL: https://www.epa.gov/environmental-economics/mortality-risk-valuation#means.

[7] Polina Alexeenko and Eilyan Bitar. "Achieving Reliable Coordination of Residential Plug-in Electric Vehicle Charging: A Pilot Study". In: *arXiv preprint arXiv:2112.04559* (2021).

[8] Yassir A Alhazmi and Magdy MA Salama. "Economical staging plan for implementing electric vehicle charging stations". In: *Sustainable Energy, Grids and Networks* 10 (2017), pp. 12–25.

[9] Somayeh Allahyari, Saeed Yaghoubi, and Tom Van Woensel. "The secure time-dependent vehicle routing problem with uncertain demands". In: *Computers & Operations Research* 131 (2021), p. 105253.

[10] Javier Alonso-Mora et al. "On-demand high-capacity ride-sharing via dynamic trip-vehicle assignment". In: *PNAS* 114.3 (2017), pp. 462–467.

[11] Department of Energy Alternative Fuels Data Center. *Electric Vehicle Charging Station Locations*. 2018. URL: https://www.afdc.energy.gov/fuels/electricity_locations.html#/find/nearest?fuel=ELEC.

[12] *Amazon house cleaning robot*. 2018. URL: https://www.amazon.com/iRobot-Roomba-Vacuum-Connectivity-Carpets/dp/B06XRT2B3P/ref=sr_1_1_sspa?s=industrial&ie=UTF8&qid=1535064752&sr=1-1-spons&keywords=irobot&psc=1.

[13] Joshua S Apte et al. "Global intraurban intake fractions for primary air pollutants from vehicles and other distributed sources". In: *Environmental science & technology* 46.6 (2012), pp. 3415–3423.

[14] Ludwig Arnold. *Random dynamical systems*. Springer Science & Business Media, 2013.

[15] Miguel Asensio, Gregorio Muñoz-Delgado, and Javier Contreras. "Bi-level approach to distribution network and renewable energy expansion planning considering demand response". In: *IEEE Transactions on Power Systems* 32.6 (2017), pp. 4298–4309.

[16] Sangjae Bae, Sang Min Han, and Scott Moura. "Modeling & Control of Human Actuated Systems". In: *IFAC-PapersOnLine* 51.34 (2019), pp. 40–46.

[17] Sangjae Bae, Sang Min Han, and Scott J Moura. "System Analysis and Optimization of Human-Actuated Dynamical Systems". In: *American Control Conference (ACC), 2018*. IEEE. 2018.

[18] Sangjae Bae et al. "Inducing Human Behavior to Alleviate Overstay at PEV Charging Station". In: *2020 American Control Conference (ACC)*. IEEE. 2020, pp. 2388–2394.

[19] Somil Bansal et al. "Plug-and-play model predictive control for electric vehicle charging and voltage control in smart grids". In: *Decision and Control (CDC)*. IEEE. 2014, pp. 5894–5900.

[20] Gordon S Bauer, Jeffery B Greenblatt, and Brian F Gerke. "Cost, Energy, and Environmental Impact of Automated Electric Taxi Fleets in Manhattan". In: *Environ. Sci. Technol.* 52.8 (2018), pp. 4920–4928.

[21] Gordon S Bauer et al. "Electrifying urban ridesourcing fleets at no added cost through efficient use of charging infrastructure". In: *Transportation Research Part C: Emerging Technologies* 105 (2019), pp. 385–404.

[22] Amir Beck and Luba Tetruashvili. "On the convergence of block coordinate descent type methods". In: *SIAM journal on Optimization* 23.4 (2013), pp. 2037–2060.

[23] David CS Beddows and Roy M Harrison. "PM10 and PM2. 5 emission factors for non-exhaust particles from road vehicles: Dependence upon vehicle mass and implications for battery electric vehicles". In: *Atmospheric Environment* 244 (2021), p. 117886.

[24] Arpita Biswas, Ragavendran Gopalakrishnan, and Partha Dutta. "Managing overstaying electric vehicles in park-and-charge facilities". In: *arXiv preprint arXiv:1604.05471* (2016).

[25] Eilyan Bitar and Yunjian Xu. "Deadline differentiated pricing of deferrable electric loads". In: *IEEE Transactions on Smart Grid* 8.1 (2016), pp. 13–25.

[26] Bill de Blasio. *For-Hire Vehicle Transportation Study*. 2016. URL: https://www1.nyc.gov/assets/operations/downloads/pdf/For-Hire-Vehicle-Transportation-Study.pdf.

[27] Michael R. Bloomberg and David Yassky. *The 2014 Taxicab Fact Book*. 2014. URL: https://www1.nyc.gov/assets/tlc/downloads/pdf/2014_tlc_factbook.pdf.

[28] Patrick M Bösch et al. "Cost-based Analysis of Autonomous Mobility Services Cost-based Analysis of Autonomous Mobility Services". In: *Transport Policy* 64.May (2017), pp. 76–91.

[29] Stephen Boyd and Lieven Vandenberghe. *Convex optimization*. Cambridge university press, 2004.

[30] Timothy Brathwaite and Joan L Walker. "Asymmetric, closed-form, finite-parameter models of multinomial choice". In: *Journal of choice modelling* 29 (2018), pp. 78–112.

[31] Maurizio Bruglieri, Simona Mancini, and Ornella Pisacane. "The green vehicle routing problem with capacitated alternative fuel stations". In: *Computers & Operations Research* 112 (2019), p. 104759.

[32] Thomas S Bryden et al. "Rating a stationary energy storage system within a fast electric vehicle charging station considering user waiting times". In: *IEEE Transactions on Transportation Electrification* 5.4 (2019), pp. 879–889.

[33] Claire Buysse and Ben Sharpe. *California's Advanced Clean Trucks regulation: Sales requirements for zero-emission heavy-duty trucks*. Tech. rep. The International Council on Clean Transportation, July 2020. URL: https://theicct.org/sites/default/files/publications/CA-HDV-EV-policy-update-jul2020.pdf.

[34] Zachary P Cano et al. "Batteries and fuel cells for emerging electric vehicle markets". In: *Nature Energy* 3.4 (2018), pp. 279–289.

[35] ChargePoint. *All Roads Lead to e-Mobility: Insights from 10 Years of Electric Vehicle Charging Data*. 2017. URL: https://info.chargepoint.com.

[36] Kalpesh Chaudhari, Nandha Kumar Kandasamy, Ashok Krishnan, et al. "Agent-Based Aggregated Behavior Modeling for Electric Vehicle Charging Load". In: *IEEE Transactions on Industrial Informatics* 15.2 (2019), pp. 856–868.

[37] Huimiao Chen, Zechun Hu, Haocheng Luo, et al. "Design and Planning of a Multiple-charger Multiple-port Charging System for PEV Charging Station". In: *IEEE Transactions on Smart Grid* (2017).

[38] Kai-Fung Chu, Albert YS Lam, and Victor OK Li. "Joint Rebalancing and Vehicle-to-Grid Coordination for Autonomous Vehicle Public Transportation System". In: *IEEE Transactions on Intelligent Transportation Systems* (2021).

[39] Hwei-Ming Chung et al. "Electric vehicle charge scheduling mechanism to maximize cost efficiency and user convenience". In: *IEEE Transactions on Smart Grid* 10.3 (2018), pp. 3020–3030.

[40] Jean-Michel Clairand. "Participation of electric vehicle aggregators in ancillary services considering users' preferences". In: *Sustainability* 12.1 (2019), p. 8.

[41] Jonathan Colmer. "What is the meaning of (statistical) life? Benefit–cost analysis in the time of COVID-19". In: *Oxford Review of Economic Policy* 36.Supplement_1 (2020), S56–S63.

[42] Cody Cook et al. *The gender earnings gap in the gig economy: Evidence from over a million rideshare drivers*. Tech. rep. National Bureau of Economic Research, 2018.

[43] Gabrielle Coppola. *Driverless cars are proving to be job creators, at least so far*. https://www.bloomberg.com/news/newsletters/2021-08-10/driverless-cars-are-proving-to-be-job-creators-at-least-so-far. [Online; accessed 19-Sept-2022]. Aug. 2021.

[44] JB Cruz Jr. "Survey of nash and stackelberg equilibrim strategies in dynamic games". In: *Annals of Economic and Social Measurement, Volume 4, number 2*. NBER, 1975, pp. 339–344.

[45] Csreinicke. *Autonomous Vehicles won't only kill jobs. they will create them, too*. https://www.cnbc.com/2018/08/10/autonomous-vehicles-are-creating-jobs-heres-where.html. [Online; accessed 19-Sept-2022]. Aug. 2018.

[46] Statista Research Department. *Median household income in New York from 1990 to 2019*. 2021. URL: https://www.statista.com/statistics/205974/median-household-income-in-new-york/#statisticContainer.

[47] Mi Diao, Hui Kong, and Jinhua Zhao. "Impacts of transportation network companies on urban mobility". In: *Nature Sustainability* (2021), pp. 1–7.

[48] Chris Dockins et al. "Value of statistical life analysis and environmental policy: A white paper". In: *US Environmental Protection Agency, National Center for Environmental Economics* (2004).

[49] Brian Donovan and Daniel B. Work. "Empirically quantifying city-scale transportation system resilience to extreme events". In: *Transportation Research Part C: Emerging Technologies* 79 (June 2017), pp. 333–346. ISSN: 0968-090X. DOI: 10.1016/j.trc.2017.03.002. URL: http://dx.doi.org/10.1016/j.trc.2017.03.002.

[50] Shane Downing. *8 electric truck and van companies to watch in 2020*. Jan. 2020. URL: https://www.greenbiz.com/article/8-electric-truck-and-van-companies-watch-2020.

[51] Anthony Downs. "Why traffic congestion is here to stay.... and will get worse". In: *Access Magazine* 1.25 (2004), pp. 19–25.

[52] Taycan & E-Mobility. *The charging process: Quick, comfortable, intelligent and universal*. 2019. URL: https://newsroom.porsche.com/en/products/taycan/charging-18558.html.

[53] *Each country's share of CO2 emissions*. URL: https://www.ucsusa.org/resources/each-countrys-share-co2-emissions.

[54] Thomas Earl et al. "Analysis of long haul battery electric trucks in EU". In: *8th Commercial Vehicle Workshop*. 2018.

[55] Organisation for Economic Co-operation and Development. *Taxi, ride-sourcing and ride-sharing services - Background Note by the Secretariat*. 2018. URL: https://one.oecd.org/document/DAF/COMP/WP2(2018)1/en/pdf (visited on 05/01/2021).

[56] Ona Egbue, Suzanna Long, and VA Samaranayake. "Mass deployment of sustainable transportation: evaluation of factors that influence electric vehicle adoption". In: *Clean Technologies and Environmental Policy* 19.7 (2017), pp. 1927–1939.

[57] Greenhouse Gas Emissions. *Comparison of lifecycle greenhouse gas emissions of various electricity generation sources*. 2011.

[58] Sevgi Erdoğan and Elise Miller-Hooks. "A green vehicle routing problem". In: *Transportation Research Part E: Logistics and Transportation Review* 48.1 (2012), pp. 100–114.

[59] Gregory D Erhardt et al. "Do transportation network companies decrease or increase congestion?" In: *Science advances* 5.5 (2019), eaau2670.

[60] *Fact sheet: Biden Administration Advances Electric Vehicle Charging Infrastructure*. Feb. 2022. URL: https://www.whitehouse.gov/briefing-room/statements-releases/2021/04/22/fact-sheet-biden-administration-advances-electric-vehicle-charging-infrastructure/.

[61] Samy Faddel, Ahmed T. Elsayed, Osama A. Mohammed, et al. "Bilayer Multi-Objective Optimal Allocation and Sizing of Electric Vehicle Parking Garage". In: *IEEE Transactions on Industry Applications* 54.3 (2018), pp. 1992–2001.

[62] John C Falcocchio and Herbert S Levinson. "Measuring traffic congestion". In: *Road Traffic Congestion: A Concise Guide*. Springer, 2015, pp. 93–110.

[63] Zhong Fan. "A distributed demand response algorithm and its application to PHEV charging in smart grids". In: *IEEE Transactions on Smart Grid* 3.3 (2012), pp. 1280–1290.

[64] Peter Fantke et al. "Global effect factors for exposure to fine particulate matter". In: *Environmental science & technology* 53.12 (2019), pp. 6855–6868.

[65] Justin Gerdes. *Next Up for Electrification: Heavy-Duty Trucks and Construction Machinery*. 2020. URL: https://www.greentechmedia.com/articles/read/next-up-for-electrification-heavy-duty-trucks-and-construction-machinery.

[66] Je B Greenblatt and Samveg Saxena. "Autonomous taxis could greatly reduce greenhouse-gas emissions of US light-duty vehicles". In: *Nature Climate Change* 5.July (2015). DOI: 10.1038/NCLIMATE2685.

[67] Krishna Murthy Gurumurthy, Kara M Kockelman, and Michele D Simoni. "Benefits and costs of ride-sharing in shared automated vehicles across austin, texas: Opportunities for congestion pricing". In: *Transportation Research Record* 2673.6 (2019), pp. 548–556.

[68] Kenneth M Gwilliam. "The value of time in economic evaluation of transport projects: Lessons from recent research". In: *World Bank (Washington DC)* (1997).

[69] Omar Hafez and Kankar Bhattacharya. "Queuing analysis based PEV load modeling considering battery charging behavior and their impact on distribution system operation". In: *IEEE Transactions on Smart Grid* 9.1 (2016), pp. 261–273.

[70] Scott Hardman, Alan Jenn, Gil Tal, et al. "A review of consumer preferences of and interactions with electric vehicle charging infrastructure". In: *Transportation Research Part D: Transport and Environment* 62 (2018), pp. 508–523.

[71] Gerhard Hiermann et al. "The electric fleet size and mix vehicle routing problem with time windows and recharging stations". In: *European Journal of Operational Research* 252.3 (2016), pp. 995–1018.

[72] Julian Hof, Michael Schneider, and Dominik Goeke. "Solving the battery swap station location-routing problem with capacitated electric vehicles using an AVNS algorithm for vehicle-routing problems with intermediate stops". In: *Transportation Research Part B: Methodological* 97 (2017), pp. 102–112.

[73] Patrick Hofstetter. *Perspectives in life cycle impact assessment: a structured approach to combine models of the technosphere, ecosphere, and valuesphere*. Springer Science & Business Media, 1998.

[74] John E Hopcroft and Richard M Karp. "An n^5/2 algorithm for maximum matchings in bipartite graphs". In: *SIAM Journal on computing* 2.4 (1973), pp. 225–231.

[75] Michael Hyland and Hani S. Mahmassani. "Dynamic autonomous vehicle fleet operations: Optimization-based strategies to assign AVs to immediate traveler demand requests". In: *Transp. Res. Part C Emerg. Technol.* 92 (2018), pp. 278–297. ISSN: 0968-090X. DOI: https://doi.org/10.1016/j.trc.2018.05.003. URL: http://www.sciencedirect.com/science/article/pii/S0968090X18306028.

[76] *Income statistics for New York ZIP codes*. https://www.incomebyzipcode.com/newyork. [Online; accessed 19-Sept-2022]. 2022.

[77] Indeed. *How much does a Taxi Driver make in New York, NY?* 2021. URL: https://www.indeed.com/career/taxi-driver/salaries/New-York--NY.

[78] Stefan Irnich and Guy Desaulniers. "Shortest path problems with resource constraints". In: *Column generation*. Springer, 2005, pp. 33–65.

[79] Akshay Jadhav. *Autonomous Vehicle Market by Automation Level (Level 3, Level 4, and Level 5), by Component (Hardware, Service and Software), by Application (Civil, Robo taxi, Ride hail, Ride share, Self-driving truck, and Self-driving bus) - Global Opportunity Analysis and Industry Forecast, 2020 – 2030*. 2020. URL: https://www.alliedmarketresearch.com/autonomous-vehicle-market (visited on 05/01/2021).

[80] Alan Jenn. "Emissions benefits of electric vehicles in Uber and Lyft ride-hailing services". In: *Nature Energy* 5.7 (2020), pp. 520–525.

[81] Surendra Reddy Kancharla and Gitakrishnan Ramadurai. "Electric vehicle routing problem with non-linear charging and load-dependent discharging". In: *Expert Systems with Applications* 160 (2020), p. 113714.

[82] Fanxin Kong et al. "Smart rate control and demand balancing for electric vehicle charging". In: *Proceedings of the 7th ICCPS*. IEEE Press. 2016.

[83] Katherine Kortum and Mark Norman. "National Academies–TRB Forum on Preparing for Automated Vehicles and Shared Mobility". In: *Transportation Research Circular* E-C234 (2018).

[84] Fred Lambert. *Tesla increases Supercharger idle fees to decrease wait times*. 2018. URL: https://electrek.co/2018/09/19/tesla-update-supercharger-idle-fees/.

[85] Heikki Liimatainen, Oscar van Vliet, and David Aplyn. "The potential of electric trucks – An international commodity-level analysis". In: *Applied Energy* 236 (2019), pp. 804–814. ISSN: 0306-2619. DOI: https://doi.org/10.1016/j.apenergy.2018.12.017. URL: http://www.sciencedirect.com/science/article/pii/S0306261918318361.

[86] Juuso Lindgren and Peter D Lund. "Identifying bottlenecks in charging infrastructure of plug-in hybrid electric vehicles through agent-based traffic simulation". In: *International Journal of Low-Carbon Technologies* 10.2 (2015), pp. 110–118.

[87] Todd Litman. "Transportation cost and benefit analysis". In: *Victoria Transport Policy Institute* 31 (2009), pp. 1–19.

[88] Yuanyuan Liu. *China Strives to Speed Up Development of EV Charging Stations*. Shelton, CT, 2018. URL: https://www.renewableenergyworld.com/storage/china-strives-to-speed-up-development-of-ev-charging-stations/#gref.

[89] Benjamin Loeb, Kara M Kockelman, and Jun Liu. "Shared autonomous electric vehicle (SAEV) operations across the Austin, Texas network with charging infrastructure decisions". In: *Transportation Research Part C: Emerging Technologies* 89 (2018), pp. 222–233.

[90] Gongyuan Lu et al. "Solving resource recharging station location-routing problem through a resource-space-time network representation". In: *arXiv preprint arXiv:1602.06889* (2016).

[91] Ioannis Lymperopoulos et al. "Ancillary Services Provision Utilizing a Network of Fast-Charging Stations for Electrical Buses". In: *IEEE Transactions on Smart Grid* 11.1 (2019), pp. 665–672.

[92] M. Schiffer and G. Walther. "An adaptive large neighborhood search for the location-routing problem with intra-route facilities". In: *Transportation Science* 52.2 (2017), pp. 331–352.

[93] M. Schiffer and G. Walther. "Strategic planning of electric logistics fleet networks: A robust location-routing approach". In: *Omega* 80 (2018), pp. 31–42.

[94] Hani S Mahmassani. "50th anniversary invited article—autonomous vehicles and connected vehicle systems: Flow and operations considerations". In: *Transportation Science* 50.4 (2016), pp. 1140–1162.

[95] Monirehalsadat Mahmoudi and Xuesong Zhou. "Finding optimal solutions for vehicle routing problem with pickup and delivery services with time windows: A dynamic programming approach based on state–space–time network representations". In: *Transportation Research Part B: Methodological* 89 (2016), pp. 19–42.

[96] Daniel McFadden and Kenneth Train. "Mixed MNL models for discrete response". In: *Journal of applied Econometrics* 15.5 (2000), pp. 447–470.

[97] Hui Miao et al. "Operating expense optimization for EVs in multiple depots and charge stations environment using evolutionary heuristic method". In: *IEEE Transactions on Smart Grid* 9.6 (2017), pp. 6599–6611.

[98] Dimitris Milakis, Bart Van Arem, and Bert Vanwee. "Policy and society related implications of automated driving: A review of literature and directions for future research". In: *J. Intell. Transport. Syst.* 21.4 (2017), pp. 324–348. ISSN: 15472442. DOI: 10.1080/15472450.2017.1291351. URL: https://doi.org/10.1080/15472450.2017.1291351.

[99] Ted R Miller. "Variations between countries in values of statistical life". In: *Journal of transport economics and policy* (2000), pp. 169–188.

[100] S Sheik Mohammed et al. "Interruptible charge scheduling of plug-in electric vehicle to minimize charging cost using heuristic algorithm". In: *Electrical Engineering* 104.3 (2022), pp. 1425–1440.

[101] Aniruddh Mohan et al. "Trade-offs between automation and light vehicle electrification". In: *Nature Energy* 5.7 (2020), pp. 543–549.

[102] Ahmadreza Moradipari and Mahnoosh Alizadeh. "Pricing and routing mechanisms for differentiated services in an electric vehicle public charging station network". In: *IEEE Transactions on Smart Grid* 11.2 (2019), pp. 1489–1499.

[103] Ana T Moreno et al. "Shared Autonomous Vehicles Effect on Vehicle-Km Traveled and Average Trip Duration". In: *J. Adv. Transport.* (2018), pp. 1–16.

[104] Sivapriya Mothilal Bhagavathy et al. "Impact of Charging Rates on Electric Vehicle Battery Life". In: *Findings* (Mar. 22, 2021). DOI: 10.32866/001c.21459.

[105] Nick Muerdter. "Alternative Fueling Station Locations". In: *U.S. Department of Energy* (July 2021). DOI: 10.25984/1810832.

[106] Subhas Chandra Mukhopadhyay. "Wearable sensors for human activity monitoring: A review". In: *IEEE sensors journal* 15.3 (2015), pp. 1321–1330.

[107] Matteo Muratori. "Impact of uncoordinated plug-in electric vehicle charging on residential power demand". In: *Nature Energy* 3.3 (2018), pp. 193–201.

[108] John Nash. "Non-cooperative games". In: *Annals of mathematics* (1951), pp. 286–295.

[109] Mehdi Nasri et al. "A robust approach for solving a vehicle routing problem with time windows with uncertain service and travel times". In: *International Journal of Industrial Engineering Computations* 11.1 (2020), pp. 1–16.

[110] Yu Marco Nie. "How can the taxi industry survive the tide of ridesourcing? Evidence from Shenzhen, China". In: *Transportation Research Part C: Emerging Technologies* 79 (2017), pp. 242–256.

[111] KOEN NOYENS. *EV charging infrastructure incentives in Europe 2021*. 2020. URL: https://blog.evbox.com/ev-charging-infrastructure-incentives-eu#Germany.

[112] Simon Oh et al. "Impacts of Automated Mobility-on-Demand on traffic dynamics, energy and emissions: A case study of Singapore". In: *Simulation Modelling Practice and Theory* (2021), p. 102327.

[113] New York Independent System Operator. *Fuel for the Wire: How We Make Energy in New York*. 2019. URL: https://www.nyiso.com/-/fuel-for-the-wire-how-we-make-energy-in-new-york.

[114] New York Independent System Operator. *Real-Time Fuel Mix*. 2020. URL: http://mis.nyiso.com/public/P-63list.htm.

[115] Christina Pakusch et al. "Traditional taxis vs automated taxis–Does the driver matter for Millennials?" In: *Travel Behaviour and Society* 21 (2020), pp. 214–225.

[116] Alex Pentland and Andrew Liu. "Modeling and prediction of human behavior". In: *Neural computation* 11.1 (1999), pp. 229–242.

[117] Dario Pevec et al. "Electric vehicle range anxiety: An obstacle for the personal transportation (R) evolution?" In: *2019 4th International Conference on Smart and Sustainable Technologies (SpliTech)*. IEEE. 2019, pp. 1–8.

[118] Andreas Poullikkas. "Sustainable options for electric vehicle technologies". In: *Renewable and Sustainable Energy Reviews* 41 (2015), pp. 1277–1287.

[119] *President Biden, U.S. Department of Transportation Releases Toolkit to help rural communities build out electric vehicle charging infrastructure*. 2022. URL: https://www.transportation.gov/briefing-room/president-biden-us-department-transportation-releases-toolkit%5C-help-rural-communities.

[120] Caroline Prodhon and Christian Prins. "A survey of recent research on location-routing problems". In: *European Journal of Operational Research* 238.1 (2014), pp. 1–17.

[121] Xinwu Qian et al. "Impact of transportation network companies on urban congestion: Evidence from large-scale trajectory data". In: *Sustainable Cities and Society* 55 (2020), p. 102053.

[122] Eric Reed. *The average salary in New York City*. https://www.yahoo.com/now/average-salary-york-city-170703352.html. [Online; accessed 19-Sept-2022]. Mar. 2019.

[123] Robert S. Kenney. "ELECTRIC SCHEDULE A-10 MEDIUM GENERAL DEMAND-METERED SERVICE". In: (2019). URL: https://www.pge.com/tariffs/assets/pdf/tariffbook/ELEC_SCHEDS_A-10.pdf.

[124] Paolo Santi et al. "Quantifying the benefits of vehicle pooling with shareability networks". In: *Proceedings of the National Academy of Sciences* 111.37 (2014), pp. 13290–13294.

[125] Bruce Schaller. *UNSUSTAINABLE? The Growth of App-Based Ride Services and Traffic, Travel and the Future of New York City*. 2017. URL: http://www.schallerconsult.com/rideservices/unsustainable.pdf.

[126] M Schiffer, S Stütz, and G Walther. "Are ECVs breaking even?-Competitiveness of electric commercial vehicles in medium-duty logistics networks". In: *Technical Report Working Paper* OM-02/2016 (2016).

[127] Maximilian Schiffer, Michael Schneider, and Gilbert Laporte. "Designing sustainable mid-haul logistics networks with intra-route multi-resource facilities". In: *European Journal of Operational Research* 265.2 (2018), pp. 517–532.

[128] Maximilian Schiffer and Grit Walther. "The electric location routing problem with time windows and partial recharging". In: *European Journal of Operational Research* 260.3 (2017), pp. 995–1013.

[129] Maximilian Schiffer et al. "Vehicle Routing and Location Routing with Intermediate Stops: A Review". In: *Transportation Science* 53.2 (2019), pp. 319–343.

[130] Michael Schimpe et al. "Comprehensive modeling of temperature-dependent degradation mechanisms in lithium iron phosphate batteries". In: *Journal of The Electrochemical Society* 165.2 (2018), A181.

[131] Andreas Schroeder and Thure Traber. "The economics of fast charging infrastructure for electric vehicles". In: *Energy Policy* 43 (2012), pp. 136–144.

[132] Toru Seo and Yasuo Asakura. "Multi-Objective Linear Optimization Problem for Strategic Planning of Shared Autonomous Vehicle Operation and Infrastructure Design". In: *IEEE Transactions on Intelligent Transportation Systems* (2021).

[133] Colin Sheppard et al. *Modeling plug-in electric vehicle charging demand with BEAM: the framework for behavior energy autonomy mobility*. Tech. rep. Lawrence Berkeley National Lab.(LBNL), Berkeley, CA (United States), 2017.

[134] Colin J. R. Sheppard et al. "Joint Optimization Scheme for the Planning and Operations of Shared Autonomous Electric Vehicle Fleets Serving Mobility on Demand". In: *Transportation Research Record* 2673.6 (Apr. 2019). ISSN: 0361-1981. DOI: 10.1177/0361198119838270. URL: https://www.osti.gov/biblio/1581070.

[135] Colin JR Sheppard, Andrew Harris, and Anand R Gopal. "Cost-effective siting of electric vehicle charging infrastructure with agent-based modeling". In: *IEEE Transactions on Transportation Electrification* 2.2 (2016), pp. 174–189.

[136] Igor RS da Silva et al. "A preference-based demand response mechanism for energy management in a microgrid". In: *Journal of Cleaner Production* 255 (2020), p. 120034.

[137] Michele D Simoni et al. "Congestion pricing in a world of self-driving vehicles: An analysis of different strategies in alternative future scenarios". In: *Transportation Research Part C: Emerging Technologies* 98 (2019), pp. 167–185.

[138] R. Sims et al. "Transport". In: *Climate Change 2014: Mitigation of Climate Change. Contribution of Working Group III to the Fifth Assessment Report of the Intergovernmental Panel on Climate Change* (2014).

[139] Carl Smith. *States show limited progress with electric vehicle policies*. Apr. 2021. URL: https://www.governing.com/now/states-show-limited-progress-electric-vehicle-policies.html.

[140] *Sources of Greenhouse Gas Emissions*. URL: https://www.epa.gov/ghgemissions/sources-greenhouse-gas-emissions.

[141] Shashank Sripad and Venkatasubramanian Viswanathan. "Quantifying the Economic Case for Electric Semi-Trucks". In: *ACS Energy Letters* 4.1 (2019), pp. 149–155. DOI: 10.1021/acsenergylett.8b02146. eprint: https://doi.org/10.1021/acsenergylett.8b02146. URL: https://doi.org/10.1021/acsenergylett.8b02146.

[142] Caltrans State of California. *Truck Lane Use*. URL: https://dot.ca.gov/programs/traffic-operations/legal-truck-access/truck-lane-use.

[143] Statista. *Digital Market Outlook Segment Report*. 2017. URL: https://www.statista.com/outlook/mmo/mobility-services/ride-hailing-taxi/worldwide (visited on 05/01/2021).

[144] Martijn van der Steen et al. "EV policy compared: an international comparison of governments' policy strategy towards E-mobility". In: *E-mobility in Europe*. Springer, 2015, pp. 27–53.

[145] Thomas Stoiber et al. "Will consumers prefer shared and pooled-use autonomous vehicles? A stated choice experiment with Swiss households". In: *Transportation Research Part D: Transport and Environment* (2019).

[146] *Story of Our Grid*. https://www.nyserda.ny.gov/About/Publications/Research-and-Development-Technical-Reports/Electric-Power-Transmission-and-Distribution-Reports/Electric-Power-Transmission-and-Distribution-Reports---Archive/New-York-Power-Grid-Study/Story-of-Our-Grid. 2021.

[147] Wencong Su, Habiballah Eichi, Wente Zeng, et al. "A survey on the electrification of transportation in a smart grid environment". In: *IEEE Transactions on Industrial Informatics* 8.1 (2012), pp. 1–10.

[148] Jeffrey A Sward et al. "Strategic planning for utility-scale solar photovoltaic development–Historical peak events revisited". In: *Applied Energy* 250 (2019), pp. 1292–1301.

[149] Seyfollah Tabrizi, Seyed Hassan Ghodsypour, and Abbas Ahmadi. "Modelling three-echelon warm-water fish supply chain: A bi-level optimization approach under Nash–Cournot equilibrium". In: *Applied Soft Computing* 71 (2018), pp. 1035–1053.

[150] Gil Tal et al. "Electric cars in California: policy and behavior perspectives". In: *Who's Driving Electric Cars*. Springer, 2020, pp. 11–25.

[151] Fei Tan, Zheng-yi Chai, and Ya-lun Li. "Multi-objective evolutionary algorithm for vehicle routing problem with time window under uncertainty". In: *Evolutionary Intelligence* (2021), pp. 1–16.

[152] Tesla Team. *Introducing V3 Supercharging*. 2019. URL: https://www.tesla.com/blog/introducing-v3-supercharging.

[153] Nathaniel Tucker and Mahnoosh Alizadeh. "An online admission control mechanism for electric vehicles at public parking infrastructures". In: *IEEE Transactions on Smart Grid* 11.1 (2019), pp. 161–170.

[154] USEPA. *Fast Facts: U.S. Transportation Sector Greenhouse Gas Emissions 1990–2018*. 2020. URL: https://nepis.epa.gov/Exe/ZyPDF.cgi?Dockey=P100ZK4P.pdf.

[155] M M Vazifeh et al. "Addressing the minimum fleet problem in on-demand urban mobility". In: *Nature* 557.7706 (2018), pp. 534–538. ISSN: 0028-0836. DOI: 10.1038/s41586-018-0095-1. URL: https://doi.org/10.1038/s41586-018-0095-1.

[156] Reza Vosooghi et al. "Shared autonomous electric vehicle service performance: Assessing the impact of charging infrastructure". In: *Transportation Research Part D: Transport and Environment* 81 (2020), p. 102283.

[157] Dai Wang et al. "Quantifying electric vehicle battery degradation from driving vs. vehicle-to-grid services". In: *Journal of Power Sources* 332 (2016), pp. 193–203.

[158] Guibin Wang, Zhao Xu, Fushuan Wen, et al. "Traffic-constrained multiobjective planning of electric-vehicle charging stations". In: *IEEE Transactions on Power Delivery* 28.4 (2013), pp. 2363–2372.

[159] Shu Wang, Zhao Yang Dong, Fengji Luo, et al. "Stochastic collaborative planning of electric vehicle charging stations and power distribution system". In: *IEEE Transactions on Industrial Informatics* 14.1 (2018), pp. 321–331.

[160] Xu Wang, Mohammad Shahidehpour, Chuanwen Jiang, et al. "Coordinated Planning Strategy for Electric Vehicle Charging Stations and Coupled Traffic-Electric Networks". In: *IEEE Transactions on Power Systems* 34.1 (2019), pp. 268–279.

[161] Dorcas Wong. *What is China's new infrastructure plan and WILL IT benefit tech investors?* `https://www.china-briefing.com/news/how-foreign-technology-investors-benefit-from-chinas-new-infrastructure-plan/`. June 2021.

[162] Yangyang Xu and Wotao Yin. "A block coordinate descent method for regularized multiconvex optimization with applications to nonnegative tensor factorization and completion". In: *SIAM Journal on imaging sciences* 6.3 (2013), pp. 1758–1789.

[163] Zhiwei Xu, Wencong Su, Zechun Hu, et al. "A hierarchical framework for coordinated charging of plug-in electric vehicles in China". In: *IEEE Transactions on Smart Grid* 7.1 (2016), pp. 428–438.

[164] Meng Xuyao, Zhang Weige, Bao Yan, et al. "Sequential Construction Planning of Electric Taxi Charging Station Considering the Development of Charging Demand". In: *Joint ICEEE and ICEIV* (2018).

[165] Qin Yan, Bei Zhang, and Mladen Kezunovic. "Optimized operational cost reduction for an EV charging station integrated with battery energy storage and PV generation". In: *IEEE Transactions on Smart Grid* 10.2 (2018), pp. 2096–2106.

[166] Jun Yang and Hao Sun. "Battery swap station location-routing problem with capacitated electric vehicles". In: *Computers & Operations Research* 55 (2015), pp. 217–232.

[167] Shuguan Yang and Zhen Sean Qian. "Turning meter transactions data into occupancy and payment behavioral information for on-street parking". In: *Transportation Research Part C: Emerging Technologies* 78 (2017), pp. 165–182.

[168] Weifeng Yao, Junhua Zhao, Fushuan Wen, et al. "A multi-objective collaborative planning strategy for integrated power distribution and electric vehicle charging systems". In: *IEEE Transactions on Power Systems* 29.4 (2014), pp. 1811–1821.

[169] Zonggen Yi, John Smart, and Matthew Shirk. "Energy impact evaluation for eco-routing and charging of autonomous electric vehicle fleet: Ambient temperature consideration". In: *Transp. Res. Part C Emerg. Technol.* 89.October 2017 (2018), pp. 344–363. ISSN: 0968090X. DOI: `10.1016/j.trc.2018.02.018`.

[170] Wang Li-ying and Song Yuan-bin. "Multiple Charging Station Location-Routing Problem with Time Window of Electric Vehicle." In: *Journal of Engineering Science & Technology Review* 8.5 (2015).

[171] Xiao Ying and Tengjing Xuan. *China's Electric Vehicle Charging Stations Idle 85% of Time*. 2018. URL: https://www.caixinglobal.com/2018-01-22/chinas-electric-vehicle-charging-stations-idle-85-of-time/-101201234.html.

[172] Dajun Yue and Fengqi You. "Stackelberg-game-based modeling and optimization for supply chain design and operations: A mixed integer bilevel programming framework". In: *Computers & Chemical Engineering* 102 (2017), pp. 81–95.

[173] Efstathios Zavvos, Enrico H Gerding, and Markus Brede. "A Comprehensive Game-Theoretic Model for Electric Vehicle Charging Station Competition". In: *IEEE Transactions on Intelligent Transportation Systems* (2021).

[174] Bo Zeng and Yu An. "Solving bilevel mixed integer program by reformulations and decomposition". In: *Optimization online* (2014), pp. 1–34.

[175] Teng Zeng, Scott Moura, and Hongcai Zhang. "Solving Overstay and Stochasticity in PEV Charging Station Planning with Real Data". In: *IEEE Transactions on Industrial Informatics* (2019).

[176] Hongcai Zhang, Zechun Hu, Zhiwei Xu, et al. "An integrated planning framework for different types of PEV charging facilities in urban area". In: *IEEE Transactions on Smart Grid* 7.5 (2016), pp. 2273–2284.

[177] Hongcai Zhang, Zechun Hu, Zhiwei Xu, et al. "Evaluation of achievable vehicle-to-grid capacity using aggregate PEV model". In: *IEEE Transactions on Power Systems* 32.1 (2017), pp. 784–794.

[178] Hongcai Zhang, Zechun Hu, Zhiwei Xu, et al. "Optimal planning of PEV charging station with single output multiple cables charging spots". In: *IEEE Transactions on Smart Grid* 8.5 (2017), pp. 2119–2128.

[179] Hongcai Zhang et al. "A Second Order Cone Programming Model for Planning PEV Fast-Charging Stations". In: *IEEE Trans. Power Syst.* 33.3 (2017), pp. 2763–2777. ISSN: 08858950. DOI: 10.1109/TPWRS.2017.2754940. eprint: 1702.01897.

[180] Hongcai Zhang et al. "A second-order cone programming model for planning PEV fast-charging stations". In: *IEEE Transactions on power Systems* 33.3 (2017), pp. 2763–2777.

[181] Hongcai Zhang et al. "Charging infrastructure demands of shared-use autonomous electric vehicles in urban areas". In: *Transportation Research Part D: Transport and Environment* 78 (2020), p. 102210.

[182] Hongcai Zhang et al. "Evaluation of achievable vehicle-to-grid capacity using aggregate PEV model". In: *IEEE Transactions on Power Systems* 32.1 (2016), pp. 784–794.

[183] Hongcai Zhang et al. "Joint fleet sizing and charging system planning for autonomous electric vehicles". In: *IEEE Transactions on Intelligent Transportation Systems* (2019).

[184] Hongcai Zhang et al. "PEV fast-charging station siting and sizing on coupled transportation and power networks". In: *IEEE Transactions on Smart Grid* 9.4 (2016), pp. 2595–2605.

[185] Hongcai Zhang et al. "PEV fast-charging station siting and sizing on coupled transportation and power networks". In: *IEEE Transactions on Smart Grid* 9.4 (2018), pp. 2595–2605.

[186] Tianyang Zhang, Xi Chen, Zhe Yu, et al. "A Monte Carlo Simulation Approach to Evaluate Service Capacities of EV Charging and Battery Swapping Stations". In: *IEEE Transactions on Industrial Informatics* 14.9 (2018), pp. 3914–3923.

[187] Xiaohu Zhang et al. "Bilevel optimization based transmission expansion planning considering phase shifting transformer". In: *2017 North American power symposium (NAPS)*. IEEE. 2017, pp. 1–6.

[188] Tianyang Zhao et al. "Real-time optimal energy and reserve management of electric vehicle fast charging station: Hierarchical game approach". In: *IEEE Transactions on Smart Grid* 9.5 (2017), pp. 5357–5370.

[189] Yu Zheng, Yue Song, David J Hill, et al. "Online Distributed MPC-based Optimal Scheduling for EV Charging Stations in Distribution Systems". In: *IEEE Transactions on Industrial Informatics* 15.2 (2019), pp. 638–649.

[190] Zhe Zhou et al. "Power-traffic network equilibrium incorporating behavioral theory: A potential game perspective". In: *Applied Energy* 289 (2021), p. 116703.